

Volume 1 Annex V1-7 Type A Water Licence Applications

Package P5-13

Hydrogeological Characterization and Modeling of the
Proposed Boston, Madrid South and Madrid North Mines,
Hope Bay Project

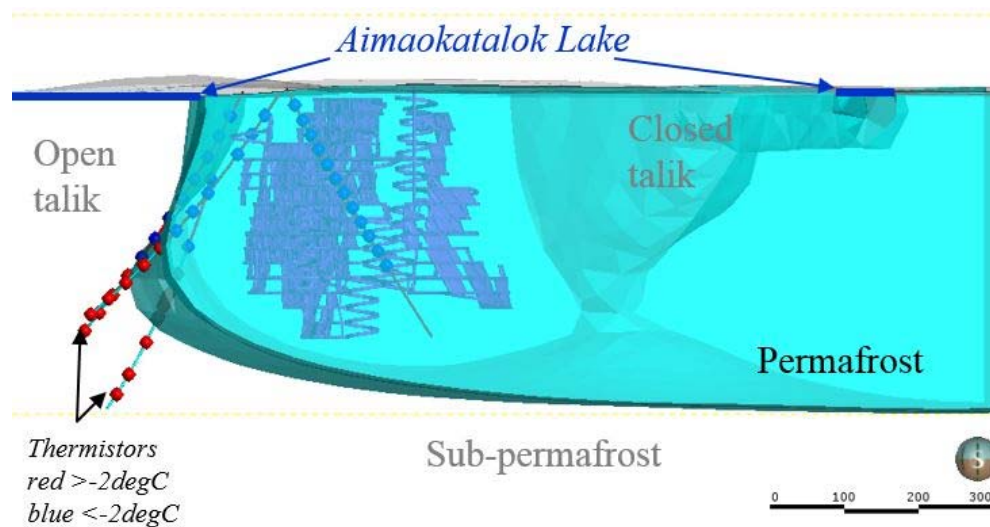




Hydrogeological Characterization and Modeling of the Proposed Boston, Madrid South and Madrid North Mines, Hope Bay Project

Prepared for

TMAC Resources Inc.



Prepared by

The logo for srk consulting, featuring a stylized orange 's' followed by the text 'rk consulting' in a bold, sans-serif font.

SRK Consulting (Canada) Inc.
1CT022.013
November 2017

Hydrogeological Characterization and Modeling of the Proposed Boston, Madrid South and Madrid North Mines, Hope Bay Project

November 2017

Prepared for

TMAC Resources Inc.
PO Box 44
Suite 1010 – 95 Wellington Street, West
Toronto, ON, M5J 2N7
Canada

Tel: +1 416 628 0216
Web: www.tmacresources.com

Prepared by

SRK Consulting (Canada) Inc.
2200–1066 West Hastings Street
Vancouver, BC V6E 3X2
Canada

Tel: +1 604 681 4196
Web: www.srk.com

Project No: 1CT022.013

File Name: Groundwater_Report_1CT022.013_20171121_CH_EMR_GF.docx

Copyright © SRK Consulting (Canada) Inc., 2017



Table of Contents

1	Introduction	1
1.1	Background	1
1.2	Scope of Work	1
1.3	Report Layout	2
2	Reference Information	3
2.1	Previous Relevant Studies	3
2.2	Mine Plan	4
2.2.1	Plan Basis	4
2.2.2	Boston Mine	4
2.2.3	Madrid North Mine	4
2.2.4	Madrid South Mine	4
3	Hydrogeological Conditions	5
3.1	Geology	5
3.1.1	Regional Setting	5
3.1.2	Local Setting	5
3.2	Hydraulic Properties	7
3.2.1	Data Sources	7
3.2.2	Overburden	7
3.2.3	Fractured Rock	8
3.3	Water Level	10
3.4	Groundwater Quality	11
3.4.1	Regional Subpermafrost Groundwater Quality Data	11
3.4.2	Hope Bay Subpermafrost Groundwater Quality Data	12
3.5	Permafrost Extent	14
3.5.1	Freezing Point Depression	14
3.5.2	Mapping of the Lake Taliks and Base of Permafrost	14
3.5.3	Regional Talik Model	16
3.5.4	Site-specific Talik Model	16
4	Hydrogeological Modeling Approach	17
4.1	Conceptual Groundwater Model	17
4.1.1	Flow System	17
4.1.2	Open Talik Properties	17
4.1.3	Groundwater Quality	17
4.1.4	Mine Interactions with Groundwater	17
4.2	Numerical Groundwater Models	18

4.2.1	Software and Model Type	18
4.2.2	Model Assumptions.....	18
4.2.3	Model Designs	18
4.2.4	Model Calibration	20
4.2.5	Model Simulations.....	20
4.2.6	Model Sensitivity and Uncertainty Analysis	20
4.2.7	Limitations of the Groundwater Model	20
5	Modeling Results	21
5.1	Current Conditions	21
5.2	Active Mining Conditions	21
5.2.1	Predicted Mine Inflows	21
5.2.2	Effects of Heated Underground Mining to Permafrost and Taliks	23
5.2.3	Mine Inflow Benchmarking.....	23
5.2.4	Predicted Groundwater Quality	26
5.3	Post-closure Conditions	29
5.3.1	Mine Reflood Time Estimation	29
5.3.2	Inflow of Mine Affected Groundwater into Lakes	30
5.4	Model Sensitivity	31
5.4.1	Results of the Sensitivity Models	31
5.4.2	Sensitivity to Flow from Exploration Drillholes	36
5.4.3	Management of the Uncertainty of the Groundwater Predictions	37
6	Conclusions	39
7	References.....	42

List of Figures

- Figure 1: Project Map
- Figure 2: Boston Mine Views
- Figure 3: Madrid North Mine and Madrid South Mine Views
- Figure 4: Mine Void Volumes over Time
- Figure 5: Regional Geology
- Figure 6: Detailed Geology Map of the Boston Area
- Figure 7: Schematic Cross West-East Section of the Boston Mineralization
- Figure 8: Detailed Geology Map of the Madrid Area
- Figure 9: Location Map of the Hydrogeological Data at Boston
- Figure 10: Location Map of the Hydrogeological Data at Doris
- Figure 11: Location Map of the Hydrogeological Data at Madrid North
- Figure 12: Location Map of the Hydrogeological Data at Madrid South
- Figure 13: Statistical Summary of the K Measurements
- Figure 14: K Vs Depth
- Figure 15: K vs Geological Units
- Figure 16: Correlation K vs Fracture Frequency
- Figure 17: TDS Concentrations with Depth in Canada's North
- Figure 18: Observed Profile of Chloride Concentration with Depth
- Figure 19: TDS versus Chloride
- Figure 20: Potential through Taliks at Boston and Madrid
- Figure 21: 3D Sections Showing the Permafrost and the Boston Mine (Looking North)
- Figure 22: 3D Sections Showing the Permafrost and the Madrid North Mine (Looking North)
- Figure 23: 3D Sections Showing the Permafrost and the Madrid South Mine (Looking North)
- Figure 24: Conceptual Groundwater System
- Figure 25: Published K values
- Figure 26: Model Domains and Boundary Conditions
- Figure 27: 3D Views of the Madrid North Numerical Model
- Figure 28: 3D Views of the Madrid South Numerical Model
- Figure 29: Madrid North Predicted Heads at Current Conditions
- Figure 30: Madrid South Predicted Heads at Current Conditions
- Figure 31: Hydraulic Head Predictions at Madrid North
- Figure 32: Hydraulic Head Predictions at Madrid South
- Figure 33: Predicted Mine Inflows
- Figure 34: Predicted Infiltrations of Water from Lakes
- Figure 35: Predicted Contributions of Lake water to Mine Inflows
- Figure 36: Chloride Concentration Predictions at Madrid North
- Figure 37: Chloride Concentration Predictions at Madrid South

Figure 38: Predicted Chloride Concentrations of Mine Inflows

Figure 39: Sensitivity Model Results

Figure 40: Sensitivity Model Results

Figure 41: Probabilities of Intercepting Open Hole Flowing at Maximum Rate at Madrid North

Figure 42: Probabilities of Intercepting Open Hole Flowing at Maximum Rate at Madrid South

List of Tables

Table 1: Hydraulic Conductivity of Doris Lake Bed Sediments.....	7
Table 2: Specific hydraulic tests that intersected geological structures	9
Table 3: Lake Level and Pore Pressure Measurements at Boston	10
Table 4: Lake Level and Pore Pressure Measurements at Madrid South and Madrid North	11
Table 5: Groundwater Quality (10WBW001) under Doris Lake	13
Table 6: Isotherm Depression Estimates based on Water Samples from 10WBW001	14
Table 7: Mine Volumes within and Outside Permafrost.....	18
Table 8: Groundwater Model Parameters.....	19
Table 9: Predicted Flow Rates at Nodes Representing Surface Water Bodies for Current Conditions	21
Table 10: Volume of Key Lakes, Annual Lake Inflow and Predicted Peak Annual Infiltration	22
Table 11: Lateral Permafrost Thaw from Heated Air in Underground Mining Areas	23
Table 12: Actual Concentration in Lakes and Groundwater	28
Table 13: Predicted Concentration in Mine Inflows during Active Mining	29
Table 14: Reflood Time Estimations	30
Table 15: Summary of the Sensitivity Model Results	35
Table 16: Drillhole Intersection Summary for Madrid South	36
Table 17: Drillhole Probabilities	37

List of Appendices

Appendix A: SRK Memo, “Hope Bay Project: Lake Talik Configuration”

Change Log

The following table provides an overview of material changes to this report from the previous version issued as Appendix V3-4B as part of the DEIS for Phase 2 of the Hope Bay Project dated December 2016.

Changes by Section

Information Request, Technical Comment, or Other Change	Section	Comments
ECCC-IR5	Section 3.4.2 Section 5.2.3	Report updated to include response to IR.
ECCC-IR6	Section 4.1.4	Report updated to include response to IR.
INAC-IR23	Section 3.2.3	Report updated to include response to IR.
INAC-IR24	Section 3.3	Report updated to include response to IR.
INAC-IR28	Section 3.2.3 Section 5.2.1	Report updated to include response to IR.
KIA-DEIS-39	Section 4.1.2 Section 5.4	Report updated to include response to IR.
KIA-IR160	Section 5.4	Report updated to include response to IR.
KIA-IR177	Section 5.2.1, Figure 14 Section 5.3.1	Report updated to include response to IR.
NRCan-IR5	Section 3.5.2	Report updated to include response to IR.
NRCan-IR7	Section 4.2.3	Report updated to include response to IR.
NRCan-IR8	Section 0	Report updated to include response to IR.
NRCan-IR9	Section 5.2.1	Report updated to include response to IR.
NRCan-IR10	Section 5.2.4	Report updated to include response to IR.
NRCan-IR11	Table 15, Section 5.4.2	Report updated to include response to IR.
NRCan-IR13	Section 5.2.1	Report updated to include response to IR.
Other change	Figure 41 and 42	Updated all dashed blue lines (i.e., infiltration rates from Patch Lake). This error was noted after the DEIS submission. The error refers to the figures only and not the actual data.

1 Introduction

1.1 Background

The Hope Bay Project (the Project) is a gold mining and milling undertaking of TMAC Resources Inc. The Project is located 705 km northeast of Yellowknife and 153 km southwest of Cambridge Bay in Nunavut Territory, and is situated east of Bathurst Inlet. The Project comprises three distinct areas of known mineralization plus extensive exploration potential and targets. The three areas that host mineral resources are Doris, Madrid, and Boston.

The Project consists of two phases; Phase 1 (Doris project), which is currently being carried out under an existing Water Licence (TMAC, 2015a), and Madrid-Boston which is in the environmental assessment stage. Phase 1 includes mining and infrastructure at Doris only, while Madrid-Boston includes mining and infrastructure at Madrid (Madrid North and Madrid South mines) and Boston (Boston Mine) located approximately 10 and 60 km south from Doris Mine, respectively (Figure 1).

The Project is located in the continuous permafrost region of Canada, and the permafrost extends to depths of 400 to 500 metres below ground surface (mbgs), except near large bodies of water where talik zones are present. Where the mines intersect talik zones and subpermafrost depths, groundwater inflow may be encountered. Water quality sampling has confirmed that the groundwater has high salinity and elevated concentrations of dissolved ammonia, boron, cadmium, chloride, fluoride, iron, manganese, molybdenum, mercury, nickel, selenium, sulfate and zinc, and therefore careful management of the groundwater is required.

Hydrogeological characterization and predictive numerical modeling of the Doris Mine groundwater inflow rates and quality was presented in SRK (2015a). This report presents the hydrogeological conditions at the Madrid North, Madrid South and Boston mines, and describes the predictive numerical groundwater models for these mines. The resultant groundwater inflow rates and quality at each of these mines are presented during all stages of the Project, including Construction, Operation, Closure and Post-closure. This information serves as a basis to assess the effect of the mines to the groundwater environment and is used as input to the Project site-wide water and load balance (SRK, 2017).

1.2 Scope of Work

The scope of work covered in this report includes:

- Review and discussion of the Phase 1 and Madrid-Boston project-wide baseline hydrogeology characterization data;
- Description of the conceptual groundwater models for each of the Madrid-Boston proposed mines;
- Description of the input variables and assumptions for each of the numerical groundwater models developed for predicting groundwater inflow rate and groundwater inflow quality over the life of the mines;

- Calibration of the numerical groundwater models;
- Sensitivity analysis of the numerical groundwater models for each of the mines to facilitate an understanding of the system uncertainties; and
- Presentation of the groundwater modeling results in a way that is compatible with the Project site-wide water and load balance model (SRK, 2017).

1.3 Report Layout

Section 2 of this report lists all of the relevant site characterization studies that have been carried out at the Project site, presents the proposed mine plans and discusses how the mines will potentially relate to groundwater. Section 3 provides the framework for understanding the current hydrogeological regime. This includes an in-depth evaluation of the available hydrogeological data. Section 4 describes the conceptual groundwater model and the details of the numerical models. The modeling results are presented in Section 5, and the conclusions in Section 6.

2 Reference Information

2.1 Previous Relevant Studies

The hydrogeological understanding for the Project is based on information from geological and structural mapping (Roscoe Postle, 2015) and site-specific field investigations completed in 2004, 2008, 2010 and 2011. A summary of the most relevant documents in this regard is described below, and a comprehensive reference list is provided in Section 7:

- **SRK 2003:** SRK carried out preliminary calculations to assess potential inflows to the underground workings at the Doris North deposit.
- **SRK 2005:** Two thermistor strings were installed in 2004 near Doris North; one along the southern extent of the Doris North deposit in deep permafrost, the other to the west of the Doris North deposit in shallow permafrost. Data for the two wells have been collected since 2004.
- **SRK 2009 (a, b, c, d):** SRK issued three geotechnical and hydrogeological assessments; one for a mine plan that included a Boston Open Pit, one for a mine plan that included Madrid Open Pit and Underground (Madrid North), one for a Doris North Open Pit and a Doris Central Underground. The assessments were based on field studies completed by SRK in 2008 that included overburden characterisation, detailed structural review, hydrogeological investigations, and geotechnical assessments (including additional thermistor drillholes).
- **SRK 2011a:** SRK conducted a field program in 2010 involving the installation of several Westbay multi-level monitoring wells for the purposes of characterizing groundwater quality at Doris North, Doris Central, and Boston. Hydraulic tests were also completed during drilling. One of these wells is within the Doris Lake talik; groundwater quality was characterized for each of the sampled zones to a depth of 490 meters below lake elevation.
- **SRK 2011b:** SRK provided a memo summarizing results of updated estimates for inflow rates and water quality for Doris Central and Connector, including provision for flow contributions from open exploration drillholes. The updated assessments used data from the 2010 field program (SRK 2011a).
- **SRK 2012:** SRK provided a report summarizing results of groundwater quality sampling and analyses from the three existing Westbay wells (Doris North, Doris Central, and Boston).
- **SRK 2014 (a, b):** SRK provided a report that reviewed all of the historical data as well as the additional field work conducted in 2011 at the Project, and updated the characterization of the geotechnical and hydrogeological conditions. This document provided information for use in mine and infrastructure design, and to support an internal pre-feasibility study. SRK provided also a memo summarizing results of updated estimates for inflow rates and water quality for the Madrid South and Madrid North mines.
- **SRK 2015a:** SRK conducted hydrogeological modeling and presented a report providing groundwater inflow and quality predictions to portions of the Doris North Mine.
- **SRK 2015b:** SRK provided a report that presented the results of a site wide water and load balance for the Doris North mine.

2.2 Mine Plan

2.2.1 Plan Basis

The Madrid-Boston mine plans are based on the following information sources:

- Personal communication with Floyd Varley, Vice President Operations, on updates of the mine plan from Roscoe Postle Associates Inc (TMAC 2016a);
- Tables detailing the mine production plan (TMAC 2016b, 2017);
- Three-dimensional resource wireframes of the Madrid North, Madrid South and Boston mines (TMAC 2016c); and
- Three-dimensional plans for the Boston, Madrid South and Madrid North Mines based on prefeasibility conditions. (TMAC 2015b).

2.2.2 Boston Mine

The Boston Mine is located on a peninsula on Aimakatalok Lake, immediately North of Stickleback Lake; the Boston prefeasibility mine design and current resource wireframes are shown on Figure 2. The Madrid-Boston mine plan assumes mining in Boston will only take place within the estimated volume of permafrost (see section 3.6.4); therefore, the Boston Mine is not expected to intercept groundwater. Mining is scheduled to start in Year 6 (January 2022) and is expected to be fully developed by Year 13 (December 2029).

2.2.3 Madrid North Mine

The Madrid North Mine is located approximately 15 km south of Roberts Bay, and about 45 km north of the Boston Mine; the Madrid North prefeasibility mine design and current resource wireframes are shown on Figure 3. The mine consists of three distinct mining zones that include the Suluk and Rand zones located within an open talik under the north extremity of Patch Lake, and the Naartok zone located inland, mostly within permafrost, partially intersecting subpermafrost in the deepest portion of the mine. All three zones have potentials for receiving groundwater inflow. A thickness of 60 m is assumed for the crown pillar under Patch Lake in unfrozen ground. Mining is scheduled to start in Year 3 (January 2019) and is expected to be fully developed by Year 15 (December 2031). Figure 4 provides details on the underground void space volumes over time.

2.2.4 Madrid South Mine

The Madrid South underground mine is located approximately 4 km south of the Madrid North mine, at the southern extremity of Patch Lake; the Madrid North prefeasibility mine design and current resource wireframes are shown on Figure 3. The mine consists of two distinct mining zones, Patch and Wolverine, which partially intersect the Patch and the Wolverine lakes, respectively. Both lakes are expected to support open taliks; therefore, the mine has potential for receiving groundwater inflow. A thickness of 60 m is assumed for the crown pillar under Patch Lake and Wolverine Lake in unfrozen ground. Mining is scheduled to start in Year 13 (January 2029) and is expected to be fully developed by Year 16 (December 2032). Figure 4 provides details on the underground void space volumes over time.

3 Hydrogeological Conditions

3.1 Geology

3.1.1 Regional Setting

The Hope Bay Volcanic Belt (HBVB) is a greenstone belt that is located in the northeast portion of the Slave Structural Province (Figure 5). The HBVB is mafic volcanic-dominated, typified by massive to pillowed tholeiitic flows interbedded with calc-alkaline felsic volcanic and volcanoclastic rocks, clastic sedimentary rocks, and rarely synvolcanic conglomerate and carbonates.

Multiple Quaternary Ice Ages produced an extensive glaciated landscape that was covered by successive Laurentide ice sheets. The Last Ice Sheet started receding about 8,800 years ago (Dyke and Prest, 1986) leaving an extensive blanket of basal till. Immediately following the de-glaciation, the entire Hope Bay region was submerged approximately 200 metres below present mean sea level (Dyke and Dredge, 1989). Fine sediment, derived from meltwater (rock flour), was deposited onto the submerged Hope Bay shelf as marine clays and silts onto the basal tills. The greatest thicknesses accumulated in the deeper water zones, now represented by valleys.

Isostatic rebound after the de-glaciation, resulted in emergent landforms and reworking of the unconsolidated marine sediments and tills along the prograding shoreface (EBA, 1996). Sediments were easily stripped off the uplands and redeposited in valleys, leaving relatively continuous north-northwest trending bedrock ridges and elongate lakes. The unconsolidated overburden, now up to 30 m in thickness, comprises locally and regionally derived tills and boulder tills with lacustrine and marine sediments and clay up to 15 m thick in the larger valleys.

3.1.2 Local Setting

Bedrock and Structural Geology

Gold mineralization is variable in terms of mineralization style and relationship to the host volcanic sequences (Sherlock et al., 2012). The Boston deposit is located near the south end of the belt and is associated with a flexure in the Hope Bay regional structure. The Madrid deposit consists of three styles of veining and brecciation.

Boston

The Boston gold deposit is situated in an area dominated by mafic metavolcanics rocks, metasedimentary rock and minor amounts of felsic metavolcanics (Figure 6). The strata are folded and form a large south-plunging synformal anticline. The mafic metavolcanics form the interior of the fold, while synvolcanic metasediments flank the east and the west sides. The transition between the metasediment and metavolcanic packages is variable, with interbedded units of metasediments and metavolcanics.

Gold mineralization is associated primarily with steep deformed quartz veins at the contact between mafic metavolcanics and metasedimentary rocks (Figure 7). Four brittle faults have been modeled to crosscut the Boston area. Additional fault lineaments have been observed in airborne geophysics.

Madrid

The general stratigraphy of the Madrid area is composed of three major volcanic packages: the Wolverine group basalts (C-type rocks), the Patch Group basalts (A-type rocks), and the pale green pillow basalts (Figure 8). Metasedimentary rocks often occur in the Patch Group metavolcanics. The western and southern portions of the Madrid area are characterized by a wide package of variably deformed and altered rocks collectively referred as the Deformation Zone (DEFZ), about 100 m – 140 m thick. The DEFZ is typically comprised of chlorite schist with a strong overprinting (regional) foliation. Diabase dykes are the youngest rocks. Two dykes occur in the vicinity of the Naartok. No dykes have been identified in proximity to the Suluk.

Gold mineralization occurs within the proximity to the DEFZ, which is not a single planar structure, but a complicated anastomosing feature with several splays and local pinch-and-swell textures. Its orientation varies from east-west in the Naartok area to north-south at Suluk. The dip of the zone at Naartok is approximately 75° to the north and is vertical at Suluk. Five distinct faults have been interpreted in the Naartok area and two in the Suluk area. Apparent discontinuities in alteration, mineralization and lithological units generally define a set of NW trending steep structures.

Surficial Geology

The overburden can be described as ice-rich (10 to 30% by volume on average, but occasionally as high as 50%) marine silty clay and clayey silt. The onshore profile consists generally of a thin veneer of hummocky organic soil covered by tundra heath vegetation. Under this organic zone is a layer of marine clay (silty clay and clayey silt) typically between 5 and 20 m thick; however, since the terrain is glaciated with significant bedrock control, there are areas where overburden is less than 5 m thick as well as areas where the overburden exceeds 30 m in thickness. In areas where the overburden exceeds 20 m in thickness, it appears to be underlain by clayey morainal till, which contains moderate amounts of cobbles and boulders (SRK, 2009a).

The overburden soils under the lakes are of the same origin as the onshore overburden soils, i.e., silty clays and clayey silts. There is a layer of limnic sediments ranging between a few centimetres to as much as 2 m thick, under which is a normally consolidated layer of marine silty clay and clayey silts between 10 and 20 m thick (SRK, 2009a).

3.2 Hydraulic Properties

3.2.1 Data Sources

Hydraulic conductivity (K) values were measured at Boston, Doris, Madrid South and Madrid North. Data are available for the sediments from 28 in-situ tests and two laboratory tests (SRK, 2009a), and for fractured rock from 112 tests (SRK, 2009b, 2009c, 2009d, 2011a, 2014a). Hydraulic testing in fractured rock included short duration packer injection tests (Short Duration Tests) at the three sites and one long-term (about 12 hours) constant head injection test (Extended Duration Test) at the Doris site. Location maps of the tests are shown for each mine area in Figures 9-12.

3.2.2 Overburden

The potential for a connection between a shallow groundwater system in the overburden units and the deeper bedrock groundwater system will be localized in areas of taliks associated with lakes. Onshore, permafrost exists at relatively shallow depths and keeps the two systems separated.

The infiltration of water from the lakes to the deeper groundwater system will be affected by hydraulic properties of sediments found on the lake bottom. Finer grained materials (e.g., clay) will have a lower hydraulic conductivity than coarse grained materials (e.g. sand), and thus allow less infiltration. The percentage of clay in these lake bottom sediments will have a significant effect on hydraulic conductivity.

Pressure dissipation tests were conducted in sediments lining the base of Doris Lake, Patch Lake and Aimakatalok Lake, during cone penetration (CPT) drilling (SRK, 2009a). Results were interpreted for hydraulic conductivity using the method of Perez and Fauriel (1988). CPT refusal was not associated with bedrock contact, but an indurated layer of lake sediment, estimated to be 3 m thick on average based on the available drillhole information. Two samples of the indurated lake bed sediment (SRK-OB-VS-14-S3 and SRK-OB-VS-31-S2) were sent to a laboratory for consolidation testing. The laboratory measured a hydraulic conductivity of 4.6×10^{-10} and 3.5×10^{-10} m/s respectively (SRK, 2009a). Table 1 summarizes the estimated properties of the lake bed sediments.

Table 1: Hydraulic Conductivity of Doris Lake Bed Sediments

Type	Number of Tests	Average Thickness (m)	Hydraulic Conductivity Geometric Mean (m/s)
Soft lake bed sediments	28	17	1×10^{-8}
Indurated lake bed sediments	2	3	4×10^{-10}

Storativity (or specific storage), influences the “drainability” of surficial material. There are no site specific overburden storativity value measurements. A value of 1×10^{-4} m⁻¹ is assumed based on scientific literature (Singhal and Gupta, 2010).

3.2.3 Fractured Rock

Frozen fractured rock is assumed to be completely impermeable, while unfrozen fractured rock is permeable. The 53 tests performed at Boston, Madrid South and Madrid North show K values are low, ranging between 1×10^{-11} and 9×10^{-7} m/s, with a geomean of 3×10^{-9} m/s (Figure 13). The only visible trend in the dataset is the progressive decrease in K with increasing depth (Figure 14), which is a reasonable relationship considering that fractures tend to close with depths. There has been no other trend identified. The spatial distribution of K values does not show a particular pattern and there is no strong relationship established between K and lithology (Figure 15) nor K and the presence of geologic structures (i.e., fractures and faults; Figure 16).

Four tests reported a K value above 1×10^{-7} m/s, between depths of 70 and 140 mbgs, all located within the Madrid South deposit. The details of these tests are provided below:

- At 11PSD269, between 105 and 150 mbgs, K was measured at 6×10^{-7} m/s. The drillers recorded a loss of return at 137 madh (meter along drillhole), and the geotechnical log the presence of a shear zone at 138 madh;
- At 11PSD276, between 60 and 85 mbgs, K was measured at 9×10^{-7} m/s. The core along the test interval showed no obvious weak zone; there was no major structure identified and the number of joints and fractures was low (fracture frequency = 0.3 per m); and
- 11PSD284 2, between 70 and 95 mbgs. K was measured at 3×10^{-7} m/s. The core along the test interval showed no obvious weak zone; there was no major structure identified and the number of joints and fractures was low (fracture frequency = 0.7 per m).

An analysis of fracture distribution was conducted for each deposit. Two dominant fracture sets were defined based on stereonet along with various other non-systematic fractures. The first fracture set occurs at a near vertical dip and strikes approximately north-south. The second fracture set is perpendicular to the dominant foliation with a near horizontal dip. There is no established relationship between K and the discontinuities frequency (Figure 16).

The specific hydraulic tests that intersected geological structures (i.e., dyke contact, major structure or fault) and/or the Deformation Zone at the Boston or Madrid Site are listed in Table 2. There is no evidence of higher K features associated with geological structures.

Table 2: Specific hydraulic tests that intersected geological structures

ID	Test #	Test Interval (mabh)	K (m/s)
08PMD668	Test#1	165.3 to 176.0	1.0×10^{-9}
08PMD671	Test#1	160.3 to 275.0	1.0×10^{-10}
08PMD650	Test#1	32.0 to 36.0	2.5×10^{-10}
08PMD650	Test#2	99.0 to 111.0	4.5×10^{-9}
08PMD657a	Test#1	92.2 to 131.0	4.7×10^{-10}
08PMD657a	Test#2	123.2 to 179.0	3.2×10^{-10}
08PMD657a	Test#3	179.2 to 241.0	3.3×10^{-10}
08PSD142	Test#2	156.0 to 182.0	6.5×10^{-8}
08PSD143B	Test#1	240.2 to 293.0	6.8×10^{-10}
08SBD382	Test#2	276.3 to 290.0	1.8×10^{-9}
08SBD383	Test#1	195.3 to 242.0	3.7×10^{-10}
10WBW003	Test#3	246.4 to 293.2	2.3×10^{-10}
10WBW004	Test#2	75.2 to 125.0	3.8×10^{-11}
10WBW004	Test#3	123.2 to 182.0	9.7×10^{-9}
10WBW004	Test#4	180.2 to 242.0	5.1×10^{-10}
11PSD267	Test#1	101.0 to 152.0	2.2×10^{-9}

While no structures have been identified to promote high K, the presence of such features cannot be ruled out; therefore, hypothetical high K structures have been considered when modeling groundwater flow (Section 5.4). On Figure 14, the black dashed line represents a simplified K function based on the moving geometric mean of the entire dataset, and the red dashed line represents a K function based on the moving arithmetic mean. The first function will be used for the “base case” model scenario, while the second will be used to test the model sensitivity to higher fractured rock K and vertical anisotropy (vertical fractures connected to lakes). A third dashed line in orange represents the highest K value reported for the Project at the Doris Mine (geomean of 3×10^{-6} m/s estimated from the 14-hour injection test in drillhole 11TDD769). Although the geological setting at Doris differs from Boston, Madrid South and Madrid North, it will be used to test the model sensitivity to hypothetical high flow conduits.

A bedrock storativity of 3×10^{-7} m⁻¹ was estimated from the extended duration test performed at the Doris site; i.e., 14-hour injection tests performed within drillhole 11TDD769, monitored in all 12 zones of the Doris Central Westbay Well 10WBW001 (SRK 2009d, 2014a).

3.3 Water Level

The lake and groundwater level measurements suggest the groundwater table is near the lake surface, which supports the interpretation that the groundwater system in open taliks and subpermafrost is controlled by lake levels.

Level measurements in Westbay wells and vibrating wire piezometers (VWP) for Boston, Madrid South and Madrid North are compiled in Table 3 and Table 4; the water levels collected for hydraulic conductivity testing are not reported because these are influenced by drilling and not representative of in-situ groundwater conditions. The pore pressure is expressed as head (in masl), corrected from the average groundwater density measured in laboratory from the Westbay well groundwater samples. Since the density varied between 1.00 and 1.03 kg/m³; the degree of accuracy on the head measurements are ± 7 m, which corresponds to a variation in density of ± 0.015 kg/m³. With such degree of accuracy, VWP data cannot be used to estimate the vertical hydraulic gradients between the lake head and the VWPs.

Table 3: Lake Level and Pore Pressure Measurements at Boston

ID	Type	Date	Water Level/ Head (masl)	Vertical Depth of sensors or Vertical depth interval of zones (m)
Aimakatalok Lake	Lake level	-	65.6 masl	Na
Stickleback Lake	Lake level	-	69.6 masl	Na
08SBD380 ⁽¹⁾	Pore pressure	Dec. 11, 2008	89.4 masl (Zone #12)	283.0
08SBD381A	Pore pressure	Dec. 11, 2008	60.0 masl (Zone #12)	400.5
08SBD382	Pore pressure	Dec. 11, 2008	63.0 masl (Zone #12)	403.4
10WBW004	Pore pressure	Sept. 14, 2011	56.2 masl (Zone #10) ^{Fz} 64.0 masl (Zone #9) ^{Fz} 66.4 masl (Zone #8) ^{Fz} 67.9 masl (Zone #7) 67.8 masl (Zone #6) 67.6 masl (Zone #5) 68.4 masl (Zone #4) 69.2 masl (Zone #3) 70.4 masl (Zone #2) 69.9 masl (Zone #1)	22.8 to 110.9 m 112.3 to 201.8 m 203.2 to 239.0 m 240.3 to 270.2 m 271.5 to 282.3 m 283.7 to 299.9 m 301.3 to 330.7 m 332.0 to 373.8 m 375.0 to 400.5 m 401.8 to 421.0 m

Notes:

1. Na, not applicable
2. FZ, Temperature in Zone <- 2 deg C. Heads likely affected by freezing conditions and not considered in the dataset 1, The level indicated by this VWP is much higher than any lake levels at this site and the nine VWP sensors installed close-by. This data is considered an outlier and dismissed from the dataset because there is no rational reason for this value.

Table 4: Lake Level and Pore Pressure Measurements at Madrid South and Madrid North

ID	Type	Date	Head (masl)	Depth of sensors or depth interval of zones (m)
Imniagut Lake	Lake level	-	27.5 masl	Na
Patch Lake	Lake level	-	25.8 masl	Na
Windy Lake	Lake level	-	18.1 masl	Na
Wolverine Lake	Lake level	-	32.1 masl	Na
08PMD669	VWP	Oct. 13, 2008	33.3 masl (Zone #12)	533.5
08PSD144	VWP	Oct. 13, 2008	23.1 masl (Zone #12)	353.0

Na = not applicable

3.4 Groundwater Quality

3.4.1 Regional Subpermafrost Groundwater Quality Data

A dataset of groundwater Total Dissolved Solids (TDS) concentrations sampled across the Canadian Shield was compiled and plotted against depth in Figure 17. The dataset regroup TDS concentrations published by Frape & Fritz (1987) and public data reported at the following mine projects: Back River (Rescan ERM, 2015), Lupin (Stotler et al, 2009), Meadow Bank (Cumberland Resources, 2005), Meliadine (Golder, 2013), Snap Lake (De Beers, 2002), Ekati (Golder, 2014), Gahcho Kue (De Beers, 2010), and Jay (Golder, 2014).

The distribution of TDS concentrations with depth shows that brackish to hypersaline water is commonly observed in permafrost environments and salinity (TDS) generally increases with depth. Concentrations on the scale of tens of grams per litre have been measured at depths of 500 mbgs, beneath continuous permafrost. The occurrence of very old, brine water in a number of places on the Canadian Precambrian Shield suggests that these deep flow systems are very sluggish and slow moving under natural conditions (i.e., pre-mining) (Frape and Fritz, 1987).

Gascoyne (2003) reported several potential sources of salinity. The potential sources are (1) rock-water interactions, including reactions with rock matrix minerals and fracture-filling minerals, (2) soluble salts present at grain boundaries and in fluid inclusions, (3) residual saline hydrothermal fluids, and (4) marine fluids (possibly more saline than present) or basinal brines that entered the rock during ancient times, pre-glacial in origin (Gascoyne, 2003). Furthermore, in situ cryogenic concentration due to ice and methane hydrate formation may have concentrated the remaining fluids, as noted for the Lupin Mine (Stotler, 2009).

3.4.2 Hope Bay Subpermafrost Groundwater Quality Data

Groundwater samples were collected at Doris from Westbay wells 10WBW001 and 10WBW002, at Madrid from drillhole 08PMD657a, and at Boston from Westbay well 10WBW004. The samples collected at 10WBW002 and 08PMD657a were not considered to be representative of true formation water because purging could not be performed adequately (i.e., the 10WBW002 sampling interval was characterized by low K, and the sample collected in 08PMD657a was a “grab” sample collected using the wireline swabbing method during drilling).

The samples were analyzed for standard parameters (conductivity, pH, etc.), cations (chloride, sulphate, etc.), total and dissolved metals. In addition, stable isotopes (O and H) were analyzed to provide improved quality assurance and quality control (QA/QC) on well purging and development, as well as to assess potential variation in water source types. 10WBW001 (i.e., Doris) and 10WBW004 (i.e., Boston) indicated comparable chemistry, but the samples collected at 10WBW001 are considered to be the most representative of true formation water with respect to development and purging (SRK 2012, 2014a). The rationale for using Doris groundwater samples is driven by the extreme difficulty of obtaining good quality groundwater quality samples in a low K and frozen environment that would be representative of the true formation water. It is recognized that there could be slight differences of metal concentrations in groundwater; however salinity is not expected to differ between the sites because it is not a function of the mineralogical make-up.

The 75th percentile concentration from post-purging samples collected in zones 1, 6 and 10 of Westbay Well 10WBW001 are presented in Table 5. The sample results suggest that the water encountered during mining, at least initially, will be saline dominated by chloride, and that salinity will likely vary with depth. The groundwater quality results were compared to the following environmental guidelines: Canadian Council of Ministers of the Environment (CCME) water quality guidelines for freshwater, irrigation, livestock, and marine (CCME, 2015) and the Metal Mining Effluent Regulations (MMER) limits for deleterious substances (MMER, 2015).

Table 5: Groundwater Quality (10WBW001) under Doris Lake

Parameters		Units	75th Percentile [n= 19 to 29 ⁽¹⁾]	MMER and CCME Guidelines
Field Parameters	pH	pH units	7.73	6.0 - 9.5 ^{a1, a2}
	Electrical Conductivity (EC)	µS/cm	52,650	na
	Dissolved Oxygen (DO)	mg/L	11.37	na
	Salinity	%	31.86	na
	Oxidation-Reduction Potential (ORP)	mV	20.5	na
Lab Physical Parameters	EC	µS/cm	48,500	na
	Density	kg/m³	1.03	na
	pH	pH units	7.63	6.0 - 9.5 ^{a1, a2}
	Total Dissolved Solids (gravimetric)	mg/L	40,800	3,000 ^e
Anions and Nutrients	Alkalinity, Total (as CaCO ₃)	mg/L	93.7	na
	Ammonia as N	mg/L	3.5	1.04-15.3 ^{b2,F}
	Chloride (Cl)	mg/L	19,000	640 ^{b1} , 120 ^{b2} , 110 ^d
	Sulfate (SO ₄)	mg/L	2,000	1,000 ^e
Dissolved Metals	Aluminum (Al)	mg/L	0.005	0.1 ^{b2} , 5 ^{d,e}
	Arsenic (As)	mg/L	0.0025	0.5 ^{a1} , 1 ^{a2} , 0.005 ^{b2} , 0.0125 ^{c2} , 0.1 ^d
	Boron (B)	mg/L	3.24	29 ^{a1} , 1.5 ^{a2} , 0.5 ^d
	Cadmium (Cd)	mg/L	0.00012	0.0086-0.0124 ^{b1,A} , 0.0020-0.0027 ^{b2,A} , 0.0051 ^{c2} , 0.0051 ^d , 0.080 ^e
	Calcium (Ca)	mg/L	2050	na
	Chromium (Cr)	mg/L	0.0005	0.001 to 0.0089 ^B
	Cobalt (Co)	mg/L	0.00019	0.05 ^d , 1 ^e
	Copper (Cu)	mg/L	0.00064	0.3 ^{a1} , 0.6 ^{a2} , 0.002 ^{b2,C} , 0.2-1.0 ^d , 0.5-1.0 ^e
	Iron (Fe)	mg/L	4.81	0.3 ^{b2} , 5 ^d
	Fluoride (F)	mg/L	0.75	0.12 ^{b2} , 1 ^d
	Lead (Pb)	mg/L	0.0003	0.2 ^{a1} , 0.4 ^{a2} , 0.001-0.0018 ^{b2,D} , 0.2 ^d , 0.1 ^e
	Lithium (Li)	mg/L	0.35	2.5 ^d
	Magnesium (Mg)	mg/L	1,370	na
	Manganese (Mn)	mg/L	1.75	0.2 ^d
	Mercury (Hg)	mg/L	0.00005	0.000026 ^{b2} , 0.000016 ^{c2} , 0.003 ^e
	Molybdenum (Mo)	mg/L	0.0187	0.073 ^{b2} , 0.01 ^d , 0.5 ^e
	Nickel (Ni)	mg/L	0.0014	0.5 ^{a1} , 1 ^{a2} , 0.025-0.068 ^{b2,E} , 0.2 ^d , 1 ^e
	Potassium (K)	mg/L	245	na
	Selenium (Se)	mg/L	0.002	0.001 ^{b2} , 0.02 ^d , 0.05 ^e
	Sodium (Na)	mg/L	8,980	na
	Strontium (Sr)	mg/L	27.6	na
	Uranium (U)	mg/L	0.00006	0.033 ^{b1} , 0.015 ^{b2} , 0.01 ^d , 0.2 ^e
	Zinc (Zn)	mg/L	0.157	0.5 ^{a1} , 1 ^{a2} , 0.03 ^{b2} , 5 ^d , 50 ^e

Source: \\IVAN-SVR0\Projects\01_SITES\Hope.Bay\IProject_Data (Not Job Specific)\04 Groundwater Chemistry\MASTER WQ Database\IMASTER Hope Bay Water Chemistry DB_jm_ja_spb Rev16.xlsx

- Notes:
- 1

n, count of values used to calculate statistics. Statistics were calculated by assuming that all values below detection limit were at the detection limit. Some samples taken early in the program had high detection limits and were therefore excluded from the statistical summary.
- a1

MMER Maximum authorized monthly mean concentration
- a2

MMER Maximum authorized concentration in a grab sample
- b1

CCME Freshwater (Short term)
- b2

CCME Freshwater (Long term)
- c1

CCME Marine (Short term)
- c2

CCME Marine (Long term)
- d

CCME Irrigation
- e

CCME Livestock
- A

Cadmium short term guideline concentration = $10^{[1.016(\log[\text{hardness}])-1.71]}$ µg/L for hardness ≥5.3 and ≤360 mg/L and the long term guideline = $10^{[0.83(\log[\text{hardness}])-2.46]}$ µg/L for hardness ≥17 to ≤280 mg/L
- B

Chromium Hexavalent 0.001 mg/L and Chromium Trivalent 0.0089 mg/L
- C

Copper guideline concentration = $0.2 \cdot e^{(0.8545[\ln(\text{hardness}))-1.465]}$ µg/L for hardness ≥82 to ≤180 mg/L and for hardness <82 mg/L a concentration of 2 µg/L applies
- D.

Lead guideline concentration = $e^{(1.273[\ln(\text{hardness}))-4.705]}$ µg/L for hardness
- E.

Nickel guideline concentration = $e^{(0.76[\ln(\text{hardness}))-1.06]}$ µg/L for hardness >60 to ≤80 mg/L and for hardness ≤60 mg/L a concentration of 25 µg/L applies
- F

Total ammonia guideline pH and temperature dependent

Based on this comparison, ammonia, boron, cadmium, chloride, fluoride, iron, manganese, molybdenum, mercury, nickel, selenium, sulfate and zinc are considered as the potential constituents of concern because concentrations are above the guideline recommendations.

Chloride is the only constituents of concern that shows a correlation with depth. Figure 18 shows the observed and modeled vertical profile for chloride concentrations. Chloride concentrations and TDS correlates well ($r^2 = 0.97$); therefore, chloride can be used to estimate TDS using the linear relationship: $[\text{Chloride}] = 0.6 \times [\text{TDS}]$. This function was estimated using the groundwater quality samples collected at 10WBW001 and 10WBW002. Figure 19 plots the observations and the linear regression curve.

3.5 Permafrost Extent

3.5.1 Freezing Point Depression

Based on measured concentrations of dominant parameters, saline water is considered to induce a freezing point depression. Table 6 summarizes calculated freezing point depression based on the most reliable groundwater quality observed at the Project site. These results suggest that water will freeze at a temperature of -2°C .

Table 6: Isotherm Depression Estimates based on Water Samples from 10WBW001

Sample Name		10WBW001 – Zone 1 (548 m)	10WBW001 – Zone 6 (246 m)	10WBW001 – Zone 10 (63 m)
Parameter	Units			
Alkalinity	mg/L	2.0	44.2	49.7
Calcium	mg/L	4,960	749	1,010
Magnesium	mg/L	69.5	702	849
Potassium	mg/L	39	117	160
Sodium	mg/L	7,290	4,130	5,400
Chloride	mg/L	1,900	9,130	11,500
Sulphate	mg/L	981	940	1,160
Calculated Salinity	%	3.2	1.6	2.0
Calculated Theoretical Freezing Point	$^{\circ}\text{C}$	-1.9	-0.9	-1.2

Source: P:\01_SITES\Hope.Bay\1CH008.054_2011 Stage 2 Geotech-Hydro\070_Reporting\Stage 2 Doris Geotech Hydro Report\020_Tables\Hydrogeo Tables\freezing_point_depression_1CH008.054_101811_jm_rev01.xlsx Mapping of the Lake Taliks and Base of Permafrost

A talik is defined as “a layer or body of unfrozen ground occurring in a permafrost area due to local anomalies in thermal, hydrological, hydrogeological or hydrochemical conditions” (Van Everdingen, 2005). In most cases, taliks are formed by lakes and other water bodies which cause a local departure in terrestrial ground temperature (Smith and Hwang, 1973; Burn, 2002). Taliks can be closed or open. A closed talik is an unfrozen zone beneath a water body that is enclosed at the base and the surrounding sides by permafrost; and an open talik is an unfrozen zone beneath a water body that penetrates the permafrost completely and may connect suprapermfrost (i.e., the layer of ground above permafrost) and subpermafrost (i.e., the non-frozen ground below the permafrost) groundwater.

Key factors influencing talik configuration include water bottom temperature, lake size (half width or radius), present and past ground thermal regime, and long-term changes to the landscape. Taliks are transient features. Present-day water bathymetry can affect talik configuration where shallow water allows for ice to seasonally freeze to the bottom (bottom-fast ice) and conduct heat from the ground (Burn, 2002, 2005; Stevens, 2010a, 2010b). The long-term thermal and physical evolution of the landscape is a factor in the present-day configuration of taliks that extend hundreds of metres below the surface. Lunardini (1995) showed temperature at depths up to 600 mbgs can be influenced by surface temperatures as far back as 100,000 years.

Ground temperatures were measured with shallow and deep thermistors. The ground temperature data are presented below:

- At Boston (Figure 9), deep ground temperature measurements have been collected from three deep inclined wells, which extended beneath Aimakatalok Lake (08SBD381A, 08SBD382, 10WBW004, and two inland wells (08SBD380 and 97NOD176):
 - At 08SBD382, the -2°C isotherm was up to 115 m from the shoreline of Aimakatalok Lake, and located at a depth of 224 mbgs. At 08SBD381A and 10WBW004, it was 17 and 42 m from shore and located at a depth between 202 and 209 mbgs. The offshore position of the -2°C isotherm cannot be explained by the present-day lake configuration nor by lateral heat flow from the adjacent land. Therefore, it is postulated that the permafrost beneath Aimakatalok Lake has been submerged with lake expansion.
 - At 08SBD380 and 97NOD176, the ground temperature has been measured to a maximum depth of 241 mbgs and 247 mbgs, respectively. The base of permafrost is not directly intercepted by these wells and the lowermost thermistor nodes indicate relatively cold permafrost temperatures (-5.1°C at 08SBD380 and -5.5°C at 97NOD176).
- At Madrid South and Madrid North (Figure 11 and 12), deep ground temperature measurements have been collected from three inclined wells (08PMD669, 08PSD144, and TM00141):
 - Well 08PSD144 is located beneath an island centred within Patch Lake. Ground temperature measurements at this site indicate relatively shallow permafrost beneath the island (base of permafrost 78 mbgs) due to the surrounding heat from the lake.
 - Well 08PMD669 is located within the area of the Madrid North underground mine workings and is instrumented to a maximum depth of 474 mbgs. The base of permafrost is 570 mbgs at this location.
 - Well TM00141 is located within the Madrid South underground mine between Wolverine Lake and Patch Lake. The well extends toward Patch Lake. Ground temperature measured from lowermost thermistor node is -2.6°C at 225 mbgs. The projected base of permafrost is 346 mbgs, intercepting the talik at the edge of the Patch Lake.

SRK used these field observations to conduct thermal analyses that assessed where through talik occurred on a regional scale, and predicted the configuration of open taliks on a local scale. The critical lake dimensions required for open talik to exist were assessed using a one-dimensional (1D) steady state analytical model. The detailed configurations of the open taliks adjacent to the Boston, Madrid South and Madrid North underground mining areas were estimated using 2D thermal modeling, then extrapolated to obtain 3D surfaces. The details of these analyses are described in Appendix A.

3.5.2 Regional Talik Model

For the base case scenario, three criteria were used to identify, on a regional scale, the lakes potentially supporting open taliks: the diameter of circular lakes, the width of elongated lakes, and the depth of the lakes. Open taliks were estimated to occur:

- Beneath circular lakes with a diameter >224 m (i.e., lake radius of >112 m) or beneath elongated lakes with a width of at least 104 m wide (i.e., lake half-width >52 m); and
- In lakes deeper than 1.3 m (i.e., two-thirds of the mean annual ice thickness) to avoid freezing to the bottom. If the bathymetry of a lake was not known, by default, the lake was considered to be deeper than 1.3 m.

Figure 20 shows a map of the potential through taliks at the Boston and Madrid areas based on the estimated critical lake dimensions. It can be noted that additional small lakes would be expected to have through taliks if warmer permafrost (i.e., permafrost temperature up to -5°C) was present. This scenario was not considered for the analysis as there is no evidence of warmer permafrost on site; furthermore, this would not be expected to modify the groundwater model predictions because these small lakes would all be outside of the hydrogeology model domain.

3.5.3 Site-specific Talik Model

For Boston, four 2D model sections were setup to simulate possible expansion of Aimakatalok Lake and to allow for talik adjustment to closely fit to the equivalent isotherm measured at 08SBD381A, 08SBD382, and 10WBW004. Figure 21 shows the estimated 3-dimensional permafrost solid and how it intercepts the 2016 resources (TMAC 2016c). The analyses show that the Boston mine will remain in permafrost.

For Madrid South and Madrid North, four and five thermal 2D model sections were setup respectively to estimate the distribution of permafrost at depth; lake expansion was not considered because it is not supported by ground temperature data. Figures 22 and 23 show the estimated 3-dimensional permafrost solids and how they intercept the 2016 resources (TMAC, 2016c). The analyses show that the Madrid South mine will intercept unfrozen ground at the edge of the open taliks formed by the Wolverine Lake and Patch Lake. At Madrid North, the Suluk and Rand zones will be mined in the open talik formed by Patch Lake, and the Naartok zone will pierce through the base of permafrost at a depth of about 430 mbgs.

These results are considered conservative since the -2°C isotherm model fit underestimates the depth of the talik compared to site ground temperatures.

4 Hydrogeological Modeling Approach

4.1 Conceptual Groundwater Model

4.1.1 Flow System

Figure 24 illustrates the hydrogeological conceptual model. The system for the entire region is considered as a low flux, lake-dominated flow system. Regional flow is primarily controlled by the presence of unfrozen zones in open-talik beneath large lakes. Away from lakes, the permafrost is widespread, deep, and considered to be essentially impermeable.

4.1.2 Open Talik Properties

At the local scale, bedrock K is fracture-controlled, comprised of a low bulk K background system intersected by distributed, relatively high K fractures and geologic structures. At the scale of the open-talik, the fractured rocks can be considered as a single unit, without distinction between lithologies, characterized by a relatively higher K at shallow depths, gradually decreasing with depth as confining pressure increases. For the overburden, observations showed that a differentiation exists between K in the lake bed sediments and the shallow fractured rock. The clay present at the bottom of the lake are characterized by a low K.

Based on the site-specific K data, the K in fractured rock and lake sediments falls within the bound of published K values, as shown in Figure 25.

4.1.3 Groundwater Quality

Deep groundwater is connate, meaning old, or emplaced when sediments were originally deposited. This connate water is highly saline and can have elevated concentrations of major ions and metals. The concentrations of calcium, chloride and sodium are high and show a general trend of increasing concentration with depth. Other constituents can also have relatively high concentrations, but do not correlate with depth. When looking at the potential discharge of groundwater to the environment, the constituents of concern are dissolved ammonia, boron, cadmium, chloride, fluoride, iron, manganese, molybdenum, mercury, nickel, selenium, sulfate and zinc.

Once mine inflow starts, constituents will come from the following sources: the lakes above the mine workings, and the groundwater contained within the unfrozen fractured rock, i.e., in an open talik or in the subpermafrost. The lakes will supply a constant source of fresh water and the subpermafrost a constant source of saline water. The groundwater concentrations for most constituents will be constant with depth, excepted for chloride which increases with depth.

4.1.4 Mine Interactions with Groundwater

The Madrid-Boston mine plan assumes that Boston's underground development and mining will be limited to the volumes of the 2016 resource encapsulated in permafrost, hence the Boston Mine will not intercept groundwater and groundwater inflow is not modeled. Measures such as pilot drilling and risk zone mapping, as undertaken at Doris, will be used to ensure mining stays within the permafrost zone.

At the Madrid North and Madrid South mines, development and mining will access the entire resource volume; therefore, the mines will potentially intercept unfrozen ground associated with open talik or subpermafrost. Table 7 presents an estimation of the mine volumes within and outside permafrost for each mine.

Table 7: Mine Volumes within and Outside Permafrost

Mine	Volume total m ³	Volume within Permafrost		Volume outside Permafrost	
		m ³	%	m ³	%
Boston Mine	1,890,370	1,890,370	100%	None	0 %
Madrid North Mine	10,447,517	4,504,317	43%	5,943,200	57%
Madrid South Mine	859,519	133,667	16%	725,852	84%

4.2 Numerical Groundwater Models

4.2.1 Software and Model Type

Numerical groundwater modeling has been completed using the modeling software FEFLOW v6.2 (P11) (DHI, 2015). FEFLOW is a professional software package for modeling fluid flow and transport of dissolved constituents and/or heat transport processes in the subsurface. This program is used extensively for mining groundwater projects around the world.

4.2.2 Model Assumptions

The model assumptions are:

- Steady state to define current conditions;
- Transient to predict mine inflow rates and quality;
- 3D saturated media within a confined aquifer;
- Groundwater density does not vary;
- Bedrock is simulated as an equivalent porous media. Use of a fracture network model is not justified for a model of this scale and scope; and
- Homogeneous and anisotropic hydraulic conductivity.

4.2.3 Model Designs

Two numerical models were developed; one for Madrid South and one for Madrid North. The two mines were modeled separately to constrain the domains and meshes to a reasonable size.

Table 8 summarizes the model parameters for each numerical model. Figure 26 shows the model domain footprints and provides additional details on the boundary conditions assigned along the external faces of the models. Figures 27 and 28 present 3D views of the Madrid North and Madrid South models, respectively.

Table 8: Groundwater Model Parameters

	Madrid North	Madrid South
Model Domain	Lateral extent defined by the anticipated flow conditions between open taliks (Figure 26).	
	Total area 6.92 km ² . Approximately 2,800 m from north to south and 2,500 m from east to west. Top surface ranging between 19 and 84 masl. Base of the model at -1,500 masl.	Total area 2.80 km ² . Approximately 1,400 m from north to south and 2,000 m from east to west. Top surface ranging between 26 and 61 masl. Base of the model at -1,130 masl.
Model Mesh	69 layers. 22,563 elements per layer.	79 layers. 21,966 elements per layer.
	Layer thickness ranging between 3 and 400 m: <ul style="list-style-type: none"> • Soft Lake bed sediment: 17 m • Indurated lake bed sediment: 3 m • Volcanic rock: 10 m thickness down to -620 masl for the Madrid North model and to -760 masl for the Madrid South model, then gradually increasing up to 400 m thickness down to the base of the models 	
	Average element size 25 m refined to approximately 10 m at and around the underground footprints.	
Hydraulic Conductivities	The hydraulic conductivities of the lake sediments and volcanic rocks are assigned with functions of K with depths, as indicated in Figure 14 (Section 3.2.3).	
Specific Storage	The storage compressibility value for the lake bed sediments is $1 \times 10^{-4} \text{ m}^{-1}$ and for the rock $3 \times 10^{-7} \text{ m}^{-1}$. The first value is reasonable for loose sediments. The second value was estimated from the extended duration test.	
Mass Transport Properties	The mass transport model assumes an effective porosity the fractured rock of 0.1%, a longitudinal dispersivity of 30 m and transverse dispersivity of 10 m. These were estimated based on literature values for fractured rock from Singhal and Gupta (2010).	
Boundary Conditions	<u>Top slice:</u> Lakes are assigned with two types of conditions, a constant head equal to the lake elevation, and a constant mass equal to the chloride concentration of the lake.	
	Madrid North: Patch: 25.8 masl, Imniagut: 27.5 masl, and 68.5 mg/L of chloride (measured average).	Madrid South: Patch: 25.8 masl, Wolverine: 32.1 masl and 68.5 mg/L of chloride (measured average).
	<u>Bottom slice:</u> There is no movement of groundwater (no flow).	
	<u>External boundaries:</u> For flow, fluid transfer boundary condition ⁽¹⁾ and No Flow as shown in Figure 26. For mass, a constant mass boundary condition (chloride concentration) is assigned to the nodes located in open talik or in subpermafrost. The concentration at each node is calculated based on the Cl-depth relationship presented in Figure 18 (Section 3.4.2).	
	<u>Internal boundaries:</u> Underground development are represented by the volumes of the resource wireframes (TMAC 2016c) and by the 3D workings of the PFS mine design (TMAC 2015b). Developments are assigned with seepage face conditions. Seepage faces allow water to exit the model (flow into underground areas), but water cannot enter the groundwater system. These conditions are activated sequentially over time (Section 4.2.5).	
Initial Head Conditions	The initial head conditions (i.e., current conditions) are calculated from the respective models under steady state conditions. Head contours map are presented in Figure 29 and 30 (Section 5.1).	
Initial Chloride Conditions	The Initial chloride concentrations are assigned through the model domain according to the Cl-depth relationship presented in Figure 18 (Section 3.4.2).	

¹ The fluid transfer (type 3) boundary conditions (BC) are constrained by the physical locations (i.e., distance) of open taliks surrounding the two mine sites and the heads (i.e., lake levels) associated with these taliks. They were defined based on the color scale map shown on Figure 26, which represents an interpolated surface of the heads between open taliks. The fluid transfer BC allowed keeping the model size reasonable while representing the large scale flow system.

4.2.4 Model Calibration

The model calibration is controlled by boundary conditions of the lakes thus predicting heads which are near lake levels. This is consistent with site observations showing head levels at or near the lake surfaces. The observed and predicted hydraulic heads at 08PMD669 are 33.3 and 24.7 masl respectively. The observed hydraulic heads at 08PSD144 cannot be compared to predictions as it is located outside the model domain. The uncertainty with respect to model parameter values was addressed through uncertainty analysis via testing a plausible range of parameter values.

4.2.5 Model Simulations

Each groundwater model simulates the progressive excavation of the mines according to a time step function implemented on a 30-day time step. This function activates the seepage nodes assuming a constant descent rate of 1.5 m in vertical height per day from the start of mining until the bottom of the resource has been reached; then the development areas remain activated for the full duration of mining as indicated by TMAC's production schedule (TMAC, 2016b).

SRK used the prefeasibility mine plan schedule to guide the sequencing of the mining zones. At Madrid South, the Patch and Wolverine zones are excavated simultaneously. At Madrid North, the developments start at Naartok ($t = 0$ days), followed by Rand after 885 days, and then Suluk after 1265 days.

4.2.6 Model Sensitivity and Uncertainty Analysis

Multiple hypothetical scenarios were conducted to assess the sensitivity of model predictions to K values, storage values, the potential presence of fault conduits, lake sediment K, and lake elevations.

4.2.7 Limitations of the Groundwater Model

The following limitations should be considered when interpreting or using model results:

- The model has been constructed based on available data, but actual conditions may vary locally, due to local variations in K, water quality or ground temperature (permafrost distribution).
- Faults that act as significant flow conduits or flow barriers, in taliks and beneath the permafrost, could be present and not identified to date.

5 Modeling Results

5.1 Current Conditions

Figures 29 and 30 show the predictions of hydraulic head at Madrid North and Madrid South for the current conditions (steady state). The predicted flow rates are low, with a total flow (i.e., in or out of the respective model domains) of 1.9 m³/d for the Madrid North model, and 2.8 m³/d for the Madrid South model. The chloride concentration in groundwater is increasing with depth as shown in the vertical profile in Figure 18 (Section 3.4.2).

Table 9 reports the predictions at the nodes representing the respective water bodies above and around the proposed mines.

Table 9: Predicted Flow Rates at Nodes Representing Surface Water Bodies for Current Conditions

Lake	Model	Outflow Rate (Discharge to the lake) (m ³ /d)	Inflow Rate (Infiltration to the rock) (m ³ /d)
Imniagut Lake	Madrid North	0	0.80
Patch Lake	Madrid South	2.1	0
	Madrid North	1.0	0.03
Wolverine Lake	Madrid South	0.2	0.60
Windy Lake	Madrid North	0.4	0

5.2 Active Mining Conditions

5.2.1 Predicted Mine Inflows

Approach

The groundwater model assumes that, on the scale modeled, flow within the fractured bedrock media will approximately flow through an equivalent porous media. In fact, much of the mine area is likely to have no inflow, with areas of inflow constrained to discrete, bedding-controlled or structurally affected areas.

The base case model uses SRK's best estimate of the site specific hydrogeological parameters. The fractured rock K is assigned based on the moving geometric mean function of K with depth (i.e., black dashed line in Figure 14); the same function is used to allocate K values to the Madrid North and Madrid South models. No preferential directions or inclinations of discontinuities are accounted in the base case model since there was no relationship established between K and the discontinuities.

The potential influence of higher K fractured rock and geological structures were assessed with sensitivity scenarios presented in Section 5.4. These include a scenario with K based on a moving arithmetic mean function of K with depth (i.e., red dashed line in Figure 14), with a high K along the vertical axis as a mean to assess the potential influence of steeply dipping permeable geological structures, and with hypothetical high K structures intersecting the mines.

Hydraulic Heads and Mine Inflows

Figures 31 and 32 present plan view maps and cross sections of hydraulic head from transient modelling at the time of pre-mining and maximum drawdown, at Madrid North and Madrid South respectively. Figure 33 presents the predicted inflow rates for the Madrid North and Madrid South mines, while Figure 34 shows the predicted infiltration rates at Patch Lake, Wolverine Lake, Windy Lake and Imniagut Lake (the infiltration rates account for active dewatering in both mines). Figure 35 presents mixing ratios over time between groundwater and lake water.

At Madrid North, mining in open talik starts in Year 4 (May 2020), 17 months after development started. The simulation predicts that mine inflow will increase gradually until Year 7 (October 2023), and remain stable at 1,180 m³/day. At Madrid South, mining in open talik starts in Year 13 (June 2029), six months after development started. The simulation predicts that mine inflow will increase gradually until Year 14 (November 2030), and remain stable at 550 m³/day.

Mine inflows draw from water stored in the rock (storage) and from the lakes. The contributions for each of these sources are predicted to vary over time. At the early stage, inflow is primarily from storage, but is quickly replaced by the inputs from the lakes primarily from Patch Lake and Wolverine Lake located directly above the two proposed mines. The proportions between these two sources are relatively stable once the influence of storage has stabilized, with inflows consisting of about 96% lake water to 4% deep groundwater at Madrid North, and 90% lake water to 10% deep groundwater at Madrid South.

The base case scenario predicts that the lakes' infiltration could peak as follows: 1,060 m³/day at Patch Lake, 185 m³/day at Wolverine Lake, 60 m³/day at Imniagut Lake and 15 m³/day at Windy Lake. To put these rates into perspective, the volumes and annual inflow (from precipitation and runoff) of the two primarily affected lake were estimated and compared to the maximum predicted annual infiltration, as shown in Table 10.

Table 10: Volume of Key Lakes, Annual Lake Inflow and Predicted Peak Annual Infiltration

Lake Name	Lake Volume (m ³)	Annual Inflow to Lakes (m ³)	Maximum Predicted Annual Infiltration (m ³)	Maximum Predicted Annual Infiltration compared to Total Lake Volume plus Annual Inflow to Lakes
Patch	23,366,304	2,010,000	498,225	2.0 %
Windy	58,694,064	830,000	5,475	0.009 %
Wolverine	1,929,650	290,000	67,525	3.0 %
Imniagut	328,325	20,000	21,900	6.3 %

5.2.2 Effects of Heated Underground Mining to Permafrost and Taliks

The heat circulated into the underground mines will generate a lateral thaw of the bedrock at some distance from the workings; this distance will be a function of the heated underground air temperature, the initial temperature of the bedrock at each depth, and the duration of time the heat source is applied.

Lateral thaw of permafrost from heated underground mining areas was estimated using a simplified one-dimensional analytical solution of temperature change for a given heat source and the bedrock thermal properties at the Project. The model assumed a constant heat source for the entire duration of mining operations and one-dimensional heat flow in the horizontal direction. Over time, the heat is transferred through the bedrock which contributes to thaw of the surrounding permafrost, with the rate of thaw decreasing with distance from the heat source. Table 11 summarizes expected lateral thaw of the permafrost from underground areas heat over a 4, 12, and 17-year period, corresponding to the respective years of active mining at the Madrid South, Boston and Madrid North mines. The initial bedrock temperatures of -8°C and -4°C represent reasonable end-member ground temperatures measured at the underground mining areas.

Table 11: Lateral Permafrost Thaw from Heated Air in Underground Mining Areas

Heated air temperature (°C)	Initial Bedrock Temperature (°C)	Horizontal Thaw from Underground (m)		
		Year 4	Year 12	Year 17
10	-8	18	32	38
10	-4	28	47	57
5	-8	14	24	29
5	-4	23	40	48

Notes:

1. Horizontal thaw based on -2°C isotherm, with a constant heat source
2. Initial bedrock temperature based on representative end-members measured at the Property

The analysis shows lateral thaw will potentially range between 14 and 28 m after 4 years, 24 to 47 after 12 years, and 29 to 57 m after 17 years. Based on these results, the effects of underground heating on permafrost will be limited. The heat will increase the volume of unfrozen ground around the mines, but it will not generate new open taliks that connects the ground surface to subpermafrost.

5.2.3 Mine Inflow Benchmarking

SRK researched groundwater inflow measurements reported by closed or operating mines located in continuous permafrost environments to benchmark the inflow predictions estimated for the Doris, Madrid North and Madrid South mines. The available public data are limited. SRK obtained useful public information on measured mine inflows for three operating mines located in the Northwest Territories: Diavik (Golder 2008a, 2008b), Ekati (Klohn Crippen 2001, 2004, 2005 and 2006; Golder 2014), and Snap Lake (Beale, 2014; Golder, 2014; Kuchling, 2000; Itasca, 2013). No information was found for closed mines such as Polaris, Nanisivik, and Rankin Inlet.

The Ekati and Diavik mines are operating open pit and underground diamond mines that started respectively in 1997 and 2001. The Snap Lake mine is an underground diamond mine that started in 2004 and stopped operating in 2016. Background information related to the hydrogeological system for each of these mines is provided below.

Ekati Mine

Hydrogeologic conditions for the Ekati mine, NT, are summarized as follows:

- Dewatering data exists for six mines at four sites: the Panda and the Koala open pits and underground mines, the Fox pit mine and the Misery pit mine.
- These mines are situated in open taliks with the respective lakes dewatered prior to mining. Permafrost is estimated to extend down to 320 to 485 mbgs.
- The competent granitic country rock at the Ekati mine site, which comprises a majority of the rock domain, is described as generally low hydraulic conductivity, between 1×10^{-9} and 1×10^{-7} m/s and decreasing with depth.
- The mines are characterized by Enhanced Permeability Zones (EPZs), which are zones of greater fracturing and good hydraulic connectivity, related to structures such as faults, found to be present at operating diamond mines in crystalline rock of the Canadian Shield. Hydraulic conductivity of the EPZs ranges between 1×10^{-6} and 1×10^{-5} m/s, across variable widths (transmissivity between about 8×10^{-5} and 1×10^{-3} m²/s).

Diavik Mine

Hydrogeologic conditions for the Diavik mine, NT, are summarized as follows:

- Combined dewatering data exists for the underground mine labelled A154/A418.
- The underground mines A154/A418 are located in an open talik associated with Lac de Gras. The lake was not dewatered prior to mining operations, but a portion of the lake is dyked off. Permafrost is estimated to extend down to 400 mbgs.
- The hydraulic conductivity of the competent bedrock ranges between 1×10^{-8} and 6×10^{-7} m/s and decreasing with depth.
- The Diavik mine is also characterized by EPZs. Hydraulic conductivity of the EPZs ranges between 1×10^{-6} and 3×10^{-6} m/s. During mining, an EPZ was found to be the source of substantial groundwater inflow.

Snap Lake Mine

Hydrogeologic conditions for the Snap Lake mine, NT, are summarized as follows:

- Inflows have been measured in the underground workings since 2004.
- The mine extends down under the permafrost and into the open talik associated with Snap Lake. The depth of the permafrost is between 140 and 180 mbgs away from the influence of the lake. Snap Lake was not dewatered prior to mining operations, but a portion of the lake is dyked off.
- The hydraulic properties of the competent country rock range between 1×10^{-9} and 4×10^{-7} m/s, which is relatively similar to the rock mass at the mine and generally decreasing with depth.
- The Snap Lake mine is also characterized by multiple EPZs. Hydraulic conductivity of the EPZs ranges between 1×10^{-8} and 8×10^{-6} m/s.

Measured and Predicted Groundwater Inflows

At the Ekati site in 2012, an annual total average mine water inflow of approximately 1,200 m³/day was reported to the Panda and Koala underground mines, and 1,000 m³/day to the Fox pit. During mining of the Misery pit, minor groundwater inflows were reported; in 2010 pit inflow was observed to range between 200 and 300 m³/day and was interpreted to originate primarily from the active zone. The measured inflows were within the bounds of the groundwater numerical model predictions completed in 2005 and 2006. The predictions ranged between 1,000 and 1,700 m³/day for the Panda and Koala underground mines, and 400 and 4,300 m³/day for the Fox pit mine.

At the Diavik site, a combined flow between 3,300 and 6,600 m³/day was reported to the underground mine labelled A154/A418, in 2009 and 2010. Several groundwater models were completed and updated prior to and after mining operations started. Because the mine plans and objective of those models changed, it is difficult to compare the predictions with the mine inflow measured in 2009 and 2010. However, it is possible to state that the incorporation of the EPZ identified during mining and calibration with data collected during mining provided accurate predictions of groundwater inflows and quality.

At the Snap Lake site, a measured inflow to the workings of approximately 50,000 m³/day was reported in 2015. With the use of real underground flow measurements for calibration, the most recent numerical models, built after 2011, predicted the same magnitude of inflow as measured in year 2015, and future peak inflow of about 60,000 m³/d for the year 2017. Earlier numerical model versions (2001, 2002) underestimated the inflows, with a predicted peak inflow between 24,000 and 34,000 m³/day for the year 2018, about half of the flow observed in 2015. The major differences between the early and late inflow predictions at Snap Lake are linked to updated field data and modifications to the mine plan. New findings changed the permafrost depth assumption, the characterization of hydrogeological units and their properties, the characterization of structural features, and the calibration of leakage factors associated with underground tunnels.

Summary

The benchmarking results do demonstrate that predictions of groundwater inflow and groundwater quality for the Madrid North and Madrid South mines are reasonable compared to predictions and observations at other mines in the Canadian North.

Between the Ekati, Diavik and Snap Lake mines, the Ekati mine has the most similarities with the Project. In terms of average hydraulic conductivity of the rock mass, the properties of the competent country rock at the Ekati mine are relatively like the properties measured at site, even though the hydrostratigraphic units differ from the units found at the Project. In terms of mine inflow, predictions for Ekati and Hope Bay are in the same range with an average flow rate in the order of 1,000 m³/day.

At the Diavik and Snap Lake mines, unlike the Ekati mine, average hydraulic conductivities are slightly more permeable and the predicted inflows are significantly higher. The higher magnitude of inflows, observed and predicted, at the Snap Lake and Diavik mines are linked to the connection with the lakes at their surface via the EPZs; however, the significance of the EPZs were not fully understood until mining commenced. A similar scenario cannot be ruled out at the Madrid North or Madrid South mines. The current dataset; however, does not show a clear increase in fracture frequency, major lithological change, or obvious structural features associated with high hydraulic conductivity. From a practical perspective, further data collection at the Madrid South and Madrid North sites may never be enough to reduce the uncertainty associated with EPZs; the only real proof of concept being actually intercepting the features as part of mining. Mining development will provide ample opportunity to learn and adjust as mining progresses, which is consistent with what has happened at the benchmarked sites.

5.2.4 Predicted Groundwater Quality

Approach

The results for groundwater quality predictions are subdivided into two subsections: one for chloride and one for the other constituents of concern (ammonia, boron, cadmium, chloride, fluoride, iron, manganese, mercury, molybdenum, nickel, sulfate and zinc).

- The prediction for chloride was calculated directly from the numerical model and accounted for the observed increase of chloride concentration with depth.

The predictions of chloride concentrations were not calibrated to steady state conditions. The transport models that simulate the underground mine excavations were assigned chloride concentrations as initial conditions (i.e., nodal concentrations as shown on Figures 27 and 28) and constant mass boundary conditions along the edges of the model domain (i.e., equals to the chloride concentrations defined by the chloride profile in Figure 18).

To simulate the chloride profile under current conditions and at steady state, the model would have to include the additional complexity of density dependent flow systems. This was not considered to be necessary because conceptually a density dependent groundwater flow system would result in the mine inflow comprising slightly less groundwater and more fresh lake water which would not be conservative to assess the potential effects mine water quality

discharges to the environment. The groundwater contribution from the bottom of the mine would be reduced by the downward forces resulting from high water density at depth, and the fresh lake water directly above the mines would still be expected to be drawn to the mine downward because of dewatering.

- Since the other constituents of concern do not vary with depth, their concentrations were calculated with a simple mixing model assuming conservation of mass and based on the calculated proportions between predicted lake infiltration rates and predicted mine inflows (Figure 35), and the estimated concentrations in lake water and groundwater. The travel times from the lake to the mine were not taken in account.

Considering the extreme difficulty of obtaining good quality groundwater quality samples in a low K and frozen environment, it is recognized that there could be slight differences of metal concentrations compared to the baseline groundwater quality (i.e., 10WBW001 at Doris). These differences are not anticipated to be significant and are not expected to affect TMAC's ability to discharge mine water. The control for discharge is related to salinity which is not expected to differ between the sites because it is not a function of the mineralogical make-up.

Concentrations of Chloride in Mine Inflow

Figure 36 and 37 presents plan view maps and cross sections of chloride concentrations from transient modelling at the time of pre-mining and maximum drawdown, at Madrid North and Madrid South respectively.

Figure 38 presents the predicted monthly inflow chloride concentration for the Madrid South and Madrid North mines.

During about the first year of mining at the Madrid South mine, the simulation predicts inflows will have a peak chloride concentration of approximately 14,500 mg/L. As the water from storage is progressively replaced by a mix of water from the lakes (90%) and the regional deep groundwater (10%), the concentration of chloride will decrease. By the end of mining, average chloride concentration is on the order of 13,000 mg/L.

During about the first year of mining at the Madrid North mine, the simulation predicts inflows will have a peak chloride concentration of approximately 17,500 mg/L. As the water from storage is progressively replaced by a mix of water from the lakes (96%) and the regional deep groundwater (4%), the concentration of chloride will decrease. By the end of mining, average chloride concentration is on the order of 8,500 mg/L.

Concentrations of Other Constituents of Concern in Mine Inflows

The simulation predicts that concentrations of the other constituents of concern will peak in the first year of mining, when background water quality from water out of storage dominates, after which concentrations reflect relatively steady inflows from the lakes (90% at Madrid South and 96% at Madrid North) and regional deep groundwater (10% at Madrid South and 4% at Madrid North). Table 12 presents the concentrations of each constituent for lakes and groundwater and for current conditions. Table 13 presents the predicted concentrations of each constituent for the mine inflows in Madrid South and Madrid North after a year of mining when concentration peaks, or at the end of mining when concentration is steady.

Table 12: Actual Concentration in Lakes and Groundwater

Constituent	Actual 75th Percentile Concentrations in Doris Lake [mg/L]	Actual 75th Percentile Concentrations in Groundwater Under Doris Lake [mg/L]
Ammonia as N	0.005	3.5
Boron	0.0443	3.24
Cadmium	0.000005	0.00012
Fluoride	0.057	0.75
Iron	0.11175	4.81
Manganese	0.026075	1.75
Molybdenum	0.00021925	0.0187
Mercury	5.7E-07	0.00005
Nickel	0.00066	0.0014
Selenium	0.0002	0.002
Sulfate	2.805	2000
Zinc	0.003	0.157

Table 13: Predicted Concentration in Mine Inflows during Active Mining

Constituent	Madrid South		Madrid North	
	Peak Concentration in the First Year of Mining [mg/L]	Steady Concentration at End of Mining [mg/L]	Peak Concentration in the First Year of Mining [mg/L]	Steady Concentration at End of Mining [mg/L]
Ammonia as N	3.28	0.32	2.80	0.16
Boron	3.03	0.34	2.60	0.18
Cadmium	0.000113	0.000016	0.000097	0.000010
Fluoride	0.71	0.12	0.61	0.09
Iron	4.51	0.54	3.87	0.32
Manganese	1.64	0.18	1.41	0.10
Molybdenum	0.018	0.002	0.015	0.001
Mercury	0.000047	0.000005	0.000040	0.000003
Nickel	0.0014	0.0007	0.0013	0.0007
Selenium	0.0019	0.0004	0.0016	0.0003
Sulfate	1872	185	1601	90
Zinc	0.147	0.017	0.126	0.010

Blasting residues associated with ore and waste rock assumed lost to groundwater are not accounted in the groundwater model; however, these residues are accounted for in the water and load balance model (SRK, 2017) as a separate loading to groundwater.

5.3 Post-closure Conditions

Once mining ceases, backfill of waste rock material and detoxified cyanide leach tailings is completed, and the mine workings have been prepared for closure, the mine dewatering pumps will be switched off and the mine will reflood. SRK estimated the time to reflood each mine under the base case scenario at any given time (i.e., in the hypothetical event that mining had to stop before the full life of the mine), and identified the final receptors of groundwater potentially affected from the mines.

5.3.1 Mine Reflood Time Estimation

The time to re-flood the mine is a function of the volume of the mine void over time, the rising water level, and the decay in groundwater inflow over time related to the decrease in head difference between the mine water level and the surrounding groundwater levels. Based on these considerations, the reflood time is estimated using an exponential decay function, the predicted mine inflow rates, and the void volumes of the mine workings including backfill. The function is:

$$\Delta h_r(t) = \Delta h_{eom} e^{-t \frac{Q_{eom}}{V_{mine}}}$$

Where Q_{eom} is the flow rate at the end of mining, V_{mine} is the effective volume of the underground mine voids, Δh_{eom} is the drawdown at the end of mining, and t is the time since the mining stopped.

The estimated reflood times were calculated for three scenarios:

- A base case reflood time estimation based on the inflow rates predicted by the base case mining scenario;
- A hypothetical low K case with a reflood inflow rate reduced by a factor of two in comparison to the base case predictions; and
- A hypothetical high K case with a reflood inflow rate based on the upper case inflow predictions (i.e., K function based on the moving arithmetic mean).

Table 14 compiles the input parameters and reflood time estimations for the three scenarios.

Table 14: Reflood Time Estimations

Scenario	Parameters	Unit	Madrid South	Madrid North
All cases	V_{mine}^1	m ³	685,808	3,135,891
	Δh_r	m	50	50
	Δh_{eom}	m	785.8	635.8
Base case	(Q_{eom})	m ³ /d	542	1164
	t₁ reflood	year	9.5	18.8
Low K case	(Q_{eom})	m ³ /d	271	582
	t₂ reflood	year	19.1	37.5
High K case	(Q_{eom})	m ³ /d	542	1164
	t₃ reflood	year	2.8	4.1

Note:

¹ The deposition of backfill was assumed to be homogeneously distributed throughout the mine voids.

When the Madrid North Mine has been fully developed, the total reflood time is estimated to be about 19 years for the base case. For the two hypothetical reflood scenarios, minimum and maximum reflood times of 4 and 38 years respectively can be observed.

When the Madrid South Mine has been fully developed, the total reflood time is estimated to be about 9.5 years for the base case. For the two hypothetical reflood scenarios, minimum and maximum reflood times of 3 and 19 years respectively can be observed.

5.3.2 Inflow of Mine Affected Groundwater into Lakes

In the long term, the mined-out areas will be completely flooded. As water saturates the mine, the heat will transfer to the surrounding permafrost and the underground areas will be expected to freeze-back where the minimum ground temperature is less than -2°C. However, it is possible that parts of the underground areas will not completely freeze back due to the large latent heat requirements combined with relatively warm permafrost temperatures at depth.

The groundwater contained in unfrozen mined out areas may have its quality modified by the backfill and/or tailings deposited underground, become part of the regional groundwater system, and travel through the open taliks via the deep groundwater system.

At post-closure, the groundwater flow system will have returned to its initial state, with the flow directions driven by the distribution of open taliks and lake levels. The flow system should be similar to what was predicted by the current conditions scenario (Figure 29 and 30) and the groundwater contained in the mined-out areas of Madrid North will flow to Windy Lake, and for Madrid South to Patch Lake. In terms of contribution, Windy Lake could receive up to 0.1 m³/d of groundwater coming from Madrid North. Patch Lake could receive 0.3 m³/day from Madrid North and 0.6 m³/d from Madrid South. In both cases, groundwater will travel very slowly; the models predicted travel times greater than 1,000 years.

5.4 Model Sensitivity

Additional models were completed to assess the effects of parameter uncertainties on mine inflow predictions. Emphasis was placed on scenarios that could result in increased inflow to the underground mine compared to the base model. The analysis involved quantification of the effects of four main uncertainties, namely:

- Increased hydraulic conductivity in the fractured rock;
- Increased hydraulic conductivity due to potential uncontrolled faults or set of fractures;
- Increased hydraulic conductivity in the lake bed sediments;
- Decreased or increased of storage in the fractured rock; and
- Increased hydraulic gradient caused by higher water elevations in the lakes.

The predictions of the sensitivity runs are compiled in Figures 39 and 40. The results were analyzed by comparing the results to the base case model predictions presented in Section 6.2.

5.4.1 Results of the Sensitivity Models

Hydraulic Conductivity of the Fractured Rock

In the base case model, the hydraulic conductivity profile was determined from the moving geometric mean of test results with depth, which is considered to be reasonably conservative, i.e., two thirds of the K tests at Madrid South and Madrid North actually reported lower K values than the modeled K function.

A more conservative scenario tested a K distribution based on the moving arithmetic mean of the site measurements, as shown by the orange curve in Figure 14. The results show inflows are sensitive to assumptions for K. The sensitivity models predicted an increase of mine inflow to a maximum of 5,340 m³/day for Madrid North and 1,870 m³/d at Madrid South, and an augmentation of lake infiltration to a maximum of 610 m³/day for Wolverine Lake, 4,580 m³/day for Patch Lake, 270 m³/day for Imniagut Lake and 40 m³/day for Windy Lake.

In terms of chloride, the augmentation of lake infiltration combined with the relatively lower salinity concentration in the lakes, and at shallow depth causes a reduction of the final chloride concentration, 3,590 mg/L of chloride at Madrid North and 8,930 mg/L at Madrid South.

Potential Influence of a Vertical Fracture Network

A sensitivity scenario tested the influence of high K along the vertical axis as a mean to assess the potential influence of steeply dipping permeable geological structures. In this scenario, K in the horizontal plane was assigned with the geometric mean function, whereas K in the vertical axis was assigned with the arithmetic mean function.

The results show inflows are sensitive to high vertical K. The sensitivity models predicted an increase of mine inflow to a maximum of 2,190 m³/day for Madrid North and 750 m³/d at Madrid South, and an augmentation of lake infiltrations to a maximum of 260 m³/day for Wolverine Lake, 2,040 m³/day for Patch Lake, and 100 m³/day for Imniagut Lake. There was no increase for Windy Lake.

In terms of chloride, the augmentation of lake infiltration combined with lower salinity concentration in the lake causes a reduction of the final chloride concentration, 4,640 mg/L of chloride at Madrid North and 10,250 mg/L at Madrid South.

Potential Influence of a Permeable Fault

A sensitivity scenario tested the influence of a hypothetical large high permeability fault that would intercept both mines and flow freely throughout the life of the mine (i.e., no groundwater management control). In this scenario, it was assumed that the DEFZ fault, running west of Patch Lake, was continuous both laterally and at depth, approximately 10 m wide (or greater at the edge of the model where mesh is less refined) and characterized by a K of 3×10^{-6} m/s, which is the highest K value observed at the Hope Bay site.

The results show inflows are sensitive to a large permeable fault. The sensitivity models predicted an increase of mine inflow to a maximum of 1,470 m³/day for Madrid North and 700 m³/d at Madrid South, and an augmentation of lake infiltrations to a maximum of 180 m³/day for Wolverine Lake, 1,280 m³/day for Patch Lake, and 60 m³/day for Imniagut Lake. Since the DEFZ fault intercepts also the Windy Lake open talik, infiltration for Windy Lake increased to a maximum of 30 m³/day.

In terms of chloride, the DEFZ fault causes an increase of the final chloride concentration, 7,820 mg/L of chloride at Madrid North and 10,950 mg/L at Madrid South because the fault can draw higher proportion of the highly saline groundwater contained in the fractured rock.

Lake Sediments

The base case model assumes the lake sediments are divided into two layers, soft lake bed sediments and an indurated lake bed sediment layer with a K of 1×10^{-8} m/s and 4×10^{-10} m/s, respectively. A sensitivity model tested the influence of more permeable lake sediments with the K of lake sediments one order of magnitude higher, 1×10^{-7} m/s and 4×10^{-9} m/s.

The results show mine inflows are sensitive to the K of lake sediments. The sensitivity models predicted an increase of mine inflow to a maximum of 1,980 m³/day for Madrid North and 830 m³/d at Madrid South, and an augmentation of lake infiltrations to a maximum of 230 m³/day for Wolverine Lake, 1,880 m³/day for Patch Lake. There was no increase of infiltration for Imniagut Lake and Windy Lake.

In terms of chloride, the augmentation of lake infiltration combined with the relatively lower salinity concentration in the lakes causes a decrease of the final chloride concentration, 5,020 mg/L of chloride at Madrid North and 7,980 mg/L at Madrid South.

Lake Elevation

A sensitivity model tested the influence of higher lake levels, with all increased by one meter. The results show mine inflows are not sensitive to the change of level. In terms of chloride, the sensitivity model predicted no change compared to the base case model.

Storage Coefficients

The base case model assumed storage coefficient values of 1×10^{-4} m⁻¹ for the overburden and 3×10^{-7} m⁻¹ for the fractured rock. Sensitivity scenarios tested the influence of storage coefficients, with either a reduction or an augmentation of the storage values by one order of magnitude.

The results showed mine inflows are sensitive to the increase of storage coefficient values (S_x). The sensitivity models predicted an increase of inflow to a maximum of 1,350 m³/day for Madrid North and 580 m³/d at Madrid South, and a slight reduction of lake infiltration to a maximum of 180 m³/day for Wolverine Lake, 1,040 m³/day for Patch Lake. There was no significant variation of infiltration for Imniagut Lake and Windy Lake.

In terms of chloride, the sensitivity model predicted an increase of the final chloride concentration, 9,100 mg/L of chloride at Madrid North and 12,050 mg/L at Madrid South. The mine inflow augmentation combined with the additional volume of groundwater stored in overburden and fractured rock drives the augmentation.

Summary

Table 15 compiles the results of all the sensitivity models.

Table 15: Summary of the Sensitivity Model Results

Scenario	Parameter	Maximum Predicted Mine Inflow (m ³ /d)		Maximum Predicted Lake Contribution (%)		Predicted Infiltration of water from lakes (m ³ /d) for the month of March, Year 2032					Chloride Concentration at End of Active Mining (mg/L)	
		(MS)	(MN)	(MS)	(MN)	Patch lake (MS)	Patch lake (MN)	Wolverine lake (MS)	Imniagut lake (MN)	Windy lake (MN)	(MS)	(MN)
Base Case	-	550	1,180	91	96	309	1056	182	57	13	12,050	8,610
Higher hydraulic conductivity of the fractured rock	K bedrock in all directions based on the moving arithmetic	1,870	5,340	73	95	743	4580	611	274	44	10,240	4,640
Well connected vertical fracture network	K bedrock based on geometric mean along horizontal plane, and arithmetic mean along vertical plane.	750	2,190	93	96	429	2037	257	103	13	10,250	4,640
Permeable fault	DEFZ fault assumed to be highly permeable (K = 3x10 ⁻⁶ m/s)	700	1,470	90	92	433	1283	188	57	24	10,950	7,820
More permeable lake sediments	K of lake sediments one order of magnitude higher relative to base case	830	1,980	97	99	580	1878	224	59	12	7,980	5,020
Higher lake elevation	All lake levels increased by one meter	550	1,180	91	96	309	1056	182	57	13	12,050	8,610
Higher storage coefficients	One order of magnitude lower than base case	580	1,350	91	91	309	1041	182	54	4	12,050	9,100
Lower storage coefficients	Higher order of magnitude lower than base case	550	1,160	91	96	309	1058	182	57	14	12,050	8,530

5.4.2 Sensitivity to Flow from Exploration Drillholes

Considerable uncertainty exists regarding the potential for inflow through open exploration drillholes that could connect the Madrid South or Madrid North mines directly to Patch Lake. Most holes should have been plugged using a method that involved setting a Van Ruth-type plug approximately 35 m into bedrock and then emplacing cement on top of the plug, but a certain number are also known to have not been cemented. SRK estimated with the Darcy-Weisbach equation that an open NQ-diameter (75.7 mm) exploration drillhole intercepted by the mine and flowing freely could reach up to 2,680 m³/day.

SRK could not verify the condition of each exploration drillhole because there are no written records of methods for cementing nor are there as-built-type descriptions of what was actually done. Therefore, to assess the potential impact of historical drillholes to the mine inflows, SRK looked at the spatial distribution of all the exploration drillholes relative to the Madrid South and Madrid North prefeasibility mine layouts, and the probabilities of intercepting open and freely flowing drillholes. Table 16 shows the counts of drillholes for each mine, classified by their distance to mine development. This analysis will be updated as mining progresses and mine plan is updated.

Table 16: Drillhole Intersection Summary for Madrid South

Level (masl)	Counts of Drillholes by Mine Levels and Distance to Mine Development							
	Madrid South				Madrid North			
	0 m	>0 to 3 m	>3 to 10 m	>10 to 30 m	0 m	>0 to 3 m	>3 to 10 m	>10 to 30 m
-40	0	0	0	0	12	8	18	51
-60	0	0	4	4	9	8	18	47
-80	0	1	1	6	10	11	19	62
-100	1	1	1	5	13	7	16	57
-120	0	1	0	6	9	6	13	45
-140	0	1	1	5	10	9	8	32
-160	1	1	1	3	6	5	14	32
-180	0	1	2	3	8	5	12	26
-200	1	1	2	5	11	4	9	23
-220	0	0	2	5	9	2	4	23
-240	0	1	0	5	6	2	6	18
-260	1	0	0	4	3	1	1	6
-280	0	0	2	4	0	0	0	0
-300	1	1	1	3	0	0	0	0
-320	2	0	0	1	0	0	0	0
Totals	7	9	17	59	106	68	138	422

For the statistical analysis, probabilities of interception were assumed to vary according to the distance between drillholes and development, i.e., the further an exploration hole is from the future development, the less likely it will be intercepted. These were then coupled to a probability of 25% that any given drillhole remained completely open, connected to the lake above, and able to discharge at the maximum rate, given the fact that most holes should be cemented and that open hole could collapsed. Probabilities are shown in Table 17. As conditions of the drillholes cannot be assessed, these probabilities must be viewed cautiously.

Table 17: Drillhole Probabilities

Distance to Underground Developments	Probability of Intercepting an Exploration Hole	Probability of Hole of Being Open, Connected to the Lake above and Flowing Freely	Probability of Intercepting an Open Hole, Connected to the Lake above and Flowing Freely
0 m	95%	25%	24%
>0 to 3 m	50%	25%	13%
>3 to 10 m	15%	25%	3%
>10 to 30 m	2%	25%	0.5%

A binomial distribution was utilized to determine the probability of encountering flowing drillholes during the development of the Madrid South and Madrid North mines. A summary of this analysis is presented in Figures 41 and 42, showing the probability for each mine that developments intercept a given number of open exploration holes that can flow at maximum rate. The analysis shows Madrid South has a low probability to intercept an exploration drillhole. Madrid North on the other hand has a more than 50% probability to intercept two fully open exploration holes.

5.4.3 Management of the Uncertainty of the Groundwater Predictions

The groundwater management system will be designed based on the base case modelled scenario, as that is considered the most realistic scenario. The more conservative sensitivity scenario, with a K distribution based on the moving arithmetic mean of the site measurements, have been considered in the Water and Load Balance model to test the sensitivity of the water management system to higher groundwater inflow.

It is recognized that there is a likelihood that flow in the mines will be dominated by specific fractures or sets of fractures, and that the mines could intercept open exploration drillholes. This uncertainty exists for all mining projects conducted in fractured rock and is never completely alleviated until structural geology and hydrogeology data is regularly collected during mining operations. Learnings from groundwater inflow at the Doris Mine will be used to inform and update Plans for the Madrid-Boston Mines.

The uncertainties associated with the groundwater predictions, fault zones and exploration holes, are acknowledged and will be managed using a Groundwater Management Plan (GWMP) implemented across all TMAC Hope Bay project sites, while still addressing site- and licence-specific needs. The objective of the GWMP is to layout the most appropriate course of action to: (i) minimize the influence of mining in taliks on lake water levels; and (ii) Integrate the mine inflow volumes and chemistry, and resulting loading into the Water Management Plan (WMP). This plan will outline the areas of uncertainty and provides triggers for implementing management and mitigation measures.

In advance of starting mine development in the talik zones, TMAC will develop operational measures in the appropriate Standard Operation Procedures (SOPs). These operational measures will be functional and concise instructions that will allow the relevant mine operations staff to manage responses to groundwater inflows. It will describe actions to be taken to routinely manage expected amounts of groundwater inflow, and actions to be taken when features carrying inflow are encountered. Actions may include the following measures:

- Proactive control measures such as:
 - Collection and interpretation of groundwater pressure and inflow data;
 - Use of surface and underground exploration information for identifying enhanced permeability that may be intercepted; and
 - Advance cover and probe drilling (i.e., exploratory drainage holes).
- Mitigation measures such as:
 - Modification and/or adjustment of the mine plan to avoid areas of concern, or the use mined-out stopes to provide surge capacity;
 - Additional sump capacity to handle higher than predicted inflows;
 - Pre-grouting of highly conductive structures prior to intersection with the mine workings; and
 - Isolation of mining sections to control or minimize mine inflow.

6 Conclusions

A hydrogeological conceptual model was developed for the Boston, Madrid South and Madrid North mines based on information from geological and structural mapping, and site specific field investigations. SRK used the field observations to assess potential structural controls on groundwater flow and conduct thermal analyses. The analysis assessed where through taliks occurred on a regional scale, and predicted the detailed configuration of open taliks on a local scale. It concluded that the Boston Mine will be encapsulated by permafrost and will not intercept an open talik or subpermafrost areas, whereas the Madrid North and Madrid South mines will intercept unfrozen ground, either at the edge of the open taliks formed by Wolverine Lake and Patch Lake or in the subpermafrost. Subsequently, two numerical models were developed to simulate the potential mine inflows at the Madrid North and Madrid South mines.

Results of the groundwater model suggest that the maximum mine inflow will be in the order of 1,180 m³/day at the Madrid North Mine and 550 m³/day at the Madrid South Mine. Water from the lakes will contribute about 96% for Madrid North and 90% for Madrid South, with the remainder coming from deep regional groundwater. Results suggest that the water encountered during mining, at least initially, will be saline and dominated by chloride. Other constituents of concern include ammonia, boron, cadmium, iron, fluoride, manganese, molybdenum, mercury, nickel, selenium, sulfate, and zinc because concentrations in background groundwater exceed water quality guidelines. The model predicts that the respective concentrations of each constituent will peak in the early mining stage when saline connate water is the dominant source of groundwater inflow, and will then progressively decrease as water from storage is progressively replaced by a mix of water from lakes and regional deep groundwater.

During mining operations, the heat circulated into the underground mines will generate a lateral thaw of the bedrock at some distance of the workings. The extent of the thaw was assessed using a one dimensional analytical solution. The analysis showed the effects of underground heating on permafrost will be limited. The heat will increase the volume of unfrozen ground around the mines but it will not generate new open taliks that connects the ground surface to subpermafrost.

Once mining ceases, backfill of waste rock material and tailings is completed, and the mine workings have been prepared for closure, the mine dewatering pumps will be switched off and the mine will reflood. The reflood time was estimated for each mine using an exponential decay function, the predicted mine inflow rates, and the void volumes of the mine workings including backfill. When the Madrid North Mine has been fully developed, the total reflood time is estimated to be about 19 years for the base case. When the Madrid South Mine has been fully developed, the total reflood time is estimated to be about 9.5 years for the base case.

Sensitivity models were completed to assess the effects of key parameter on the mine inflow predictions. Results of the sensitivity models suggest that the predictions of inflows are sensitive to the hydraulic conductivities of the fractured rock and lake bed sediment, the interception of an hypothetical high permeability fault flowing freely into the working (i.e., not managed/controlled by mining operations), and variations in storage values.

The potential inflows from open exploration drillholes connecting the Madrid South or Madrid North mines directly to Patch Lake were assessed because there are drillholes which are known to have remained open. It was estimated that an open NQ-diameter (75.7 mm) exploration drillhole intercepted by the mine and flowing freely could reach up to 2,680 m³/day. SRK looked at the spatial distribution of all the exploration drillholes relative to the Madrid South and Madrid North mine layouts, and the probabilities of intercepting open and freely flowing drillholes. The analysis showed Madrid South has a low probability to intercept an exploration drillhole. Madrid North on the other hand has a more than 50% probability to intercept two open exploration holes.

To balance the uncertainty on the model parameters, TMAC will develop a functional groundwater management plan to routinely manage expected amounts of groundwater inflow, and define actions to be taken when high permeability formations or open exploration drillholes are anticipated and require to be controlled. Active control measures may include advance probe drilling and pre-grouting of highly conductive structures prior to intersection with the mine workings, and additional pumping capacity to handle potentially higher than predicted inflows.

This final report, *Hydrogeological Characterization and Modeling of the Proposed Boston, Madrid South and Madrid North Mines, Hope Bay Project, Nunavut*, was prepared by SRK Consulting (Canada) Inc.

This signature was scanned with the author's approval for exclusive use in this document; any other use is not authorized.

Gregory Fagerlund, MSc, PGeo
Senior Consultant

and reviewed by

This signature was scanned with the author's approval for exclusive use in this document; any other use is not authorized.

Maritz Rykaart, PhD, PEng
Principal Consultant

All data used as source material plus the text, tables, figures, and attachments of this document have been reviewed and prepared in accordance with generally accepted professional engineering and environmental practices.

Disclaimer—SRK Consulting (Canada) Inc. has prepared this document for TMAC Resources Inc.. Any use or decisions by which a third party makes of this document are the responsibility of such third parties. In no circumstance does SRK accept any consequential liability arising from commercial decisions or actions resulting from the use of this report by a third party.

The opinions expressed in this report have been based on the information available to SRK at the time of preparation. SRK has exercised all due care in reviewing information supplied by others for use on this project. Whilst SRK has compared key supplied data with expected values, the accuracy of the results and conclusions from the review are entirely reliant on the accuracy and completeness of the supplied data. SRK does not accept responsibility for any errors or omissions in the supplied information, except to the extent that SRK was hired to verify the data.

7 References

- Beale, G. and J. Read, 2014. Guidelines for Evaluating Water in Pit Slope Stability. CRC Press.
- Burn CR. 2002. Tundra lakes and permafrost, Richards Island, western Arctic coast, Canada. Canadian Journal of Earth Sciences 39: 1281–1298.
- Burn CR. 2005. Lake-bottom thermal regimes, western arctic coast, Canada. Permafrost and Periglacial Processes 16: 355–367.
- Canadian Council of Ministers of the Environment (CCME), 2015. Canadian Environmental Quality Guidelines Summary Table. <http://st-ts.ccme.ca/>. Accessed April 2015.
- Cumberland Resources Ltd., 2005. Meadowbank Gold Project: Final Environmental Impact Statement.
- De Beers Canada Inc. 2002. Snap Lake Diamond Project: Environmental Assessment Report. Submitted to the Mackenzie Valley Review Board. February 2002.
- De Beers Canada Inc. 2010. Gahcho Kue Project: Environmental Impact Statement. December 2010.
- DHI, 2015. FEFLOW v6.2 (P11) Advanced Groundwater Modelling. <http://www.mikepoweredbydhi.com/products/feflow>. March 2015.
- Dyke, A.S., and Prest, V.K. 1986. Late Wisconsin and Holocene retreat of the Laurentide Ice Sheet. Geological Survey of Canada, Map 1702A
- Dyke, A.S., and Dredge, L.A. 1989. Quaternary Geology of the Northwestern Canadian Shield. In Quaternary Geology of Canada and Greenland. Ed. R.J.Fulton. Ottawa: Geological Survey of Canada.
- EBA. 1996. Report on the Boston Gold Project. Surficial geology and Permafrost features. Prepared for Rescan Environmental Services Ltd. Vancouver, BC.
- Frape, S., & Fritz, P., 1987. Geochemical trends for groundwater from the Canadian Shield, in saline water and gases from crystalline rocks. Geological Association of Canada Special Paper, 33, 19-38.
- Gacoyne M., 2003. Hydrogeochemistry, groundwater ages and sources of salt in a granitic batholith on the Canadian Shield, southeastern Manitoba. Applied Geochemistry 19 (2004) 519-560.
- Golder Associates Inc., 2008a. A154 & A418 Geotechnical and Hydrogeological Data Summary: Diavik Diamond mine. September 2008.
- Golder Associates Inc., 2008b. Water Management Drainage Gallery Design and Predicted Mine Inflows to End of 2023. December 2008.

- Golder Associates Inc., 2013. Meliadine Draft Environmental Impact Statement - Volume 7
Freshwater Environment - Appendix 7.2-A Groundwater Quality Baseline Report.
- Golder Associates Inc., 2014. Hydrogeology Baseline Report for the Jay Project. September
2014.
- Itasca Consulting Group, 2013. Executive Summary of Groundwater Flow Model Update. Memo.
Aug 2013. Obtained on the web in Aug. 2015 from
http://www.reviewboard.ca/upload/project_document/EA1314-02_Underground_Model_Memo.PDF.
- Klohn Crippen. 2001. Phase II Hydrogeological Evaluation of Panda Pit. File: 878802
- Klohn Crippen. 2004. Ekati Mine Hydrogeological Evaluation of Misery Pit and Underground. File:
M08788 07.500.
- Klohn Crippen. 2005. Ekati Mine 2004 Hydrogeological Investigation of Fox Pit. File:
0304A01.500.
- Klohn Crippen. 2006. Ekati Mine 2005 Koala Feasibility Report Underground Mine Dewatering
Final Report. File: A03040A02.500.
- Kuchling, K., Chorley, D., & Zawadzki, W., 2000. Hydrogeological Modelling of Mining Operations
at the Diavik Diamonds Project. Proceedings of the Sixth International Symposium on
Environmental Issues and Waste Management in Energy and Mineral Production.
- Lunardini V.J. 1995. Permafrost Formation Time. CRREL Report 95-8, US Army Corps of
Engineers, Cold Regions Research & Engineering Laboratory, April 1995.
- Metal Mining Effluent Regulations (MMER), 2015. Authorized Limits of Deleterious Substances -
Schedule 4. Last amended February 20, 2015. [http://laws-
lois.justice.gc.ca/eng/regulations/SOR-2002-222/](http://laws-lois.justice.gc.ca/eng/regulations/SOR-2002-222/). Accessed April 2015.
- Mvondo, H., Lentz, D., Bardoux, M., James, D.T. 2012. Geology and mineralization of the link
between Hope Bay and Elu Greenstone Belts, northeast Slave Craton, Nunavut.
Geological Survey of Canada, Open File 7007.
- Parez and Fauriel (1988). "Le piezocone ameliorations apportees a la reconnaissance de sols."
Revue Francaise de Geotech 44: 13-27.
- Rescan ERM, 2015. Back River - 2014 Sub-permafrost Groundwater Quality Baseline Report.
June 2015.
- Roscoe Postle Associates Inc. 2015. Technical Report on the Hope Bay Project, Nunavut,
Canada. Project #2325, Toronto.
- Sherlock, R.L., Shannon, A., Hebel, M., Lindsay, D., Madsen, J., Sandeman, H., Hrabi, B.,
Mortensen, J.K., Tosdal, R., Friedman, R. 2012. Volcanic Stratigraphy, Geochronology,

and Gold Deposits of the Archean Hope Bay Greenstone Belt, Nunavut, Canada.
Economic Geology 107: 991-1042.

Singhal, B.B.S., and Gupta, R.P., 2010. Applied Hydrogeology of Fractured Rocks. Springer Science + Business Media B.V. 2nd Ed. 2010.

Smith, M.W. and Hwang, C.T., 1973. Thermal Disturbance Due To Channel Shifting, Mackenzie Delta. N.W.T., Canada; in Proceedings Second International Permafrost Conference, North American Contribution; National Academy of Sciences, Washington, D.C., p51-60.

SRK Consulting (Canada) Inc., 2003. Preliminary Groundwater Inflow Study Doris Crown Pillar. Prepared for: Miramar Mining Corporation. September 2003.

SRK Consulting (Canada) Inc., 2005. Groundwater Assessment, Doris North Project, Hope Bay Nunavut, Canada. Report prepared for Miramar Hope Bay Limited. 1CM014.006. October 2005.

SRK Consulting (Canada) Inc. 2009a. Hope Bay Gold Project Overburden Characterization Report. Prepared for Hope Bay Mining Limited. Project No.: 1CH008.002. June 2009.

SRK Consulting (Canada) Inc. 2009b. Geotechnical and Hydrogeological Assessment for the Boston Open Pit, Nunavut, Canada. Prepared for Hope Bay Mining Limited. Project No. 2CH009.000. June 2009.

SRK Consulting (Canada) Inc. 2009c. Geotechnical and Hydrogeological Assessment for the Madrid Open Pit and Underground, Nunavut, Canada. Prepared for Hope Bay Mining Limited. Project No. 2CH009.000. June 2009.

SRK Consulting (Canada) Inc. 2009d. Geotechnical and Hydrogeological Assessment for the Doris North Open Pit and Doris Central Underground, Nunavut, Canada. Prepared for Hope Bay Mining Limited. Project No. 2CH009.000. June 2009.

SRK Consulting (Canada) Inc., 2011a. Hope bay 2010 Westbay Program Data Report. Report prepared for Hope Bay Mining Limited. 1CH008.013. February 2011.

SRK Consulting (Canada) Inc., 2011b. Groundwater Inflows and Inflow Water Quality for the Revised Doris North Project Water Licence Amendment Package. 2011.

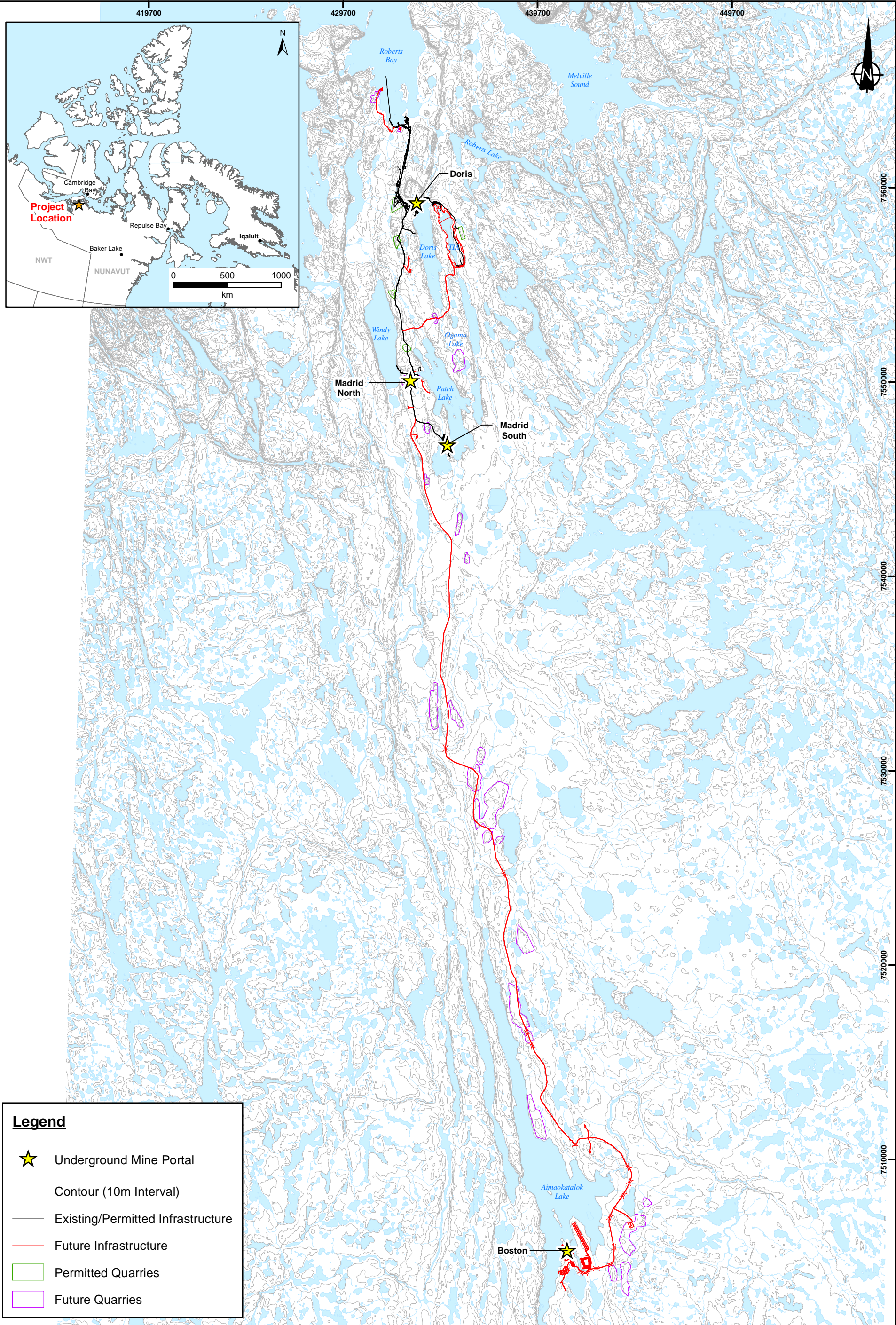
SRK Consulting (Canada) Inc., 2012. Hope Bay 2011 Groundwater Quality Report. Report prepared for Hope Bay Mining Limited. 1CH008.060. April 2012.

SRK Consulting (Canada) Inc., 2014a. 2011 Stage 2 Geotechnical and Hydrogeological Assessment for Doris Central and Connector Underground Mines. Report prepared for TMAC Resources Inc. 1CT022.001. April 2014.

SRK Consulting (Canada) Inc., 2014b. Hope Bay Project: Madrid Advanced Exploration Project: Underground Inflow Estimates. Memo prepared for TMAC Resources Inc. 1CT022.001. October 2014.

- SRK Consulting (Canada) Inc., 2015a. Hydrogeological Modeling of the Proposed Doris North Project, Hope Bay, Nunavut. Report prepared for TMAC Resources Inc. 1CT022.002. June 2015.
- SRK Consulting (Canada) Inc., 2015b. Doris North Project, Hope Bay - Water Quality Model Report. Report prepared for TMAC Resources Inc. 1CT022.002. May 2015.
- SRK Consulting (Canada) Inc., 2017. Madrid-Boston Project Water and Load Balance, Hope Bay Project. Report Prepared for TMAC Resources Inc. 1CT022.013. November 2017.
- Stevens CW. 2010a. Interannual Changes in Seasonal Ground Freezing and Near-surface Heat Flow beneath Bottom-fast Ice in the Near-shore Zone, Mackenzie Delta, NWT, Canada. Permafrost and Periglacial Processes 21: 256-270.
- Stevens CW. 2010b. Modeling Ground Thermal Conditions and the Limit of Permafrost within the Nearshore Zone of the Mackenzie Delta, Canada. Journal of Geophysical Research. 115: F04027.
- Stotler R.L., Shaun K. Frape, Ruskeeniemmi T., Ahonen L., Onstott T.C., Hobbs M.Y. 2009. Hydrogeochemistry of groundwaters in and below the base of thick permafrost at Lupin, Nunavut, Canada. Journal of Hydrology 373 (2009) 80–95.
- TMAC Resources Inc., 2015a. Revisions to TMAC Resources Inc. Amendment Application No. 1 of Project Certificate No. 003 and Water Licence 2AM-DOH1323. Prepared for the Nunavut Water Board. June 2015
- TMAC Resources Inc., 2015b. Electronic files. 3D Mine Plans for the Boston, Madrid South and Madrid North Mines, parsed with dates, based on Prefeasibility conditions. Sent by email from TMAC to SRK on December 7, 2015.
- TMAC Resources Inc., 2016a. Personal communication with Floyd Varley, Vice President Operations. Mine plan updated from Roscoe Postle Associates Inc. NI 43-101 Technical Report on the Hope Bay Project, Nunavut, Canada, March 2015.
- TMAC Resources Inc., 2016b. Electronic file. Excel spreadsheet "NEW DEIS Mine Production Plan -FINAL_20161013.xlsx". Sent by email from TMAC to SRK on October 13, 2016.
- TMAC Resources Inc., 2016c. Electronic file. Autocad 3D resource wireframes in dxf format. "TMAC_Resource.zip". Sent by email from TMAC to SRK on October 18, 2016.
- TMAC Resources Inc., 2017, Madrid—Boston of the Hope Bay Project, FINAL ENVIRONMENTAL IMPACT STATEMENT, Volume 3 - Project Description and Alternatives. December 2017
- Van Everdingen, 1998 revised May 2005. Multi-language Glossary of Permafrost and Related Ground-ice Terms. Boulder, CO: National Snow and Ice Data Center.

Figures



Legend

- ★ Underground Mine Portal
- Contour (10m Interval)
- Existing/Permitted Infrastructure
- Future Infrastructure
- Permitted Quarries
- Future Quarries

Notes:
1. Coordinate System: NAD 1983 UTM Zone 13N
2. Base Topo Data: CanVec, Natural Resources Canada



Project No: 1CT022.004.200.10
Filename: 1CT022.004.200.10_Fig_1_GroundwaterSite_mzs

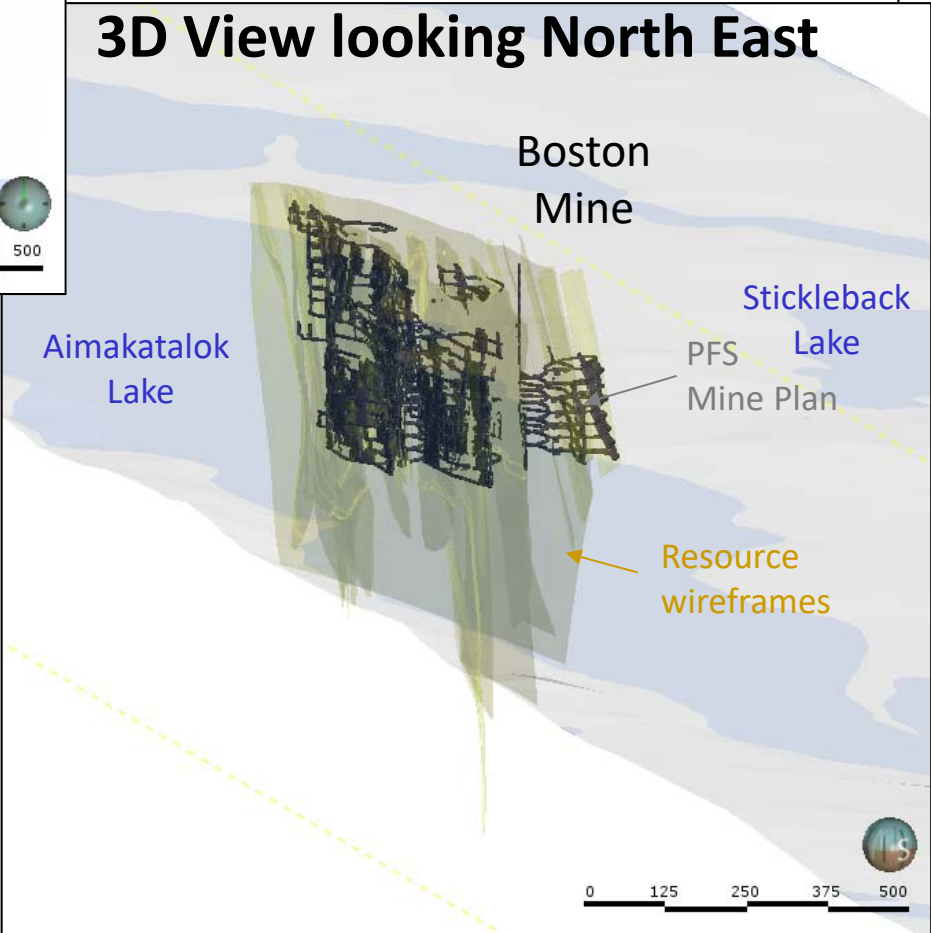
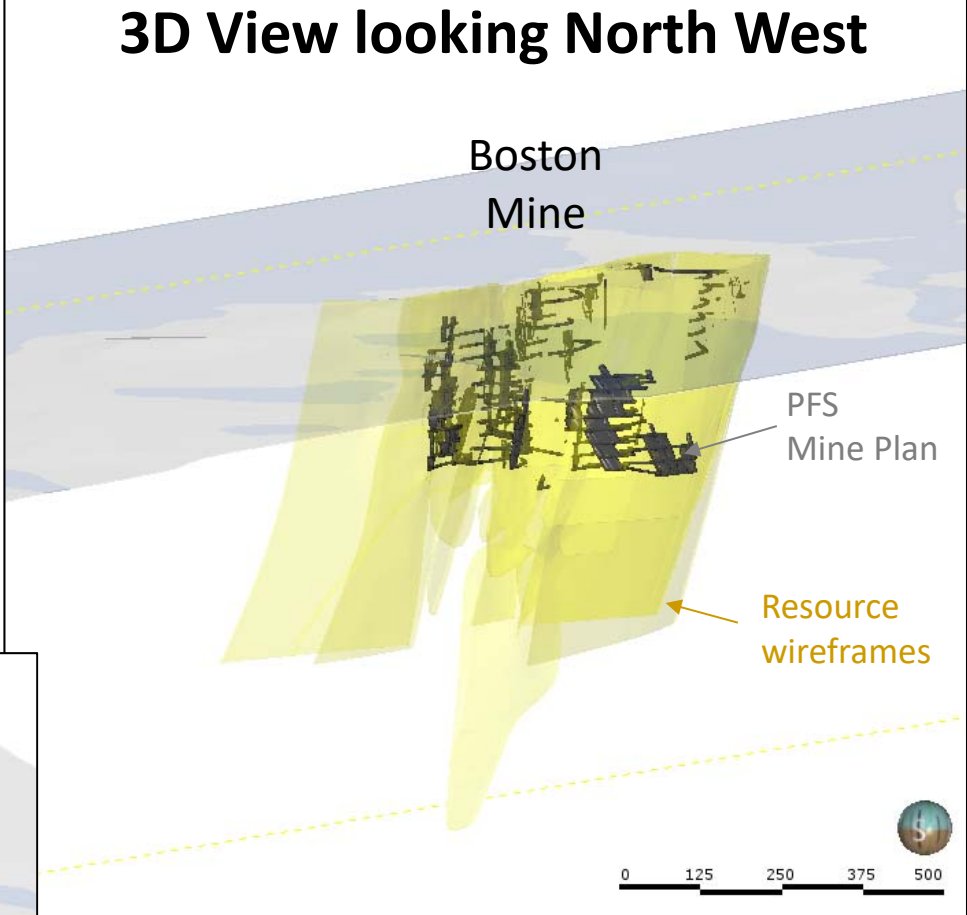
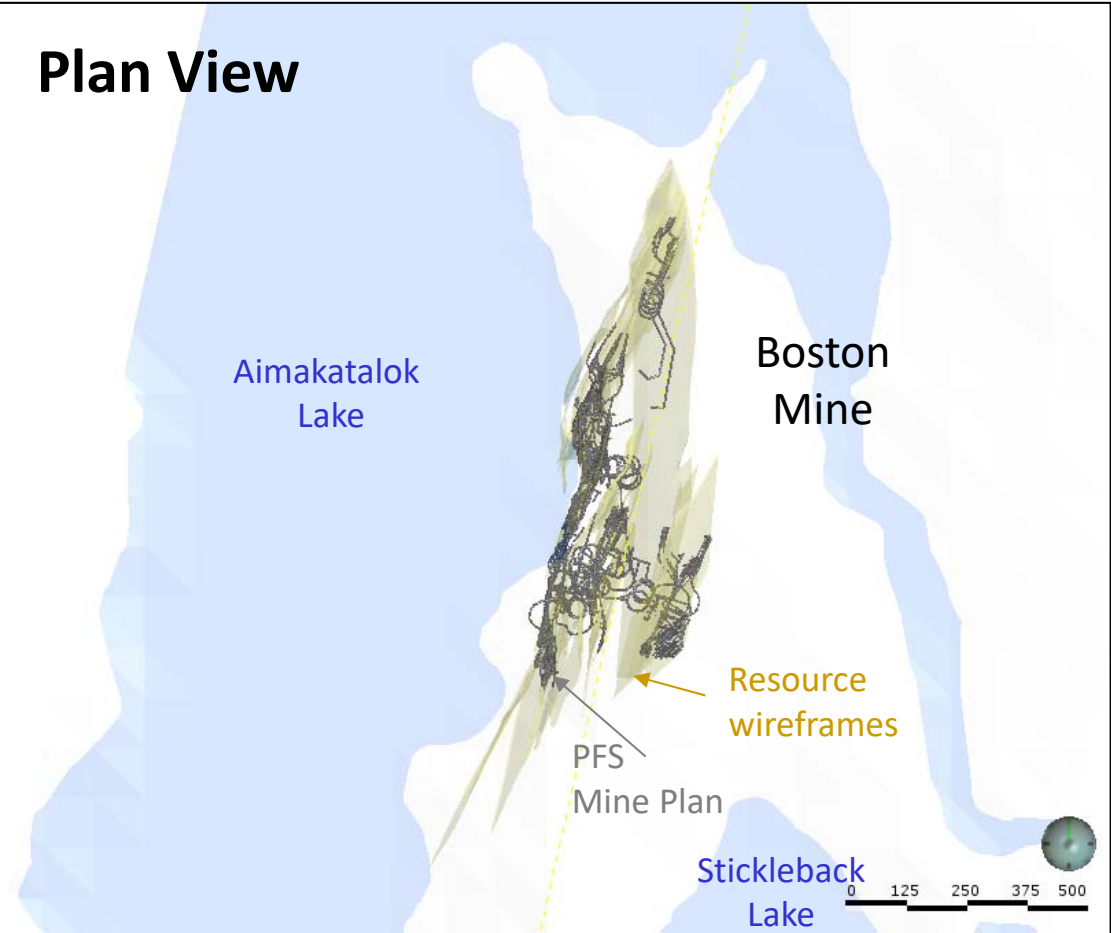


HOPE BAY PROJECT

Groundwater Modeling Report

Site Location Map

Date: Oct 2017	Approved: GF	Figure: 1
-------------------	-----------------	---------------------



Note:
 Prefeasibility mine plan shown, which will be updated as mining progresses.



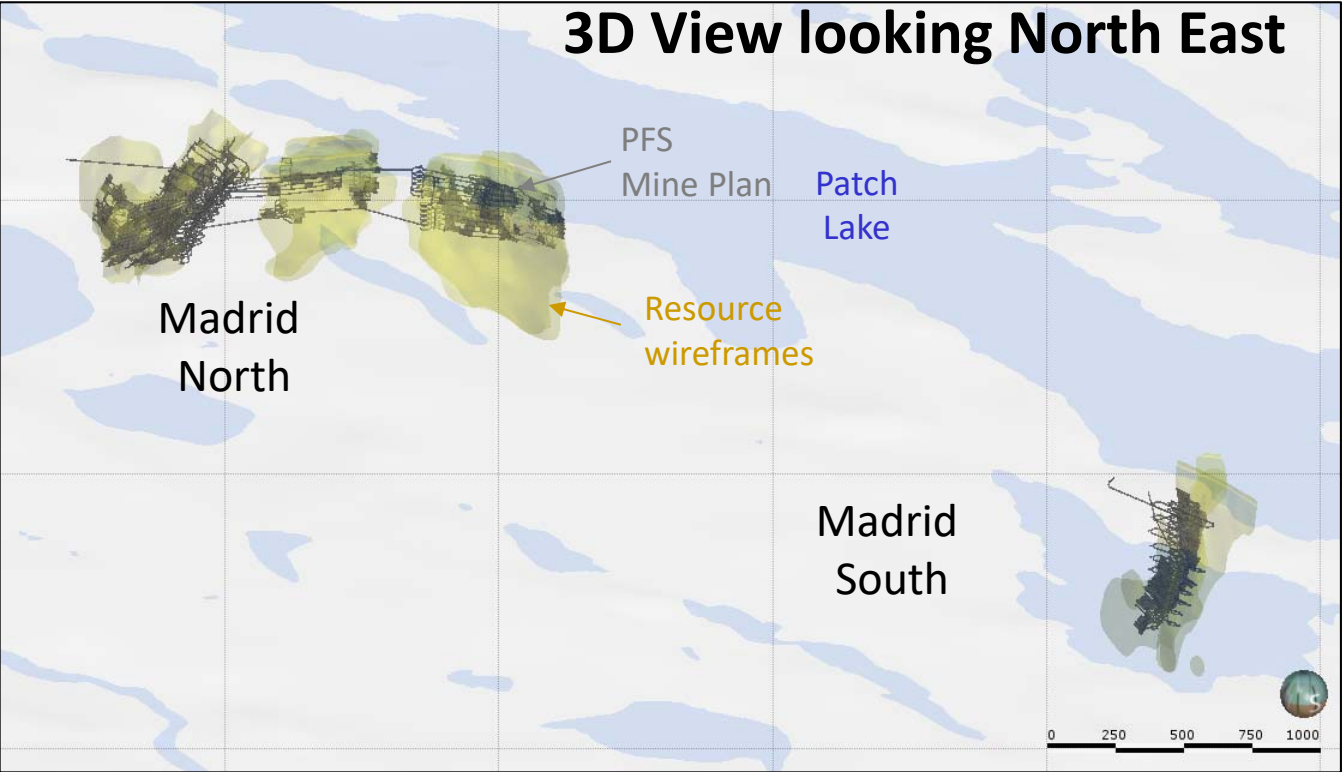
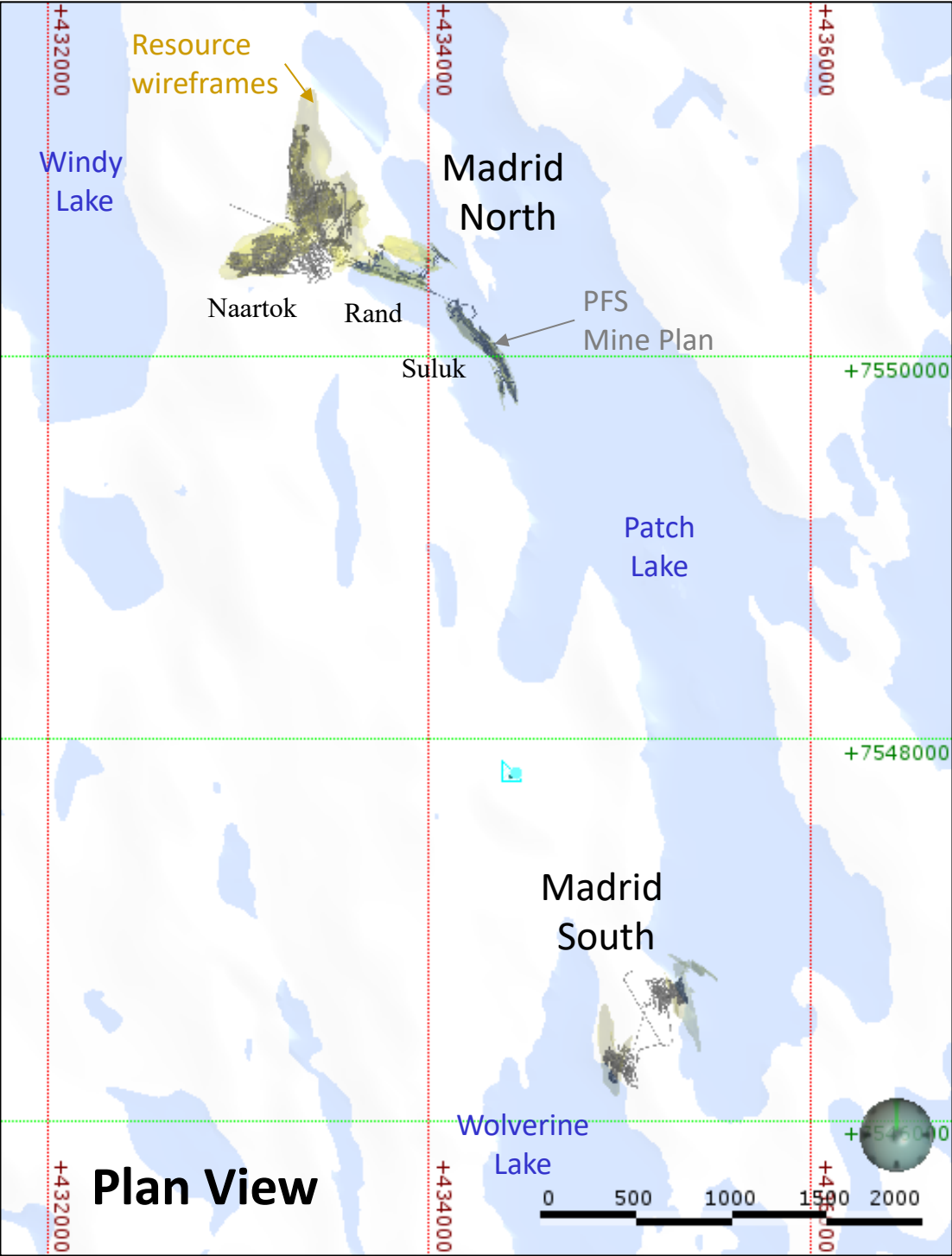
Hydrogeological Modeling

Boston Mine Views

Job No: 1CT022.013
 Filename: 1CT022.013_FEIS_Fig_11x17_Lndscp.pptx

Hope Bay Project

Date: Nov. 2017	Approved: GF	Figure: 2
--------------------	-----------------	---------------------



Note:
Prefeasibility mine plan shown, which will be updated as mining progresses.



Job No: 1CT022.013
Filename: 1CT022.013_FEIS_Fig_11x17_Lndscp.pptx

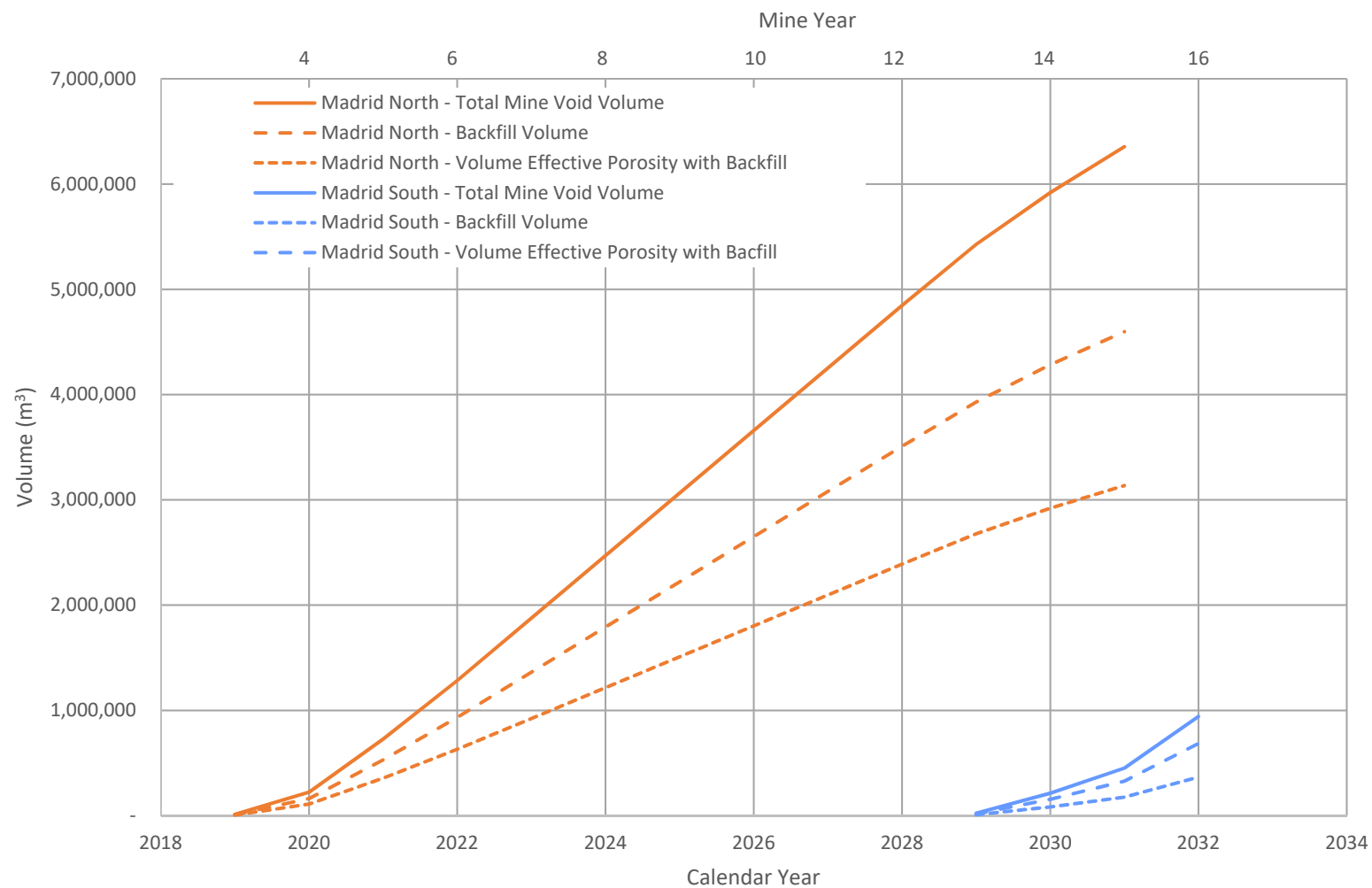


Hope Bay Project

Hydrogeological Modeling

**Madrid South and Madrid North
Mine Views**

Date: Nov. 2017	Approved: GF	Figure: 3
--------------------	-----------------	---------------------



Note:

The assumed in-place density and porosity of backfill is respectively 1.6 t/m³ and 30%.



Hydrogeological Modeling

Mine Void Volumes Over Time

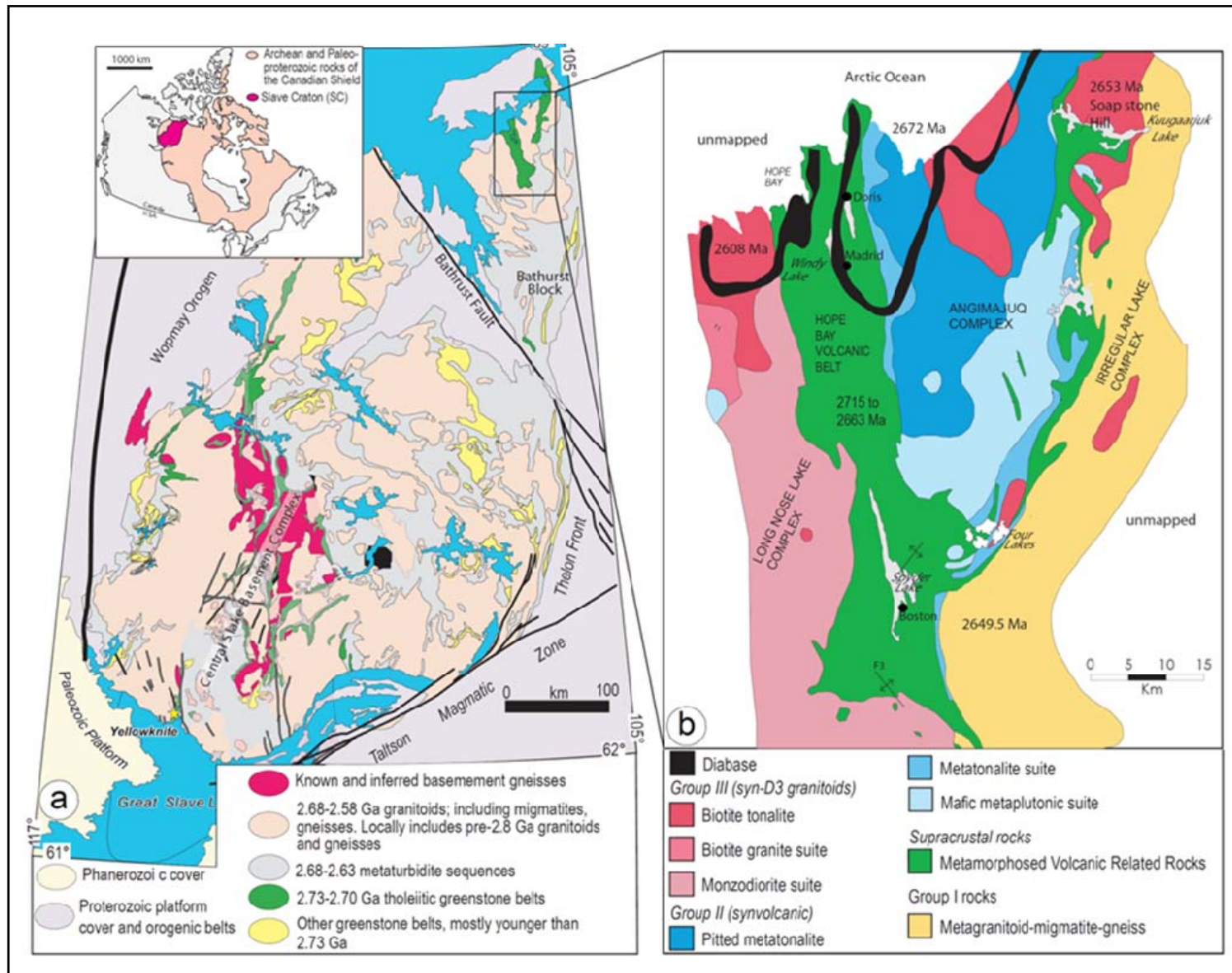
Job No: 1CT022.013
Filename: 1CT022.013_FEIS_Fig_8x11_Lndscp.pptx

Hope Bay Project

Date:
Nov. 2017

Approved:
GF

Figure: **4**



Note:

a) Regional geology of the Slave Structural Province (Craton).

b) Simplified geology of the Hope Bay Volcanic Belt (greenstone belt), from Mvondo et al. (2012).

srk consulting

Job No: 1CT022.013
Filename: 1CT022.013_FEIS_Fig_8x11_Lndscp.pptx

TMAC
RESOURCES

Hope Bay Project

Hydrogeological Modeling

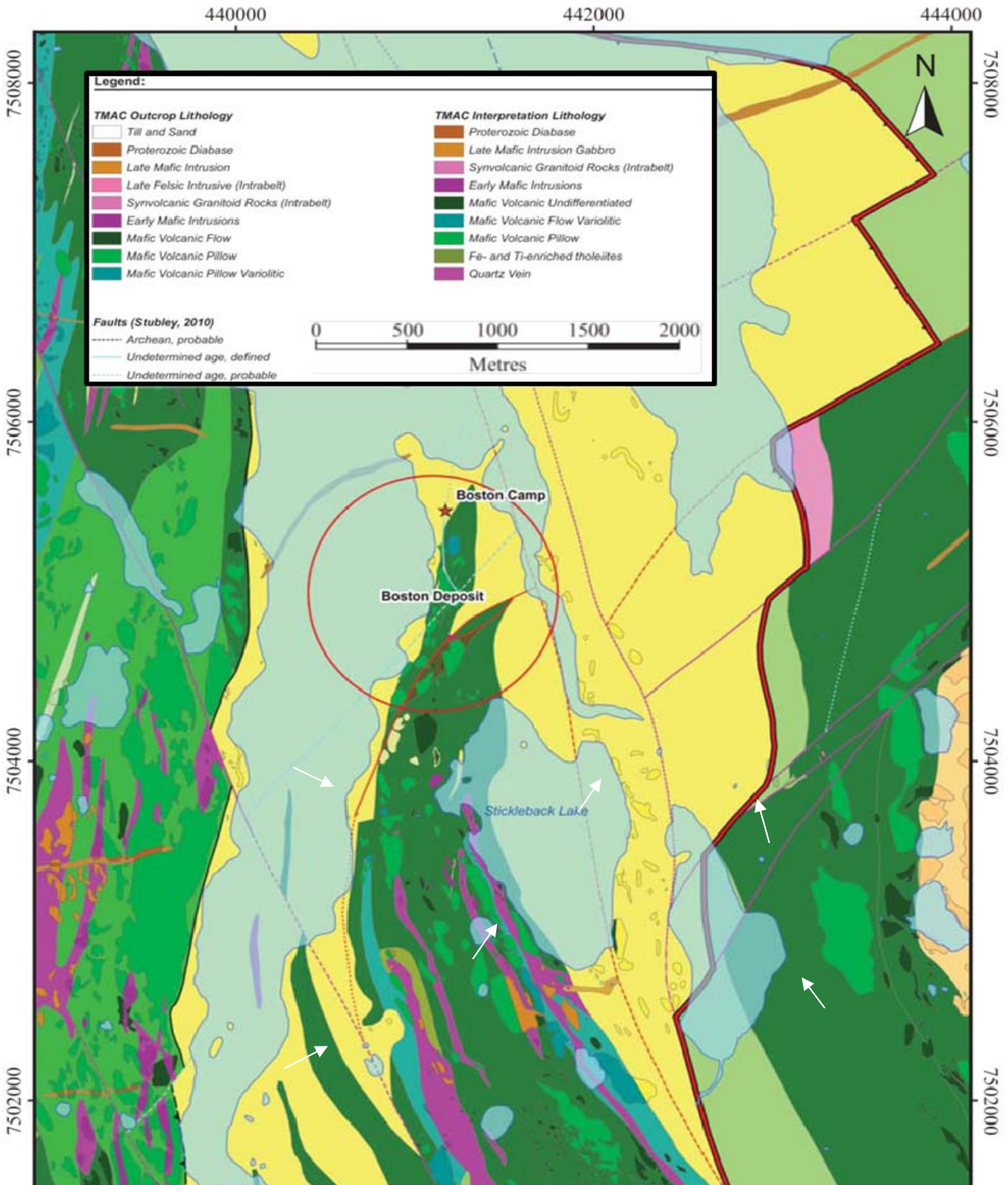
Regional Geology

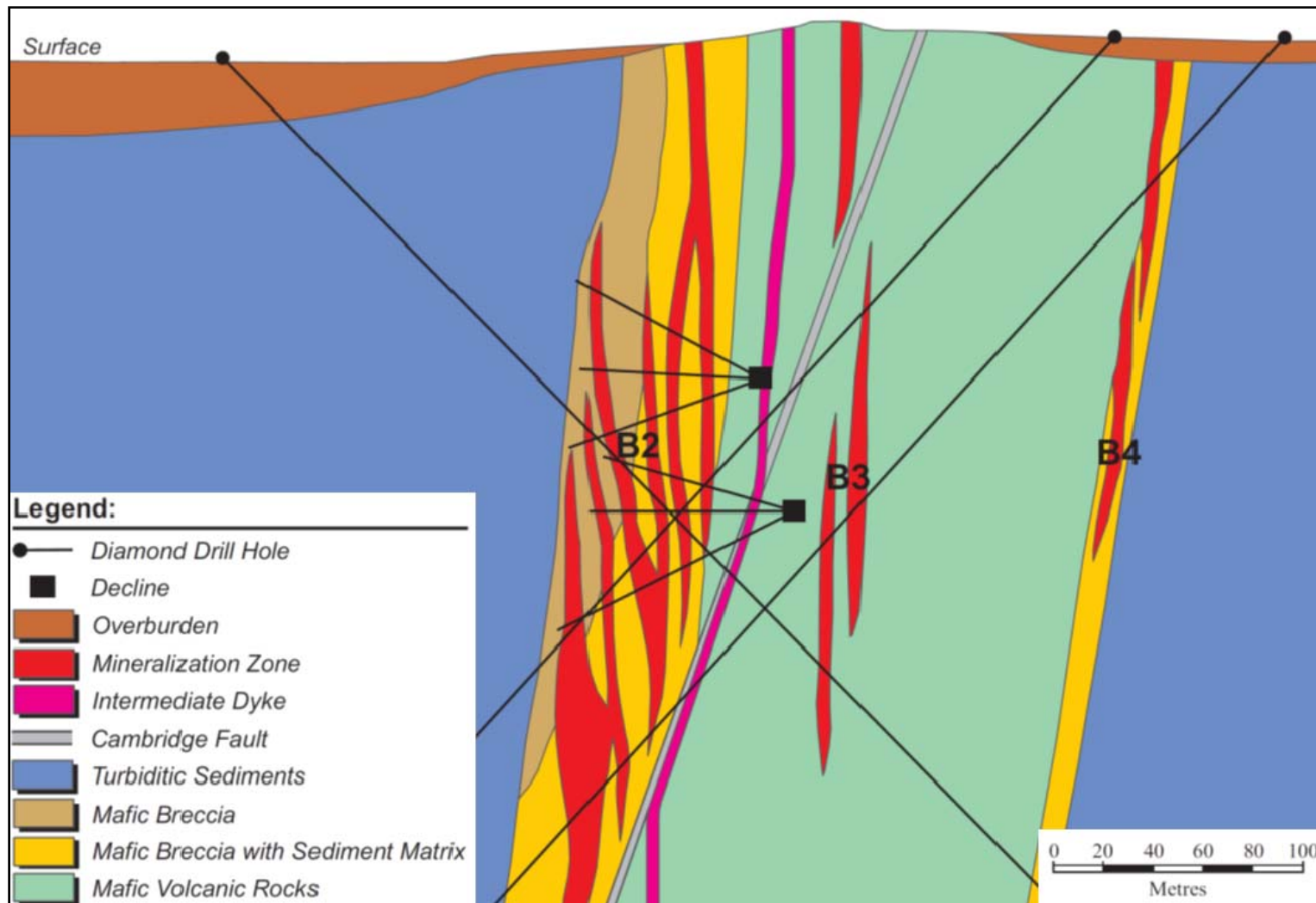
Date:
Nov. 2017

Approved:
GF

Figure:
5

Quaternary surficial sediments are shown in yellow.
Roscoe Postle Associates Inc., 2015





Source: Roscoe Postle Associates Inc., 2015

srk consulting

MAC
RESOURCES

Hydrogeological Modeling

Schematic Cross West-East
Section of the Boston Mineralization

Job No: 1CT022.013
Filename: 1CT022.013_FEIS_Fig_8x11_Lndscp.pptx

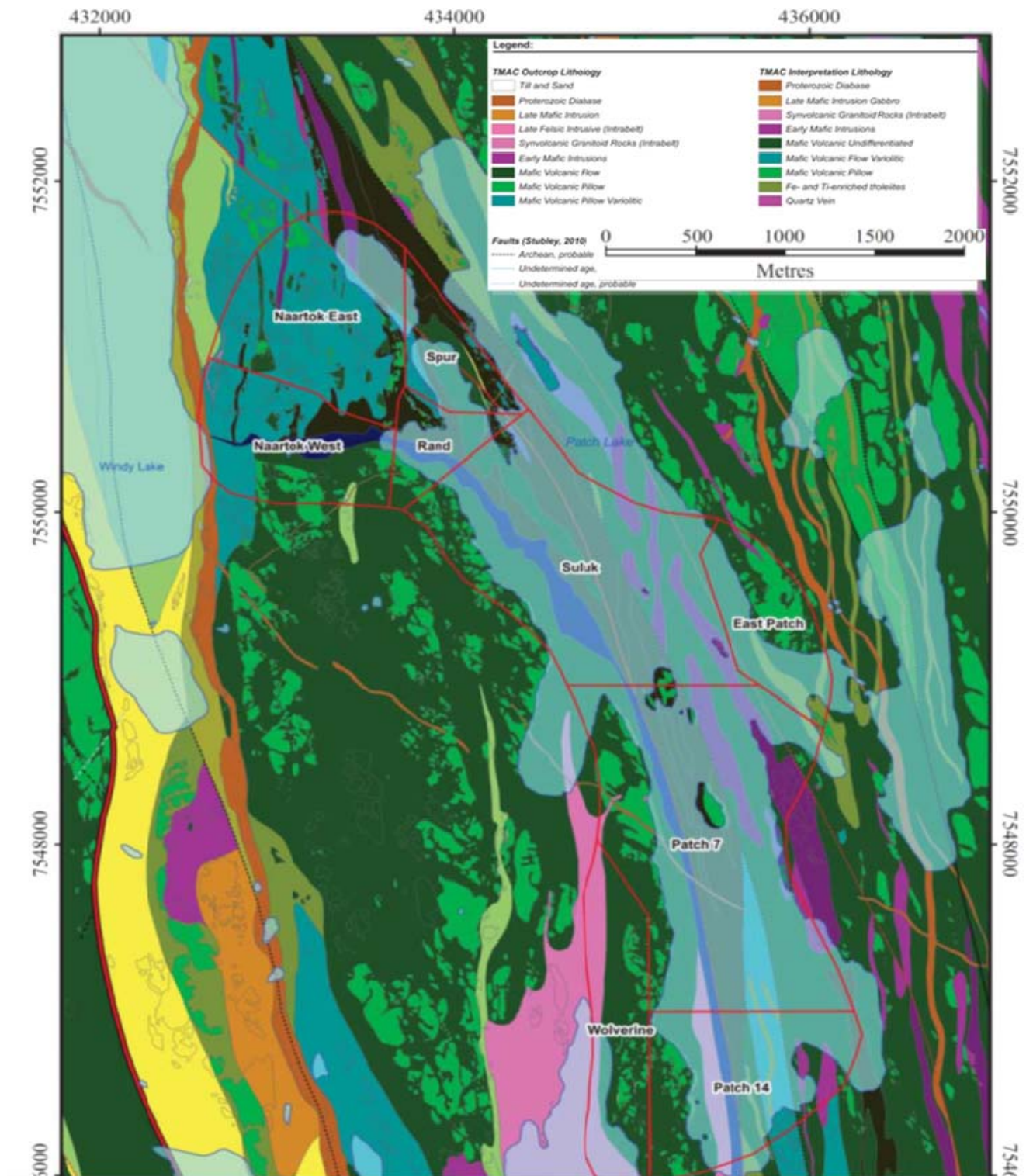
Hope Bay Project

Date:
Nov. 2017

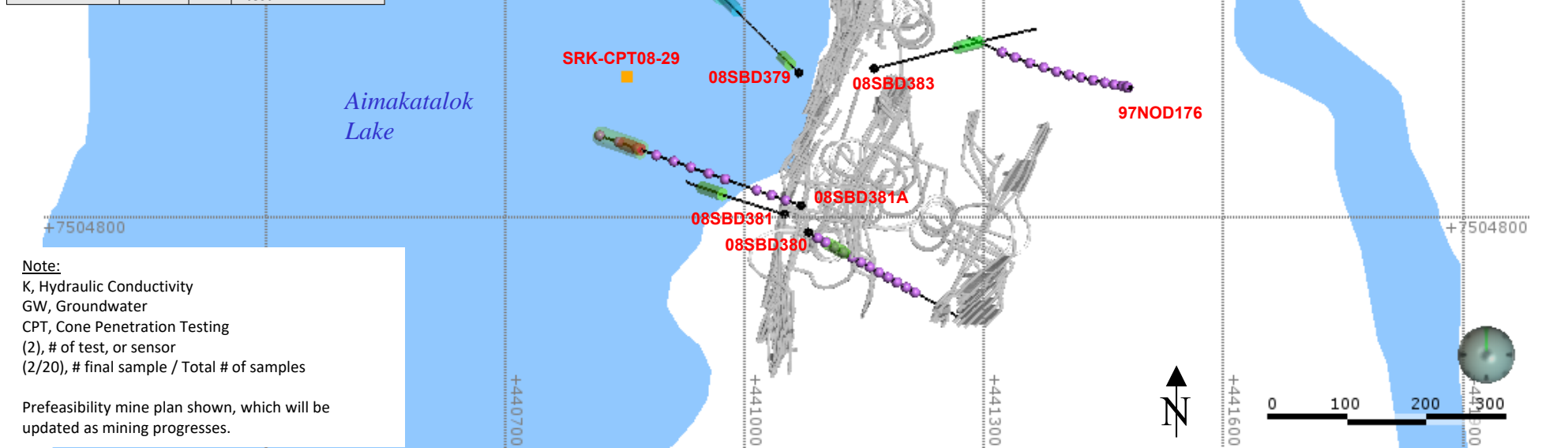
Approved:
GF

Figure: **7**

Quaternary surficial sediments are shown in yellow.
Roscoe Postle Associates Inc., 2015



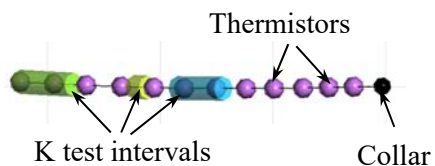
Hole ID	Length (m)	Dip (deg)	Data Type
08SBD379	332	52	K tests (3)
08SBD380	401	56	K tests (1) Thermistors (12)
08SBD381	244	58	K tests (1)
08SBD381A	401	48	K tests (2) Thermistors (12)
08SBD382	404	53	K tests (3) Thermistors (12)
08SBD383	356	54	K tests (1)
10WBW004	470	65	Westbay well K tests (9) Thermistors GW Samples (2/20)
97NOD176	367	54	Thermistors (14)
SRK-CPT08-29	6.1	90	CPT pressure dissipation Test
SRK-CPT08-31	12.8	90	CPT pressure dissipation Test
SRK-OB-VS-31	12.8	90	Lab. Consolidation test



Note:

K, Hydraulic Conductivity
 GW, Groundwater
 CPT, Cone Penetration Testing
 (2), # of test, or sensor
 (2/20), # final sample / Total # of samples

Prefeasibility mine plan shown, which will be updated as mining progresses.



srk consulting

Job No: 1CT022.013
 Filename: 1CT022.013_FEIS_Fig_8x11_Lndscp.pptx

TMAC
 RESOURCES

Hope Bay Project

Hydrogeological Modeling

Location Map of the
 Hydrogeological Data at Boston

Date: Nov. 2017	Approved: GF	Figure: 9
--------------------	-----------------	---------------------

Hole ID	Hole Length (m)	Dip (deg)	Data Type
08TDD628	141	61	K tests (1)
08TDD630	317	63	K tests (5) GW sample (1/1)
08TDD631	122	82	K tests (2)
08TDD632	401	61	K tests (4) Thermistors (12)
08TDD633	401	52	K tests (4)
08TDD634	140	59	K tests (1)
10WBW001	564	62	Westbay well K tests (17) Thermistors (12) GW samples (20/40)

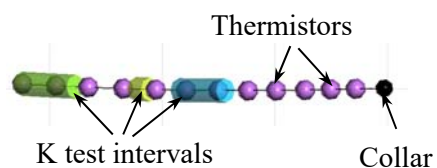
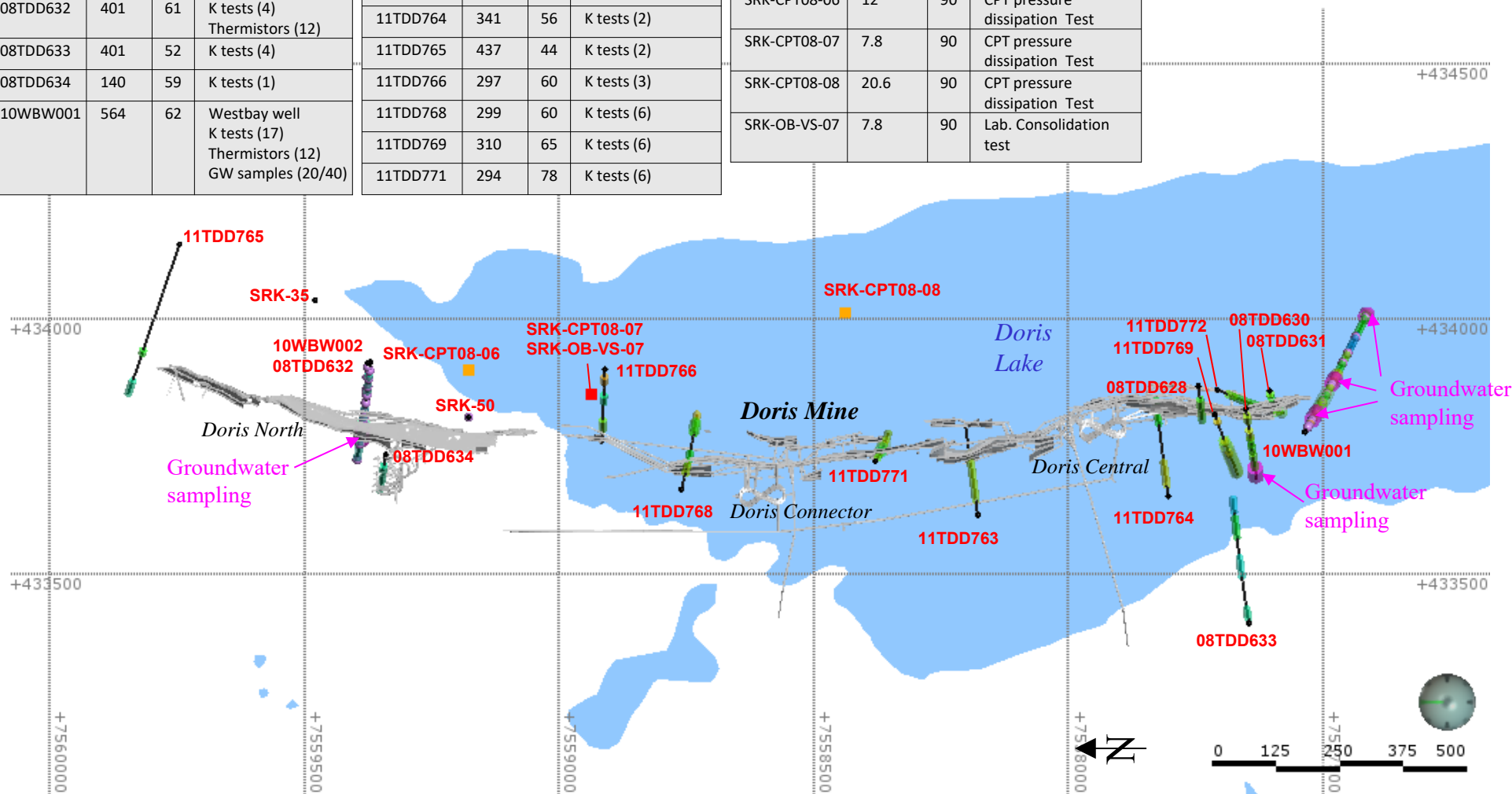
Hole ID	Hole Length (m)	Dip (deg)	Data Type
10WBW002	602	75	Westbay well K tests (5) Thermistors (8) GW Samples (0/15)
11TDD763	285	52	K tests (1)
11TDD764	341	56	K tests (2)
11TDD765	437	44	K tests (2)
11TDD766	297	60	K tests (3)
11TDD768	299	60	K tests (6)
11TDD769	310	65	K tests (6)
11TDD771	294	78	K tests (6)

Hole ID	Hole Length (m)	Dip (deg)	Data Type
11TDD772	330	65	K tests (5)
SRK-35	10	90	Thermistors (6)
SRK-50	200	90	Thermistors (13)
SRK-CPT08-06	12	90	CPT pressure dissipation Test
SRK-CPT08-07	7.8	90	CPT pressure dissipation Test
SRK-CPT08-08	20.6	90	CPT pressure dissipation Test
SRK-OB-VS-07	7.8	90	Lab. Consolidation test

Note:

K, Hydraulic Conductivity
GW, Groundwater
CPT, Cone Penetration Testing
(2), # of test, or sensor
(2/20), # final sample / Total # of samples

Prefeasibility mine plan shown, which will be updated as mining progresses.



srk consulting

Job No: 1CT022.013
Filename: 1CT022.013_FEIS_Fig_8x11_Lndscp.pptx

TMAC
RESOURCES

Hope Bay Project

Hydrogeological Modeling

Location Map of the
Hydrogeological Data at Doris

Date:
Nov. 2017

Approved:
GF

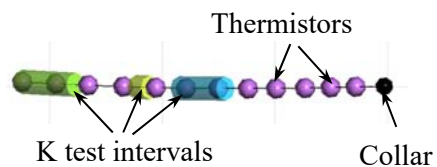
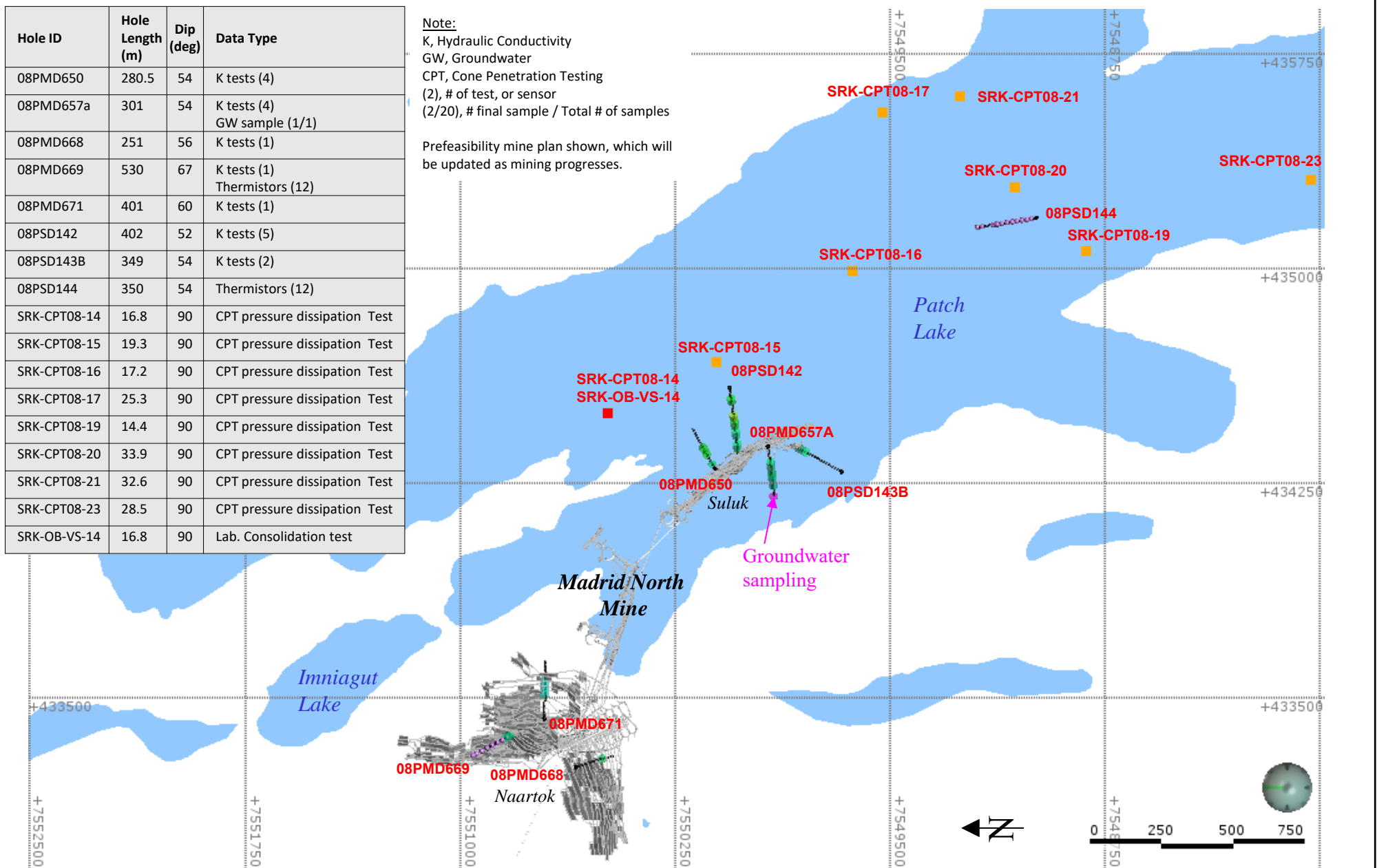
Figure:
10

Hole ID	Hole Length (m)	Dip (deg)	Data Type
08PMD650	280.5	54	K tests (4)
08PMD657a	301	54	K tests (4) GW sample (1/1)
08PMD668	251	56	K tests (1)
08PMD669	530	67	K tests (1) Thermistors (12)
08PMD671	401	60	K tests (1)
08PSD142	402	52	K tests (5)
08PSD143B	349	54	K tests (2)
08PSD144	350	54	Thermistors (12)
SRK-CPT08-14	16.8	90	CPT pressure dissipation Test
SRK-CPT08-15	19.3	90	CPT pressure dissipation Test
SRK-CPT08-16	17.2	90	CPT pressure dissipation Test
SRK-CPT08-17	25.3	90	CPT pressure dissipation Test
SRK-CPT08-19	14.4	90	CPT pressure dissipation Test
SRK-CPT08-20	33.9	90	CPT pressure dissipation Test
SRK-CPT08-21	32.6	90	CPT pressure dissipation Test
SRK-CPT08-23	28.5	90	CPT pressure dissipation Test
SRK-OB-VS-14	16.8	90	Lab. Consolidation test

Note:

K, Hydraulic Conductivity
 GW, Groundwater
 CPT, Cone Penetration Testing
 (2), # of test, or sensor
 (2/20), # final sample / Total # of samples

Prefeasibility mine plan shown, which will be updated as mining progresses.



srk consulting

Job No: 1CT022.013
 Filename: 1CT022.013_FEIS_Fig_8x11_Lndscp.pptx

TMAC
 RESOURCES

Hope Bay Project

Hydrogeological Modeling

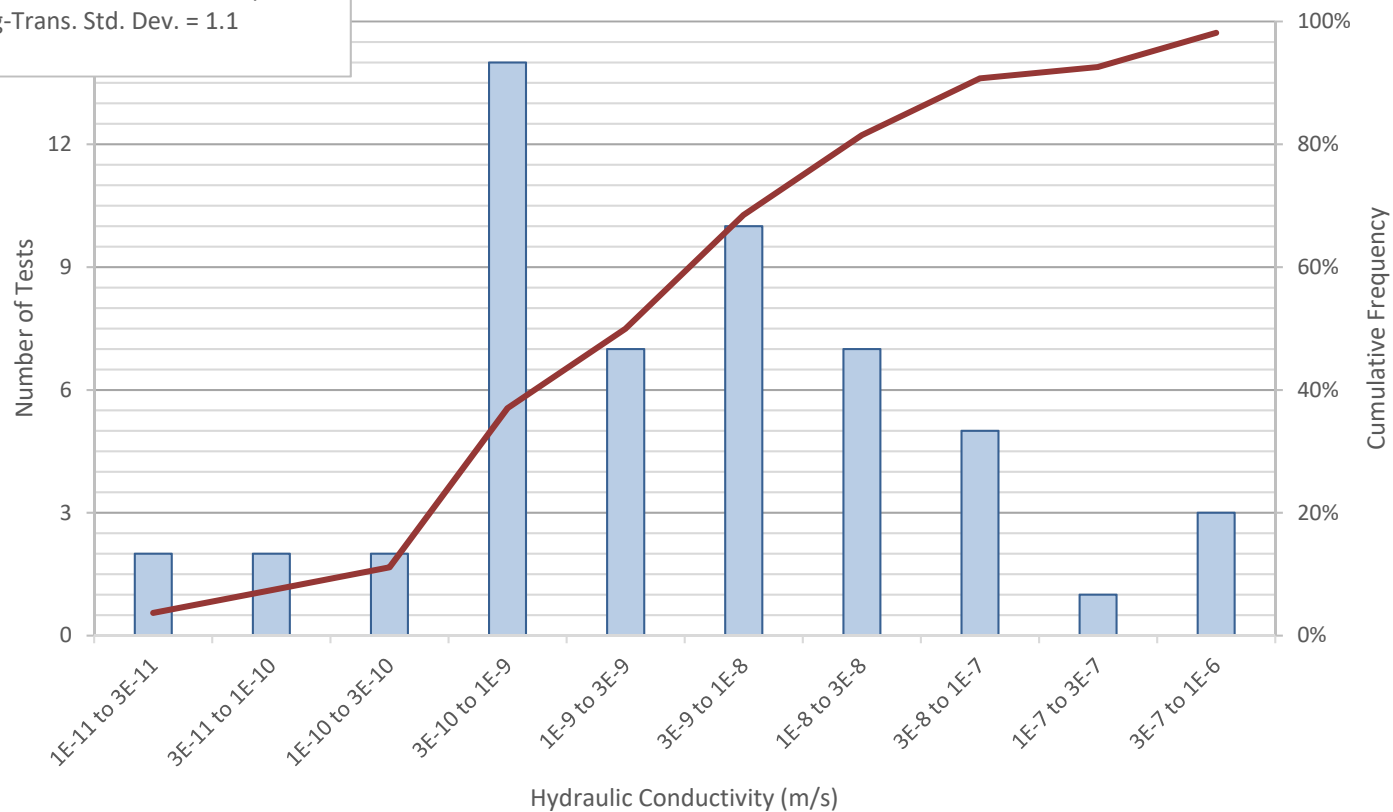
Location Map of the
 Hydrogeological Data
 at Madrid North

Date:
 Nov. 2017

Approved:
 GF

Figure:
11

Arithmetic Mean = 5E-8 m/s
 Geometric Mean = 3E-9 m/s
 Harmonic Mean = 2E-10 m/s
 Log-Trans. Std. Dev. = 1.1



■ Histogram
 — Cumulative Frequency

Source: Boston_Madrid_K_Statistical Summary.xlsx



Hydrogeological Modeling

Statistical Summary of
the K Measurements

Job No: 1CT022.013
 Filename: 1CT022.013_FEIS_Fig_8x11_Lndscp.pptx

Hope Bay Project

Date:
Nov. 2017

Approved:
GF

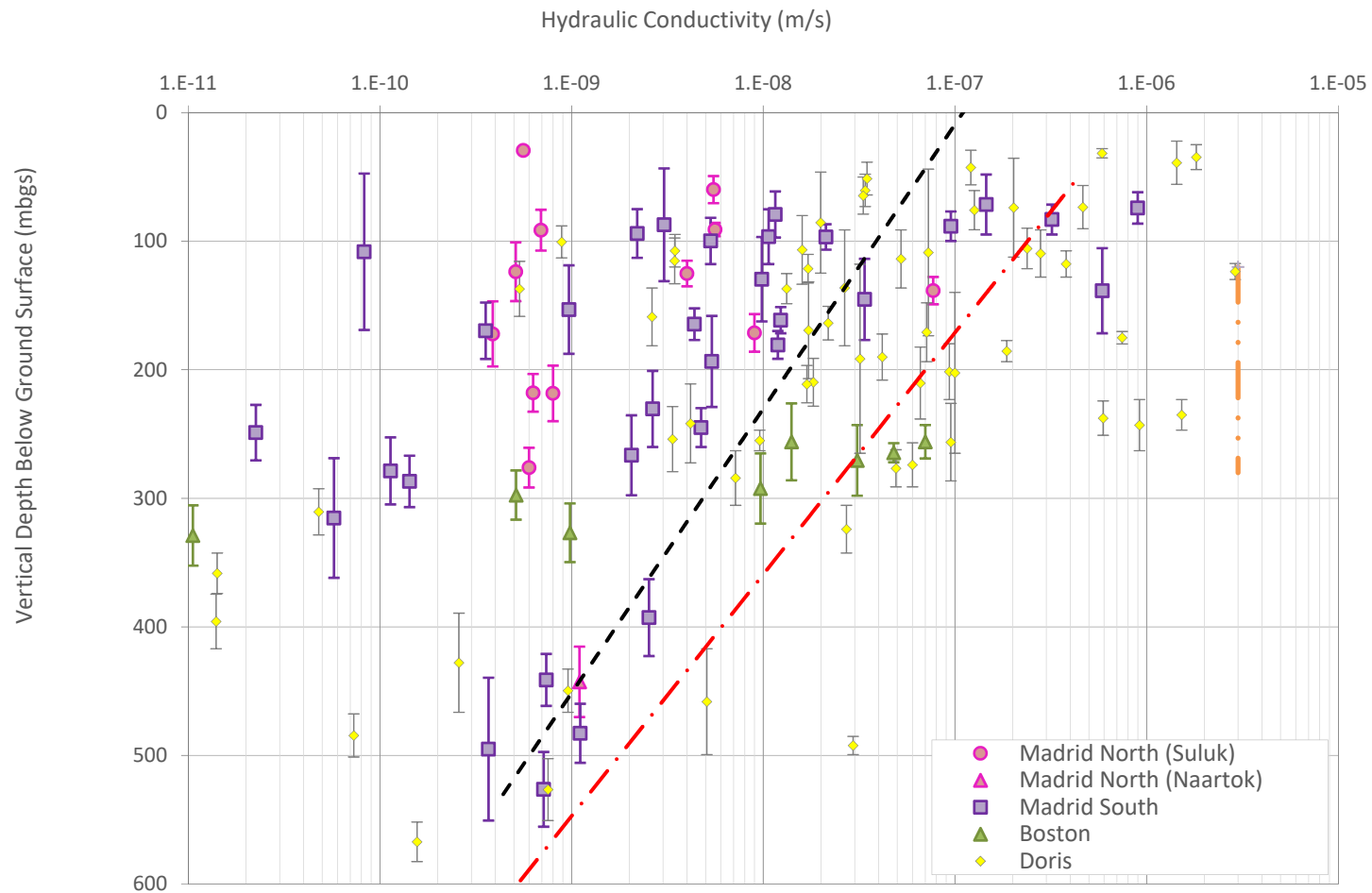
Figure: **13**

Note:

The black dashed line is a function of K with depth based on a moving geometric mean (i.e., function used in base case model).

The red dashed line is a function of K based on a moving arithmetic mean (i.e., function used to test model sensitivity to high K).

The orange dashed line is a function based on the highest K values of the Hope Bay project, reported at Doris North (i.e., to test model sensitivity to permeable faults).



Source: !HB_Master_PackerDataSummary.rev16.gf.xlsx



Hydrogeological Modeling

K vs Depth

Job No: 1CT022.013

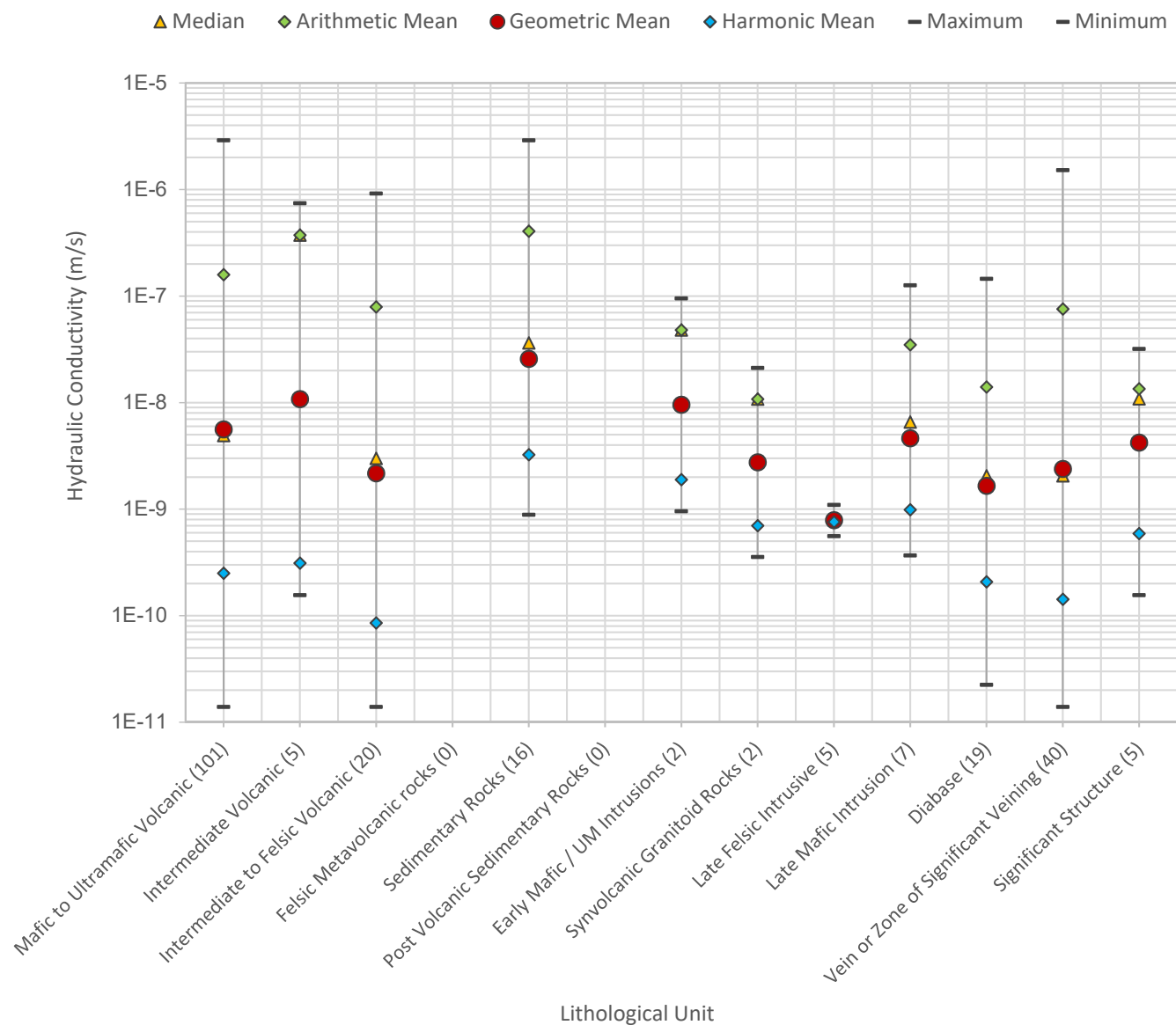
Filename: 1CT022.013_FEIS_Fig_8x11_Lndscp.pptx

Hope Bay Project

Date:
Nov. 2017

Approved:
GF

Figure: **14**



Source: KvsLithoFF_Rev02.xlsx



Hydrogeological Modeling

K vs Geological Units

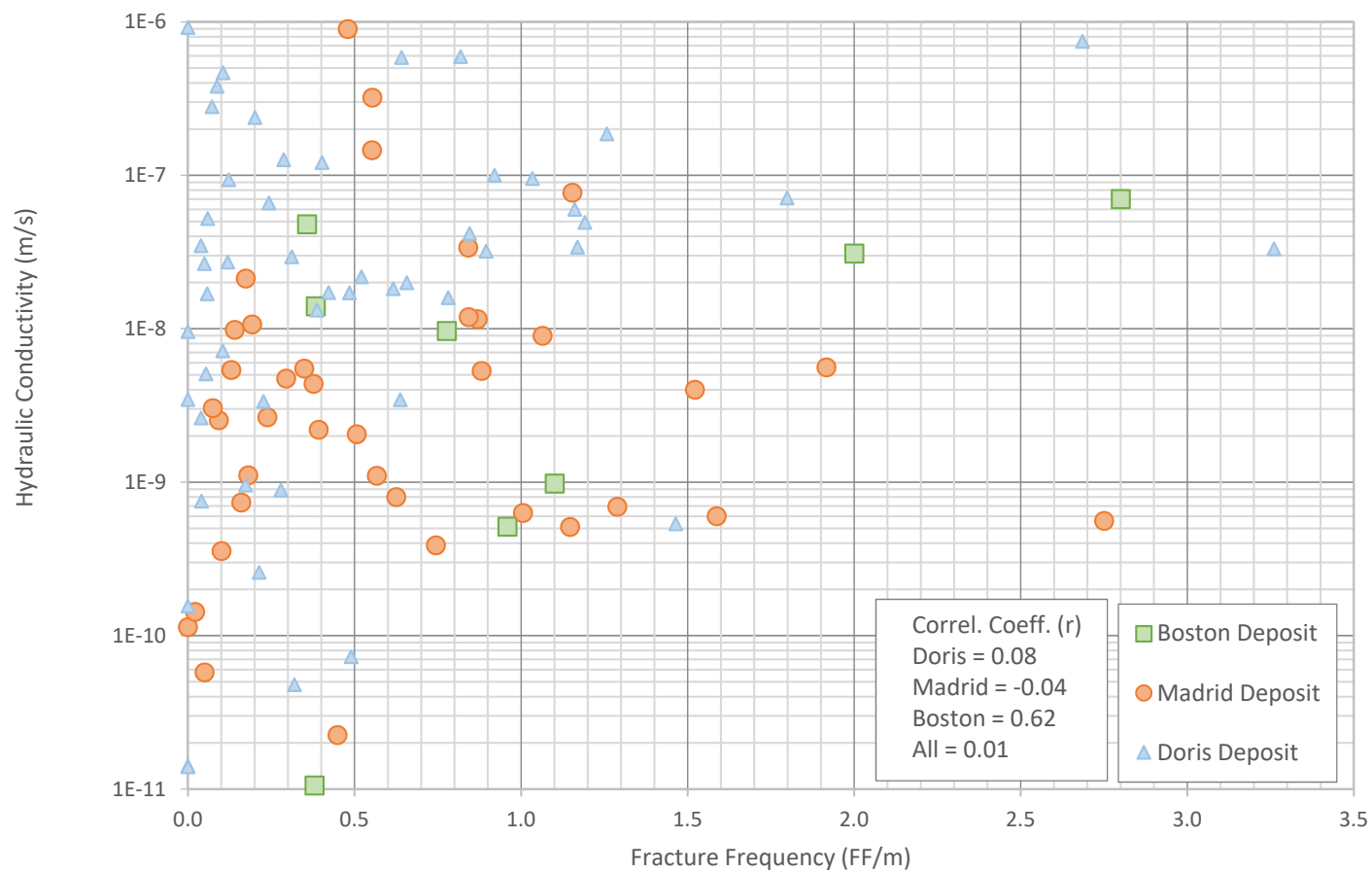
Job No: 1CT022.013
Filename: 1CT022.013_FEIS_Fig_8x11_Lndscp.pptx

Hope Bay Project

Date:
Nov. 2017

Approved:
GF

Figure: **15**



Source: KvsLithoFF_Rev02.xlsx



Hydrogeological Modeling

Correlation K vs Fracture Frequency

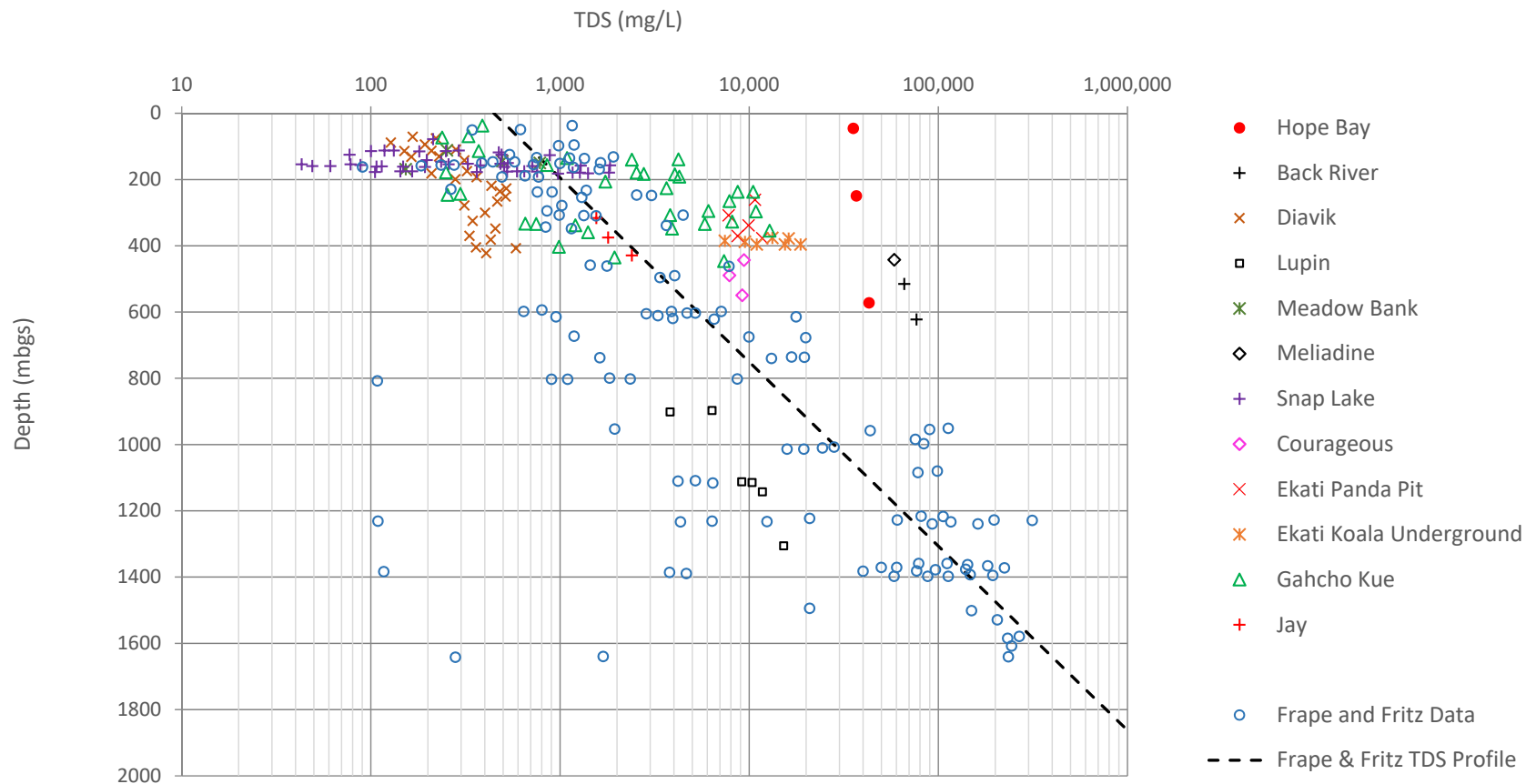
Job No: 1CT022.013
 Filename: 1CT022.013_FEIS_Fig_8x11_Lndscp.pptx

Hope Bay Project

Date:
 Nov. 2017

Approved:
 GF

Figure: **16**



Source: Compilation of TDS data Versus Depth_20151130.GF.xlsx



Hydrogeological Modeling

TDS Concentrations with Depth
in Canada's North

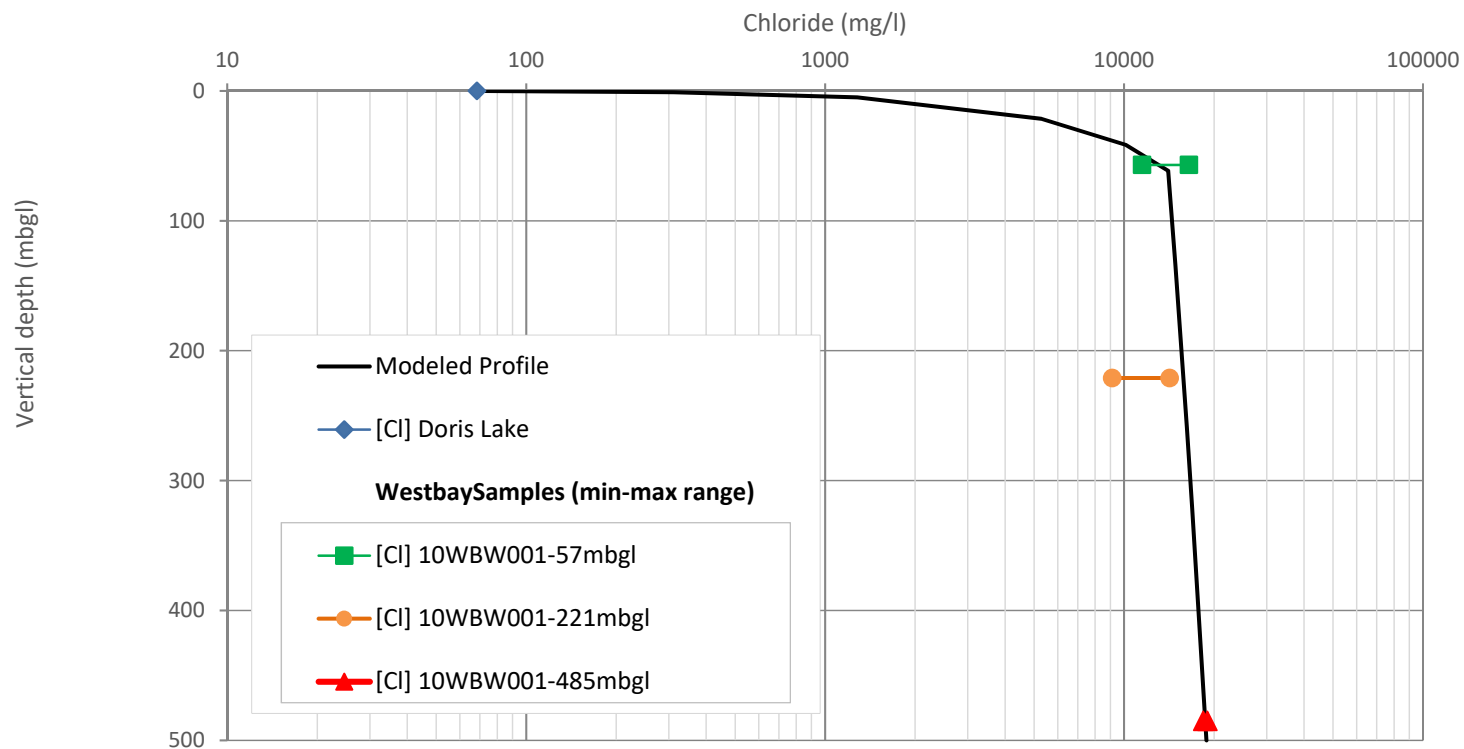
Job No: 1CT022.013
Filename: 1CT022.013_FEIS_Fig_8x11_Lndscp.pptx

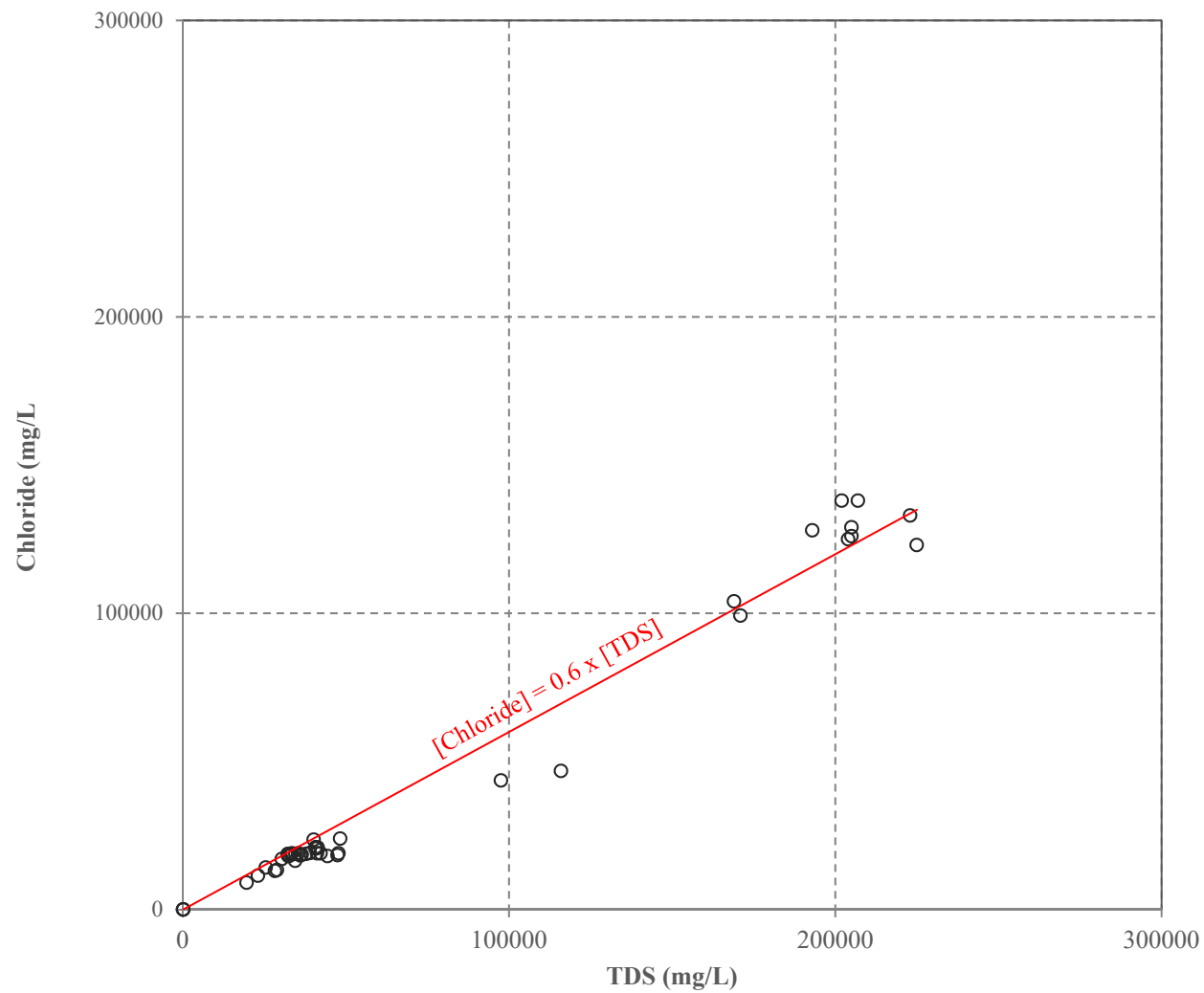
Hope Bay Project

Date:
Nov. 2017

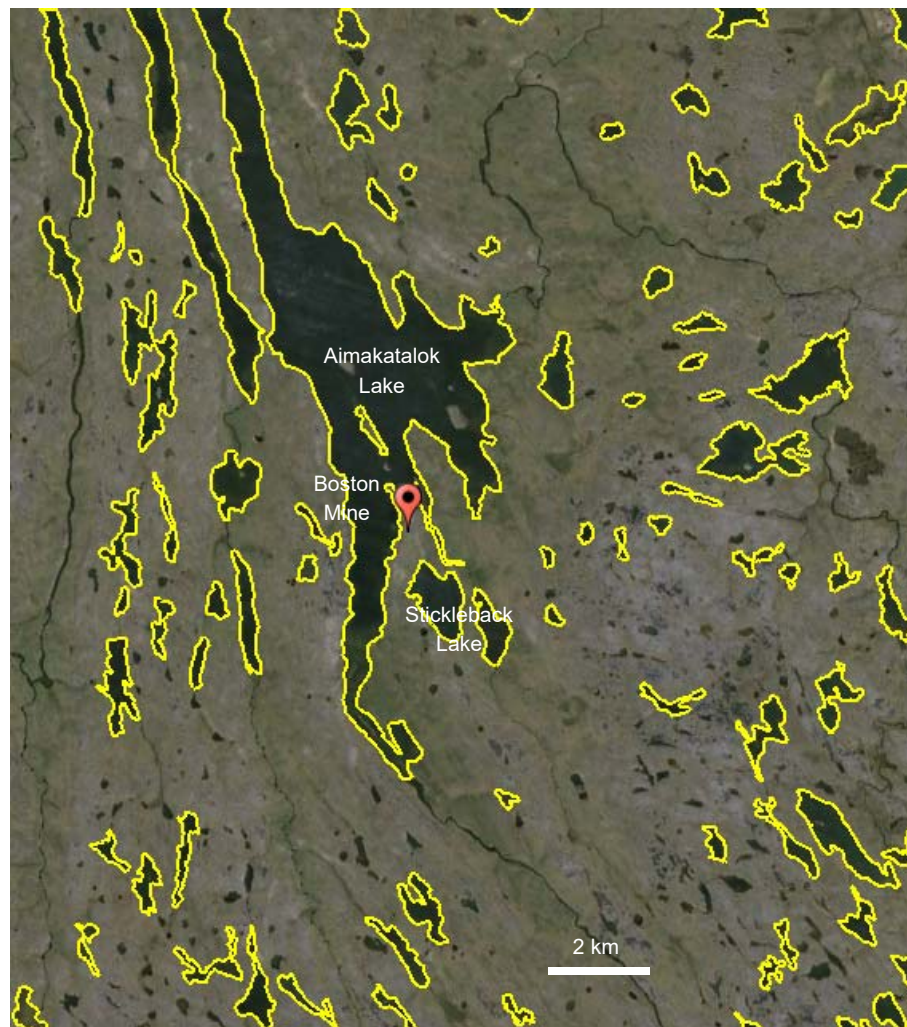
Approved:
GF

Figure: **17**

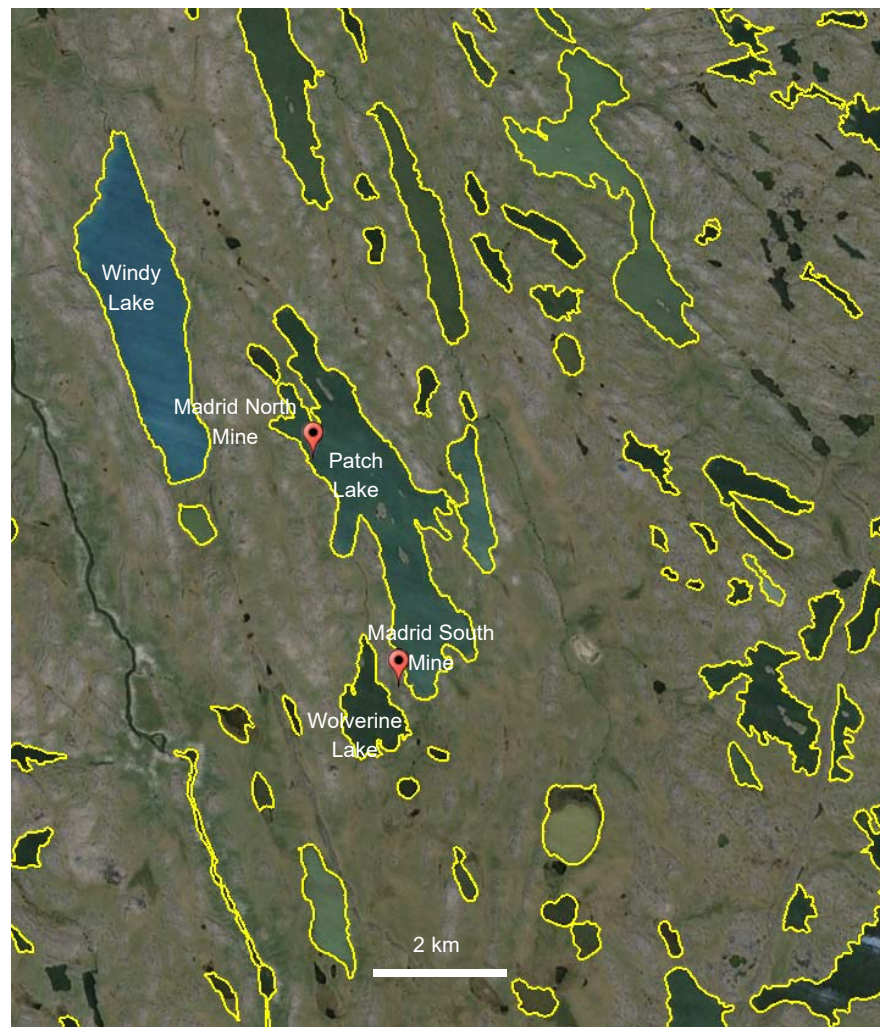




Boston Area



Madrid Area



Lakes with yellow contours are estimated to be potential open taliks



Job No: 1CT022.013
Filename: 1CT022.013_FEIS_Fig_8x11_Lndscp.pptx



Hope Bay Project

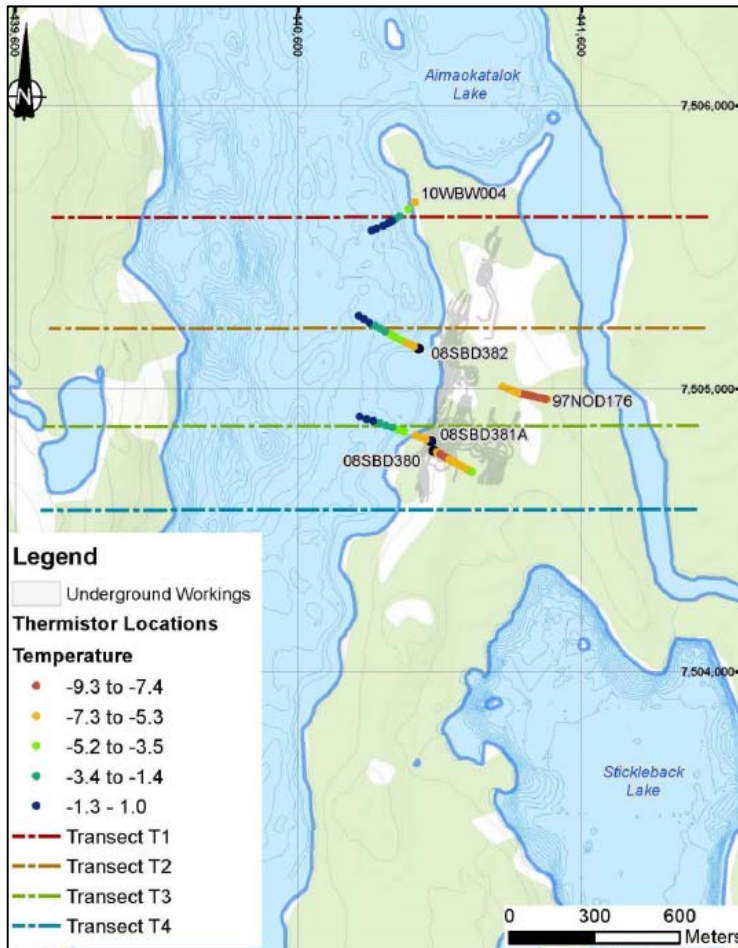
Hydrogeological Modeling

Potential Through Taliks
at Boston and Madrid

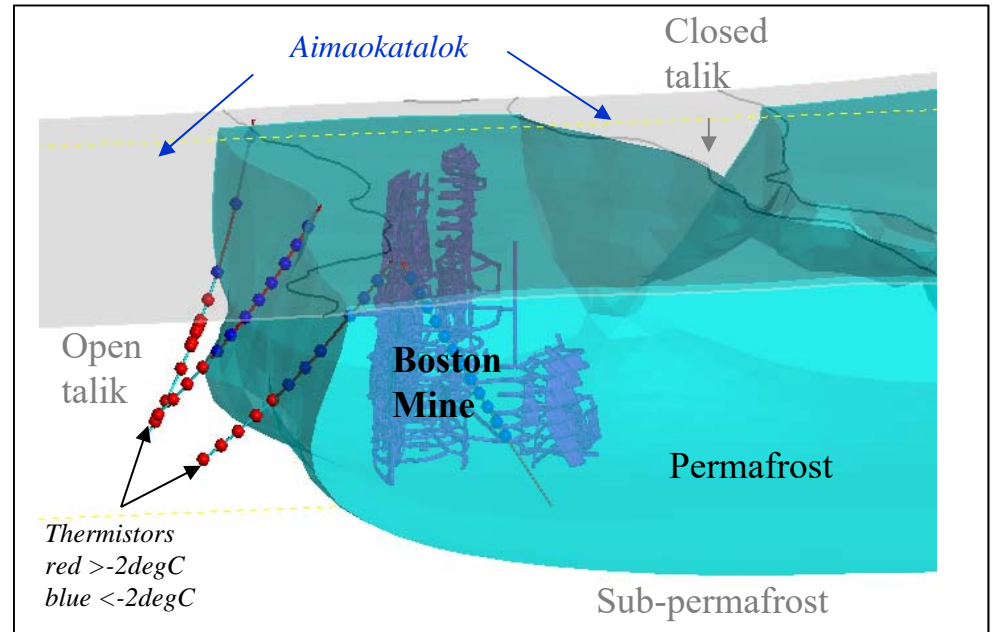
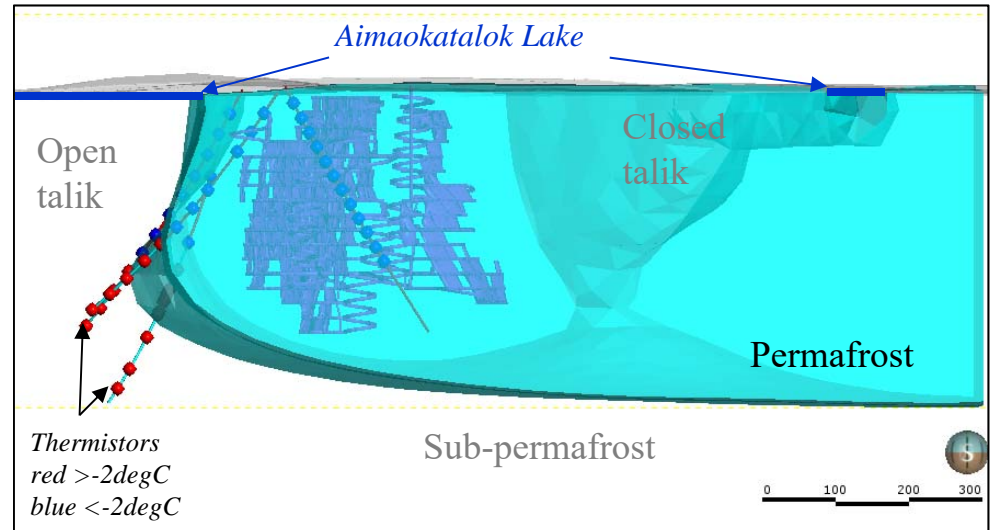
Date:
Nov. 2017

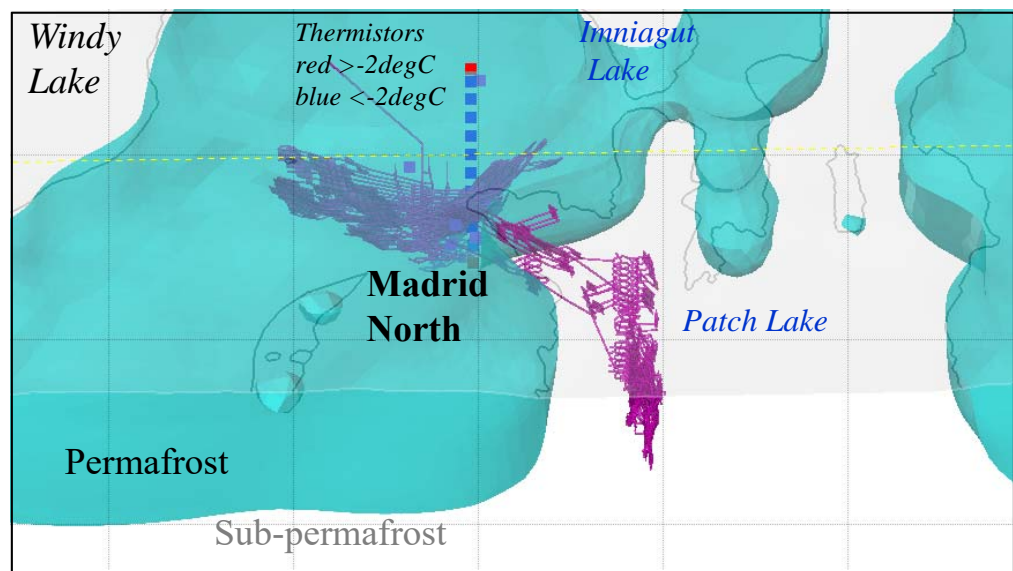
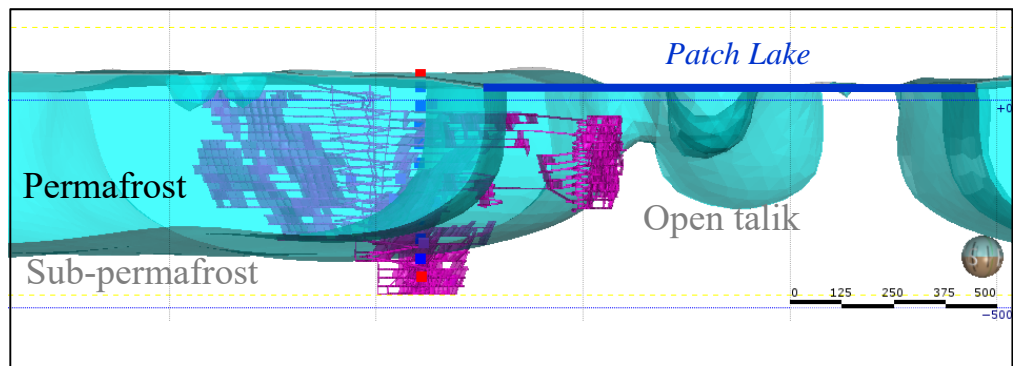
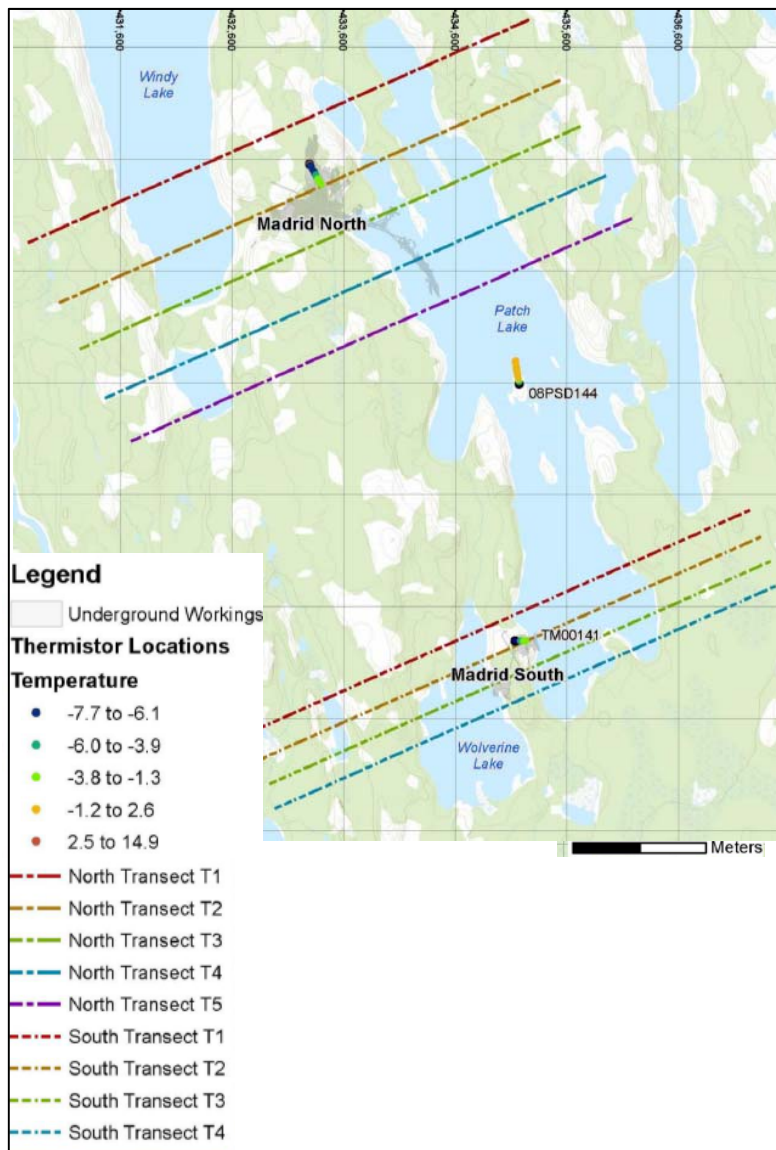
Approved:
GF

Figure: **20**

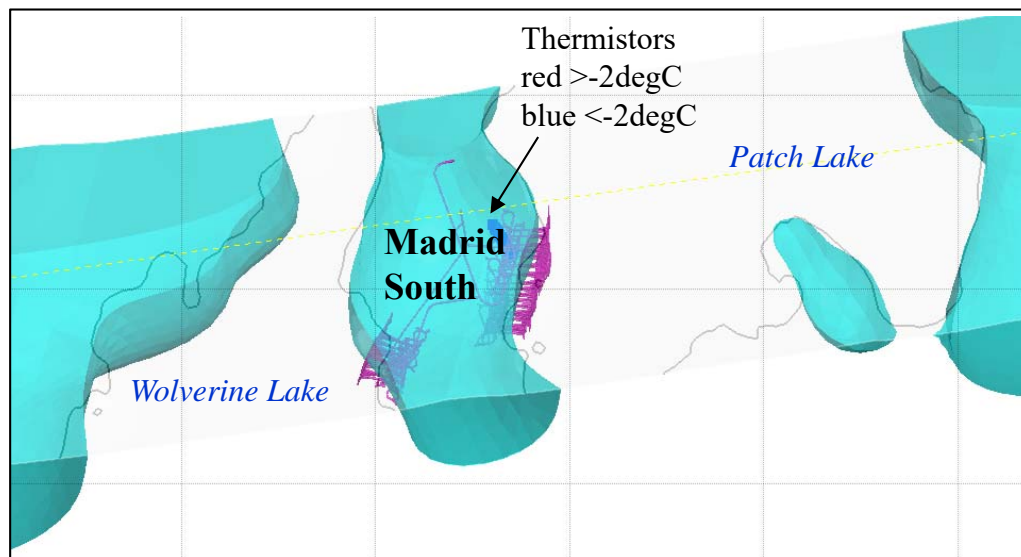
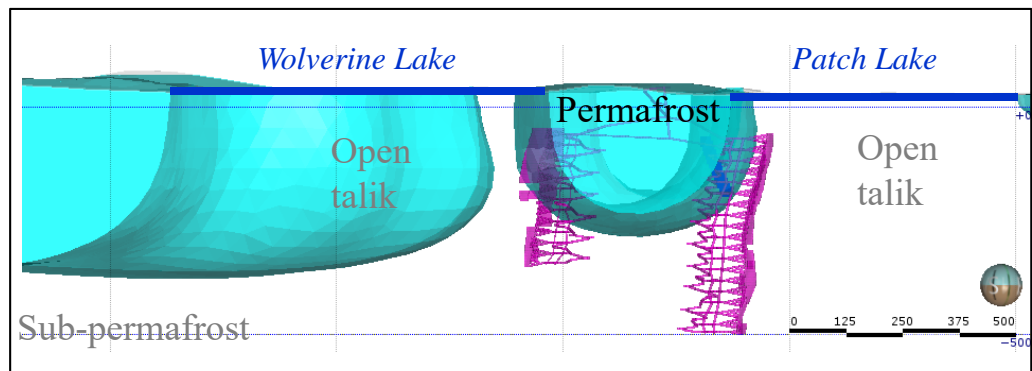
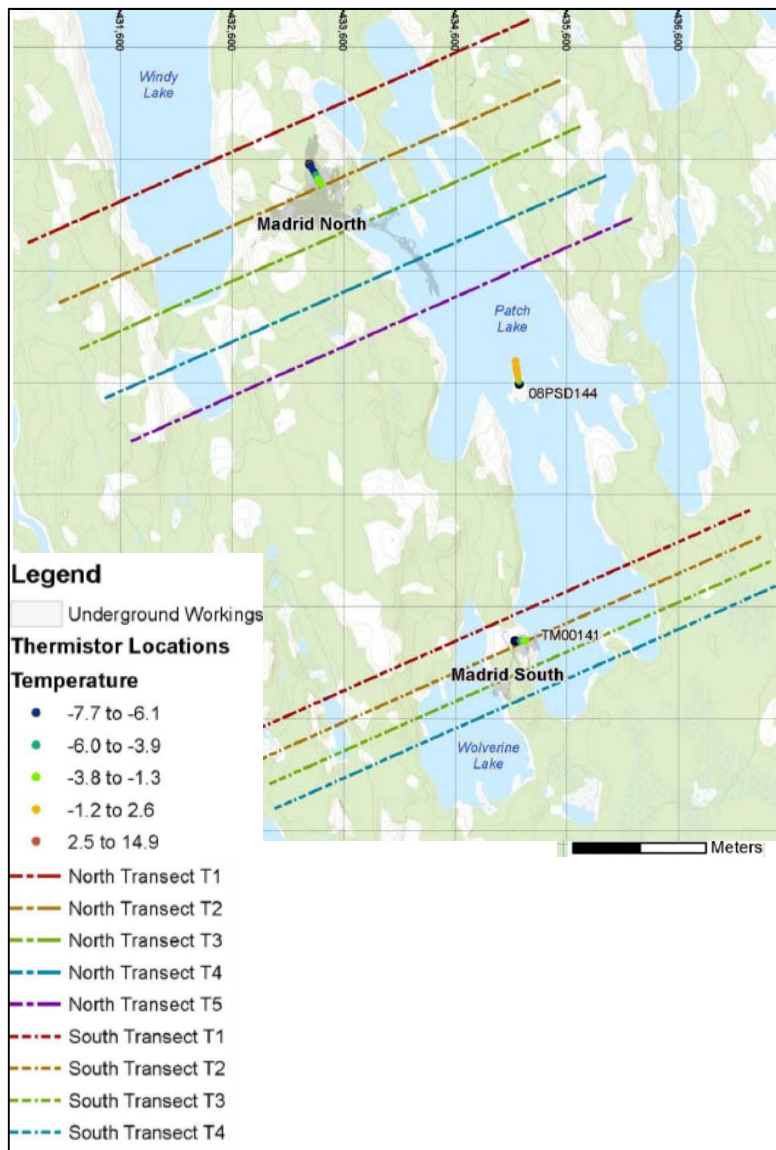


Note:
Prefeasibility mine plan shown, which will be updated as mining progresses.

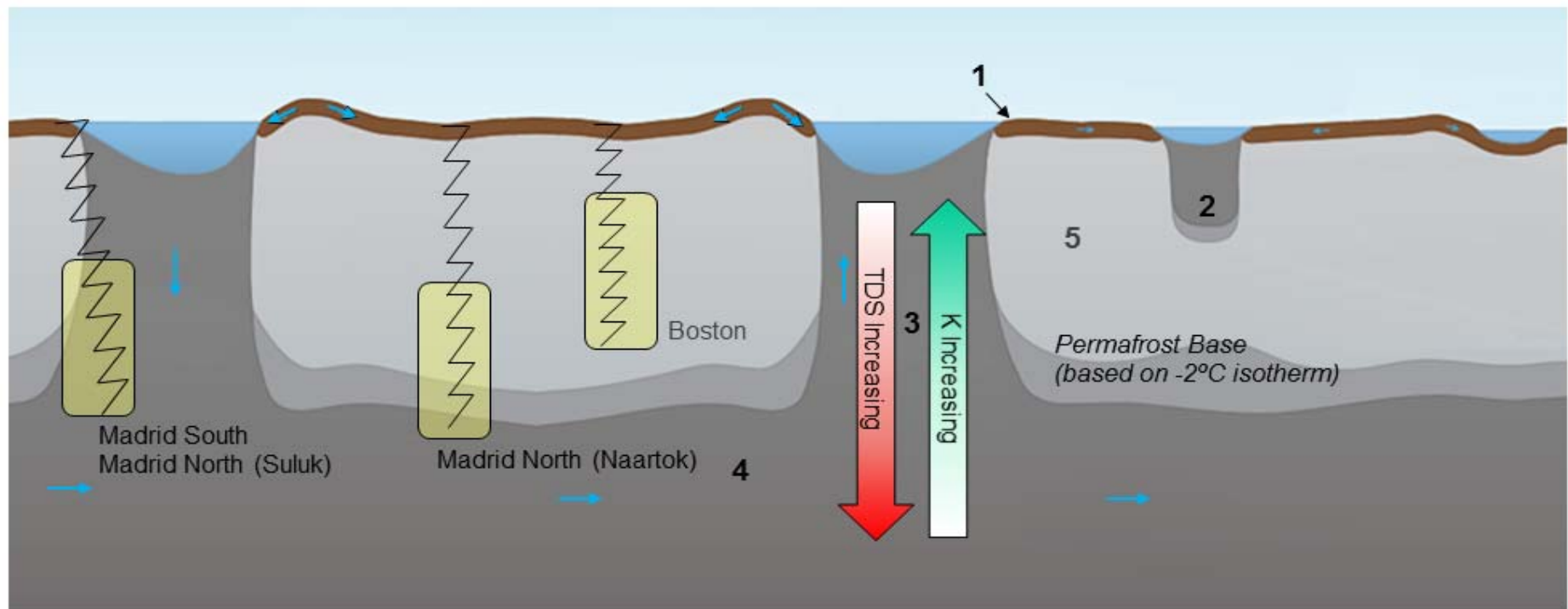




Note:
Prefeasibility mine plan shown, which will be updated as mining progresses.



Note:
Prefeasibility mine plan shown, which will be updated as mining progresses.



PERMAFROST COMPONENTS:

- 1 – Active layer.
- 2 – Closed talik caused by mid-size lake, pond or stream.
- 3 – Open talik caused by large lake or river.
- 4 – Sub-permafrost.
- 5 – Permafrost.

GROUNDWATER FLOW REGIMES

- 1 – Seasonally flowing
- 2 – Flowing, not connected to sub-permafrost.
- 3 – Flowing, connected to sub-permafrost.
- 4 – Flowing, connected to open taliks.
- 5 – No flow.

LEGEND

- Decline
- Underground
- Groundwater Flow Direction

srk consulting

Job No: 1CT022.013
Filename: 1CT022.013_FEIS_Fig_8x11_Lndscp.pptx

**TMAC
RESOURCES**

Hope Bay Project

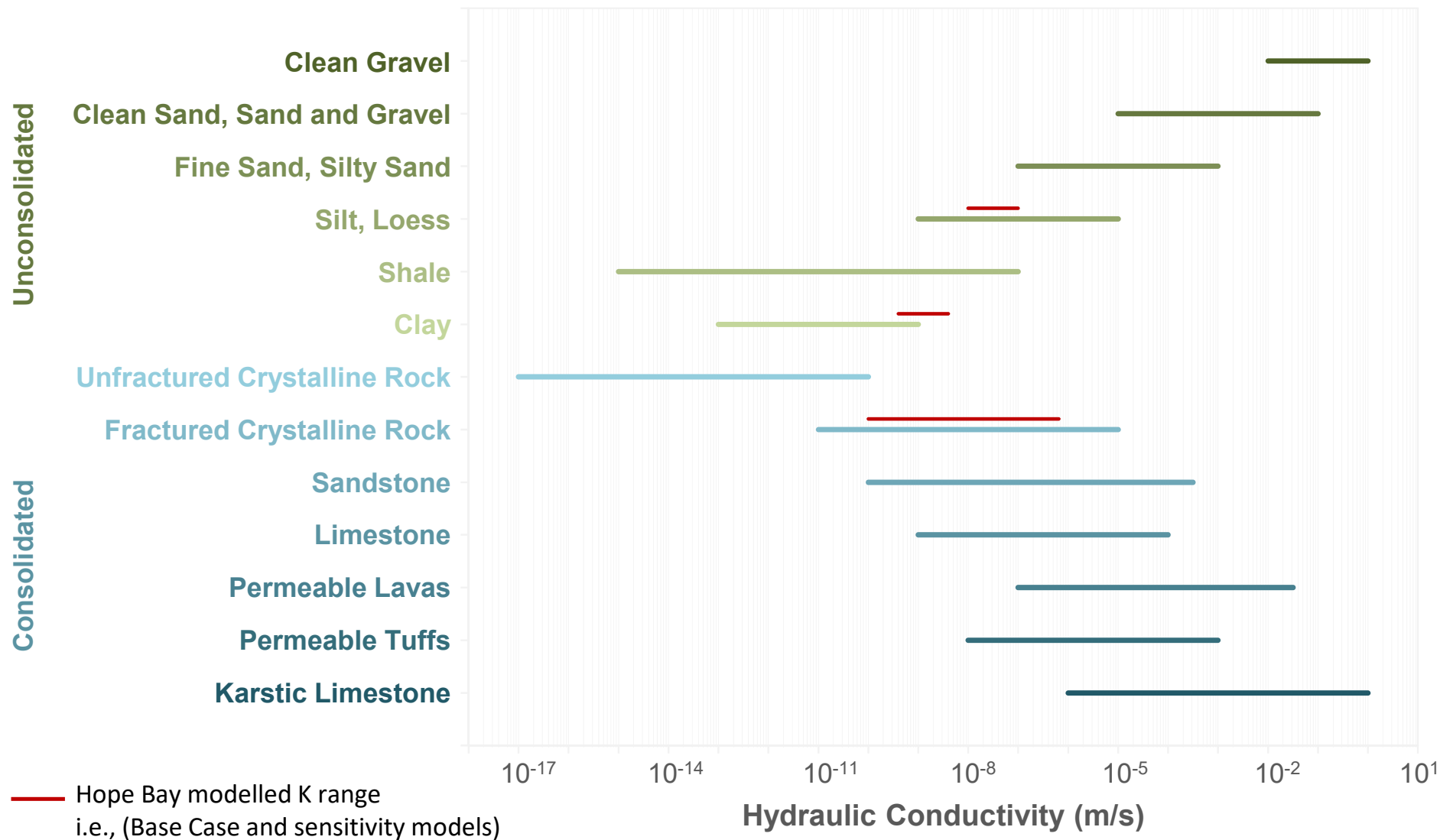
Hydrogeological Modeling

Conceptual Groundwater System

Date:
Nov. 2017


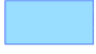


Approved:
GF

Figure: **24**



Source: Beale G, and J Reed. 2013. Guidelines for evaluating water in pit slope stability. CSIRO Publishing, Collingwood, Australia. 600 p.

		Hydrogeological Modeling		
		Published K values		
Job No: 1CT022.013 Filename: 1CT022.013_FEIS_Fig_8x11_Lndscp.pptx	Hope Bay Project	Date: Nov. 2017	Approved: GF	Figure: 25

-  Model Domain
-  Potential Open talik
-  Underground Mine
-  Lake Elevation in masl

Note:

Prefeasibility mine plan shown,
which will be updated as mining progresses.

Madrid North

Edge	BC Type	Head (masl)	Distance (m)
AB	Trsf	43	1000
BC	Trsf	25.8	1 to 850
CD	Trsf	20.2	1
DE	No Flow	-	-
EF	Trsf	18.1	1
FG	No Flow	-	-
GA	Trsf	18.1	1900

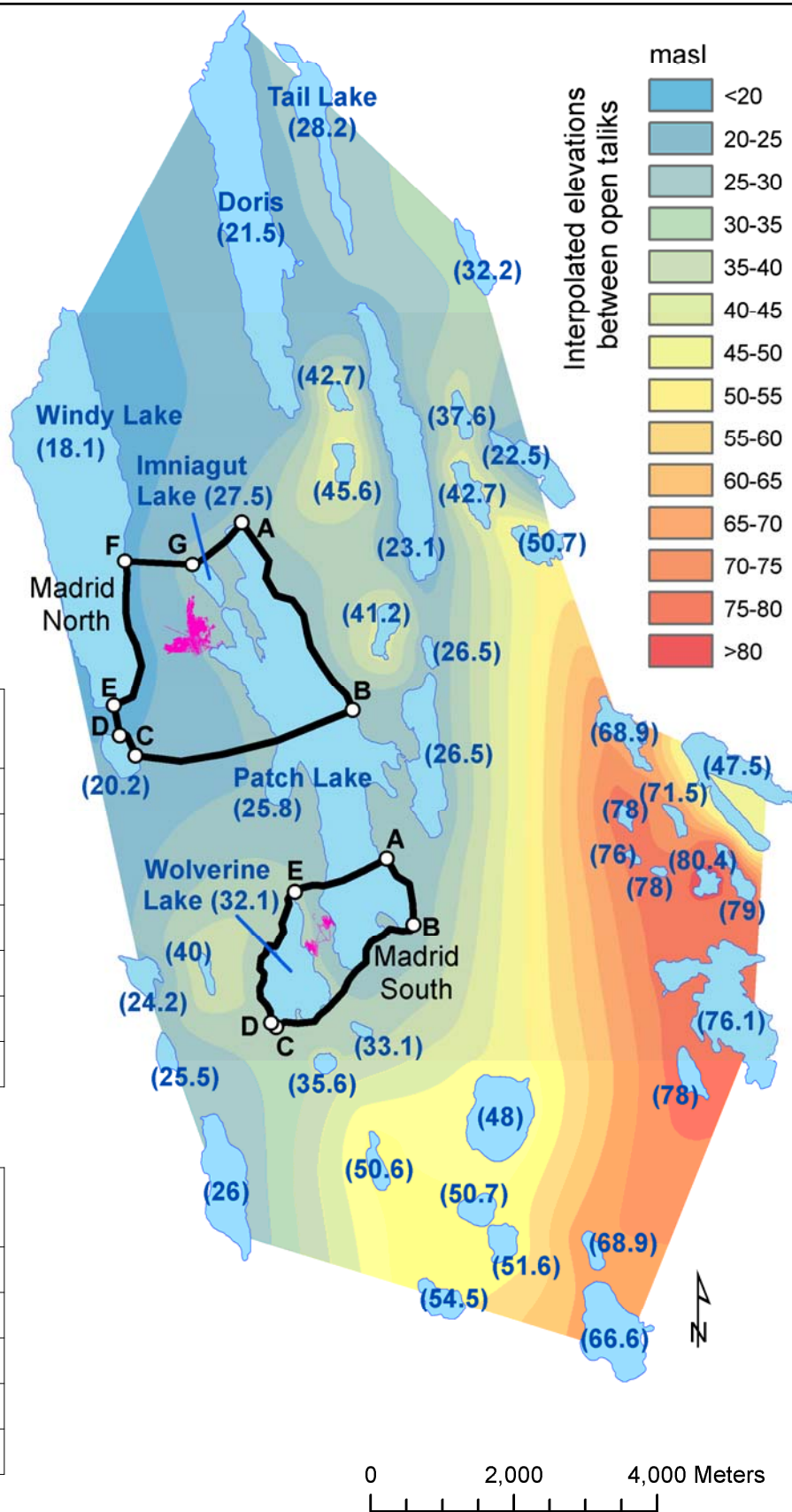
Madrid North

Edge	BC Type	Head (masl)	Distance (m)
AB	Trsf	76	4000
BC	Trsf	49	2100
CD	Trsf	26	1500
DE	Trsf	40	800
EA	Trsf	25.8	1 to 1700

Trsf = fluid-transfer boundary condition

H_{ref} = Reference water level

d_{ref} = Distance from the model to the reference water level



Hydrogeological Modeling

Model Domains and Boundary Conditions

Job No: 1CT022.013

Filename: 1CT022.013_FEIS_Fig_8x11_Prtt.pptx

Hope Bay Project

Date:
Nov. 2017

Approved:
GF

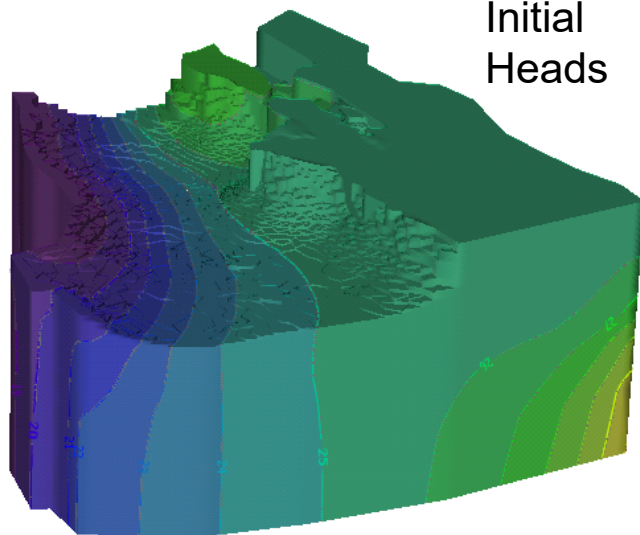
Figure:

26

Hydraulic head
- Fringes -
[m]

33 ... 33.7155
32 ... 33
31 ... 32
30 ... 31
29 ... 30
28 ... 29
27 ... 28
26 ... 27
25 ... 26
24 ... 25
23 ... 24
22 ... 23
21 ... 22
20 ... 21
19 ... 20
18.0976 ... 19

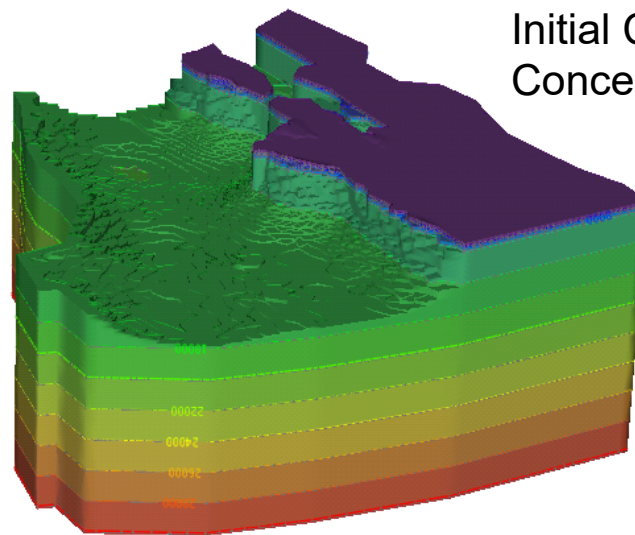
Initial
Heads



Mass concentration - Chloride (f)
- Fringes -
[mg/l]

30000 ... 30194
28000 ... 30000
26000 ... 28000
24000 ... 26000
22000 ... 24000
20000 ... 22000
18000 ... 20000
16000 ... 18000
14000 ... 16000
12000 ... 14000
10000 ... 12000
8000 ... 10000
6000 ... 8000
4000 ... 6000
2000 ... 4000
68.5 ... 2000

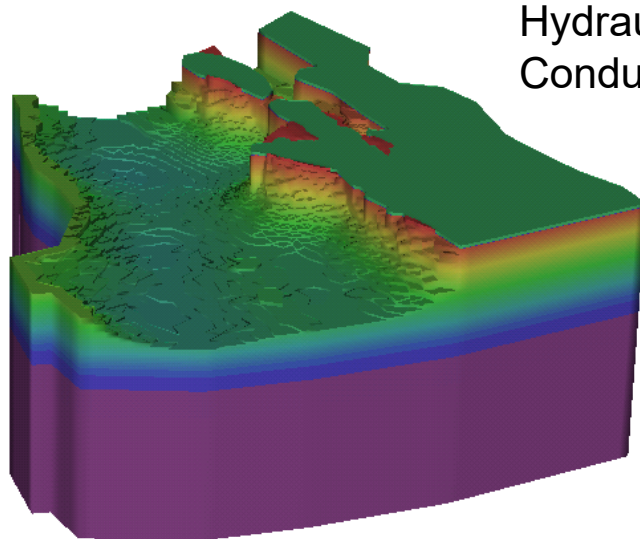
Initial Chloride
Concentrations



FEFLOW (R)
Conductivity: K_{xx}
- Patches -
[m/s]

7.7E-07
3.1E-07
1.3E-07
5.2E-08
2.1E-08
8.8E-09
3.6E-09
1.5E-09
6.0E-10
2.4E-10
1.0E-10

Hydraulic
Conductivity



FEFLOW (R)

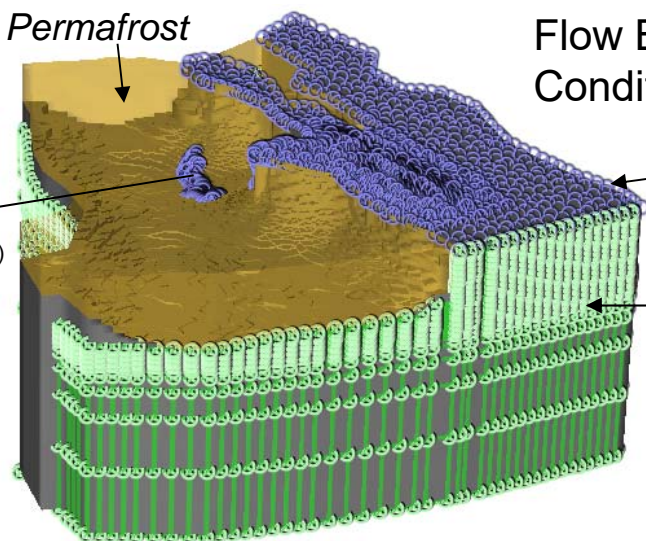
Permafrost

Flow Boundary
Conditions

Seepage
BC (Underground)

Constant head
BC

Fluid-Transfer
BC



FEFLOW (R)

FEFLOW (R)

srk consulting

**TMAC
RESOURCES**

Hydrogeological Modeling

3D Views of the Madrid North
Numerical Model

Job No: 1CT022.013
Filename: 1CT022.013_FEIS_Fig_8x11_Lndscp.pptx

Hope Bay Project

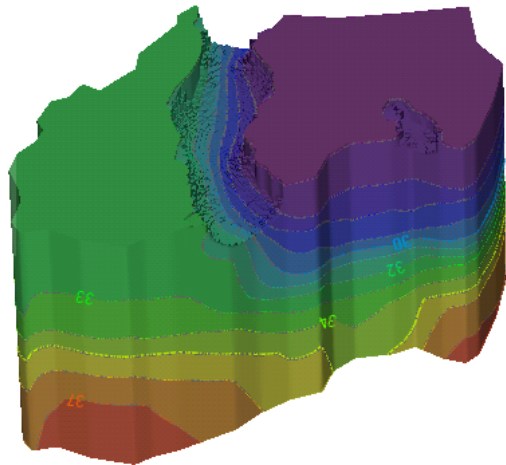
Date:
Nov. 2017

Approved:
GF

Figure: **27**

Hydraulic head
- Fringes -
[m]

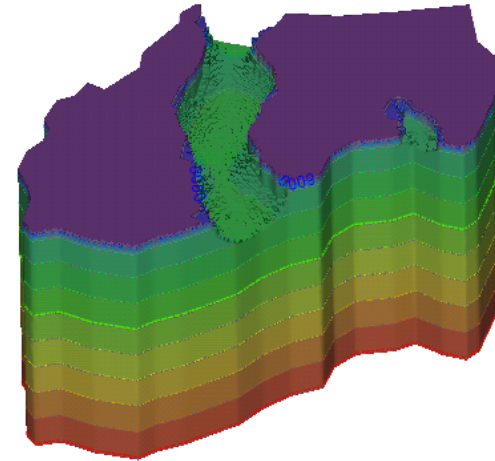
37 ... 37.8968
36 ... 37
35 ... 36
34 ... 35
33 ... 34
32 ... 33
31 ... 32
30 ... 31
29 ... 30
28 ... 29
27 ... 28
26 ... 27
25.8 ... 26



Initial
Heads

Mass concentration - Chloride (f)
- Fringes -
[mg/l]

30000 ... 30194
28000 ... 30000
26000 ... 28000
24000 ... 26000
22000 ... 24000
20000 ... 22000
18000 ... 20000
16000 ... 18000
14000 ... 16000
12000 ... 14000
10000 ... 12000
8000 ... 10000
6000 ... 8000
4000 ... 6000
2000 ... 4000
68.5 ... 2000

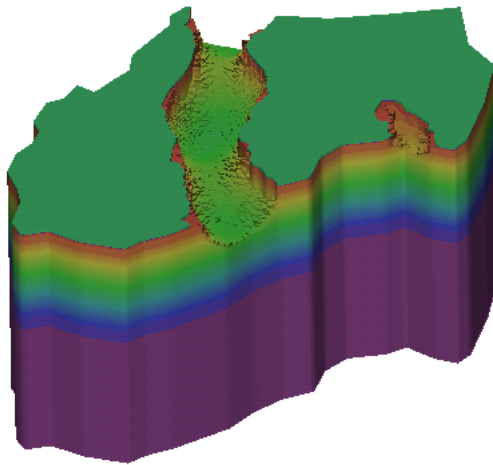


Initial Chloride
Concentrations



FEFLOW (R)
Conductivity: K_{xx}
- Patches -
[m/s]

7.7E-07
3.1E-07
1.3E-07
5.2E-08
2.1E-08
8.8E-09
3.6E-09
1.5E-09
6.0E-10
2.4E-10
1.0E-10

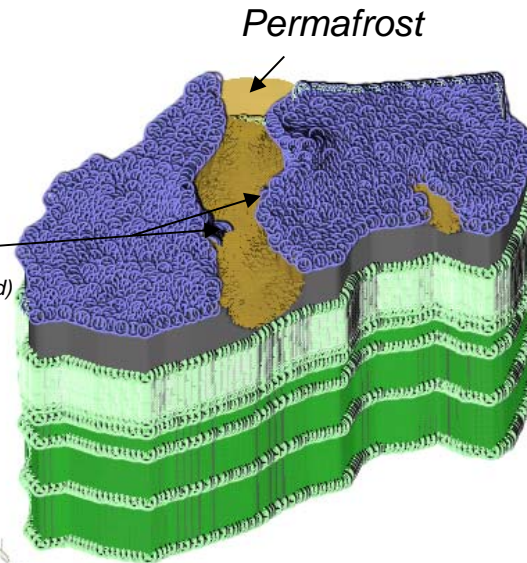


Hydraulic
Conductivity



FEFLOW (R)

Seepage
BC (Underground)



Permafrost

Flow Boundary
Conditions

Constant head
BC

Fluid-Transfer
BC



FEFLOW (R)



FEFLOW (R)

srk consulting

TMAC
RESOURCES

Hydrogeological Modeling

3D Views of the Madrid South
Numerical Model

Job No: 1CT022.013

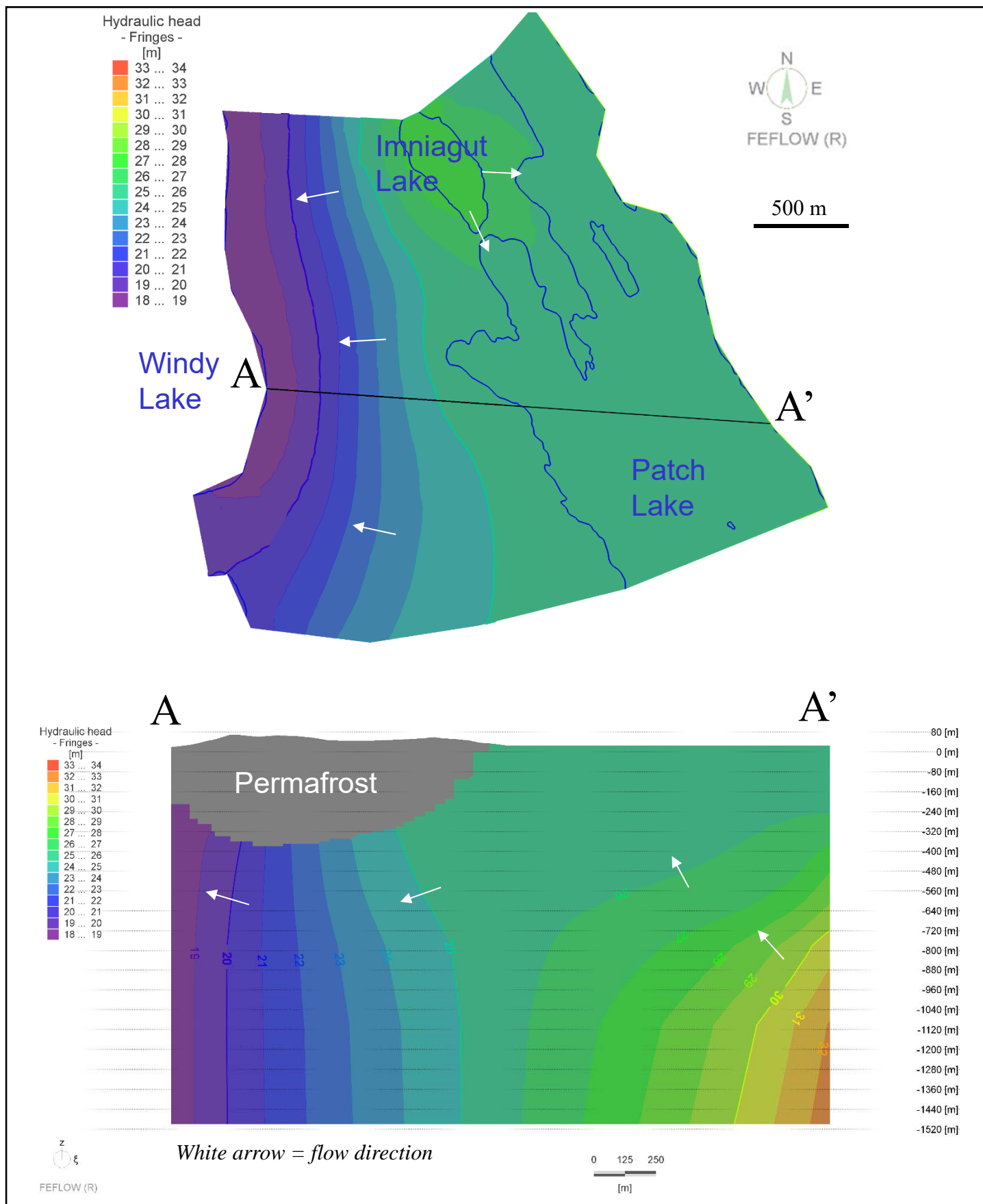
Filename: 1CT022.013_FEIS_Fig_8x11_Lndscp.pptx

Hope Bay Project

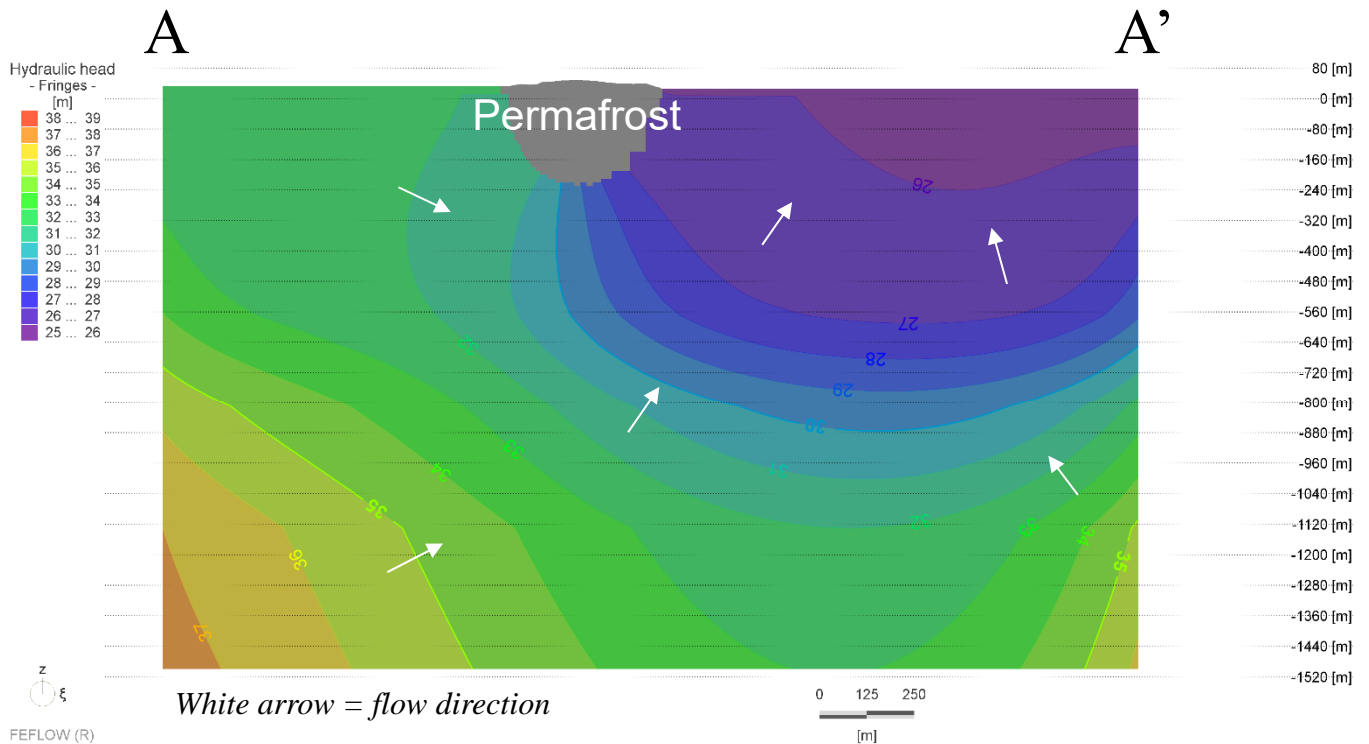
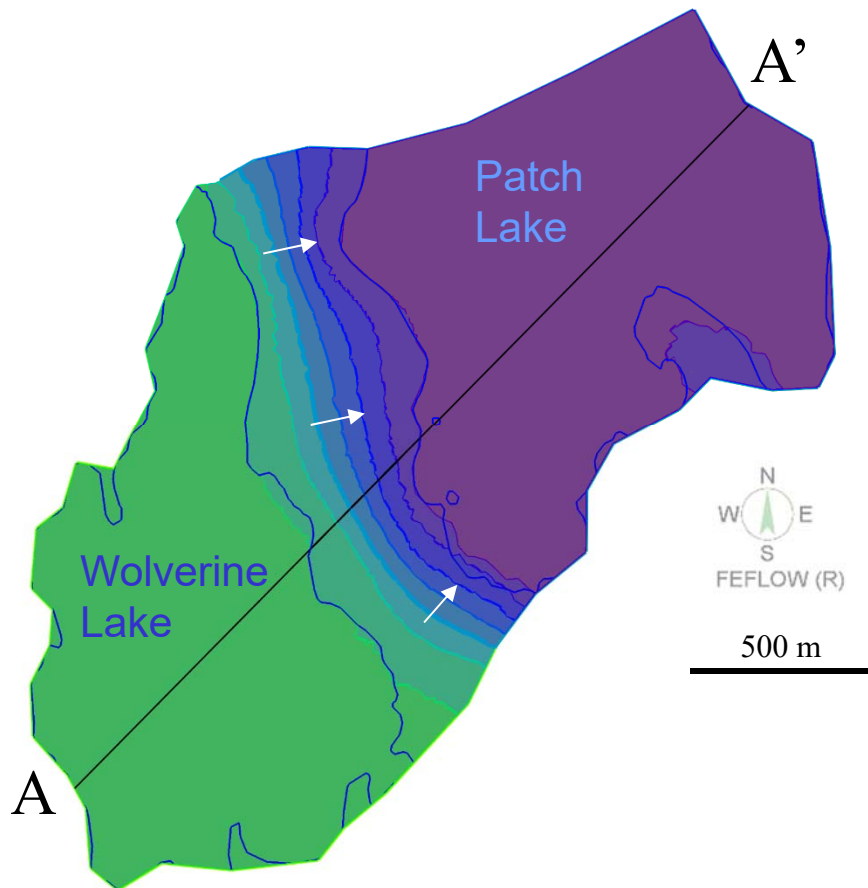
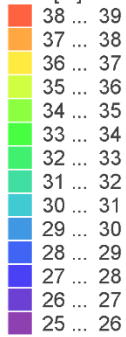
Date:
Nov. 2017

Approved:
GF

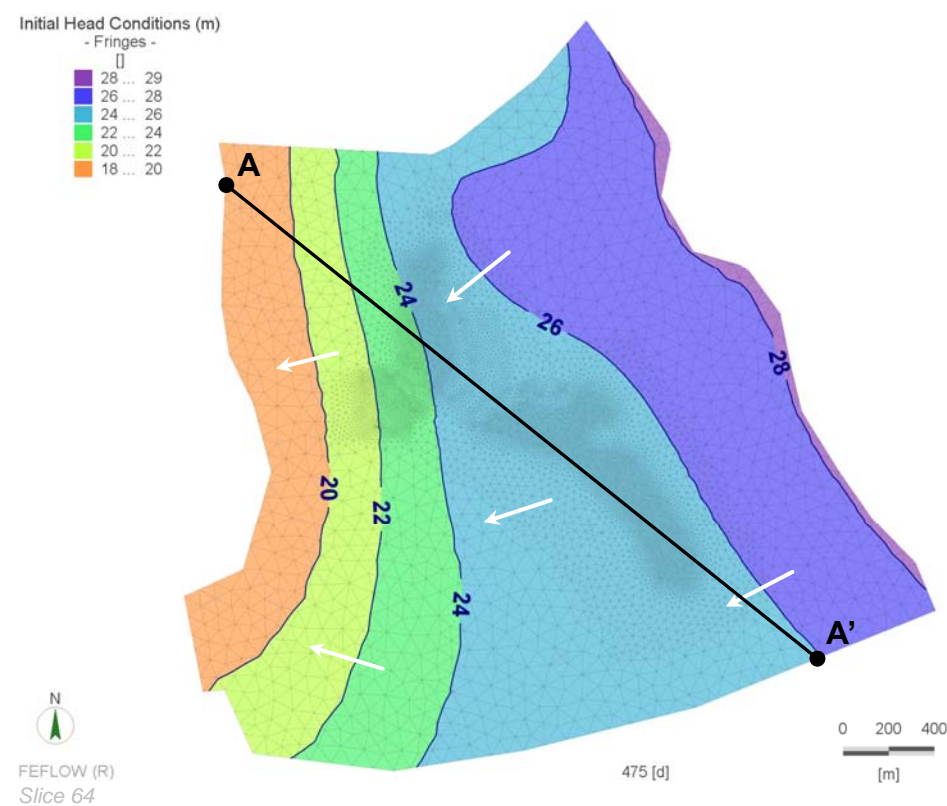
Figure: **28**



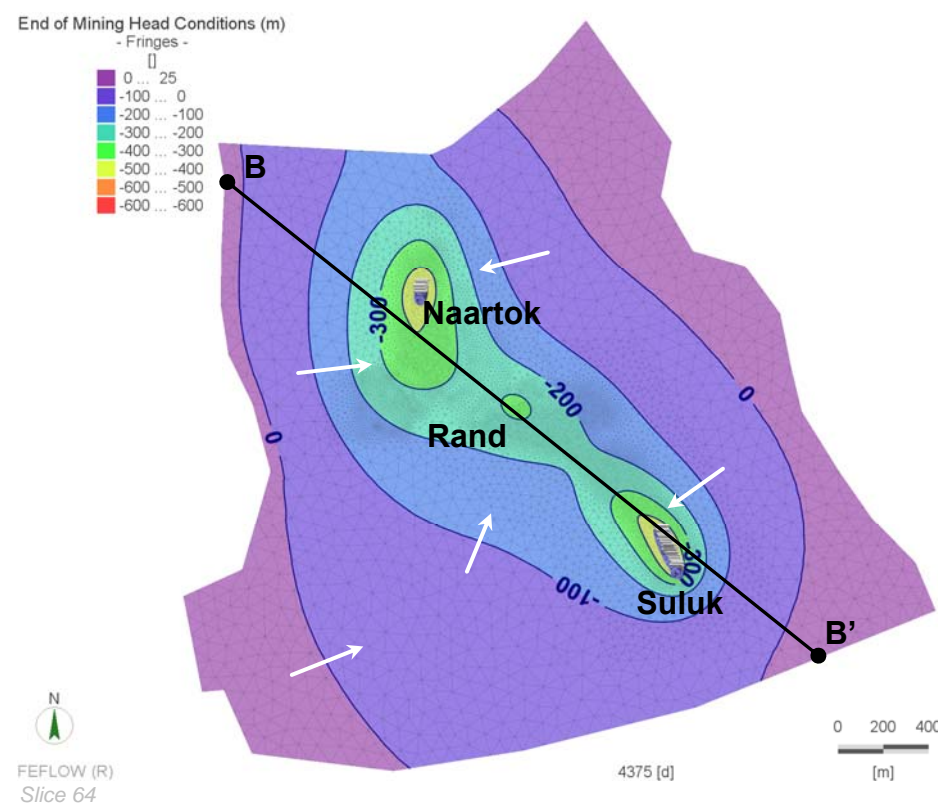
Hydraulic head
- Fringes -
[m]



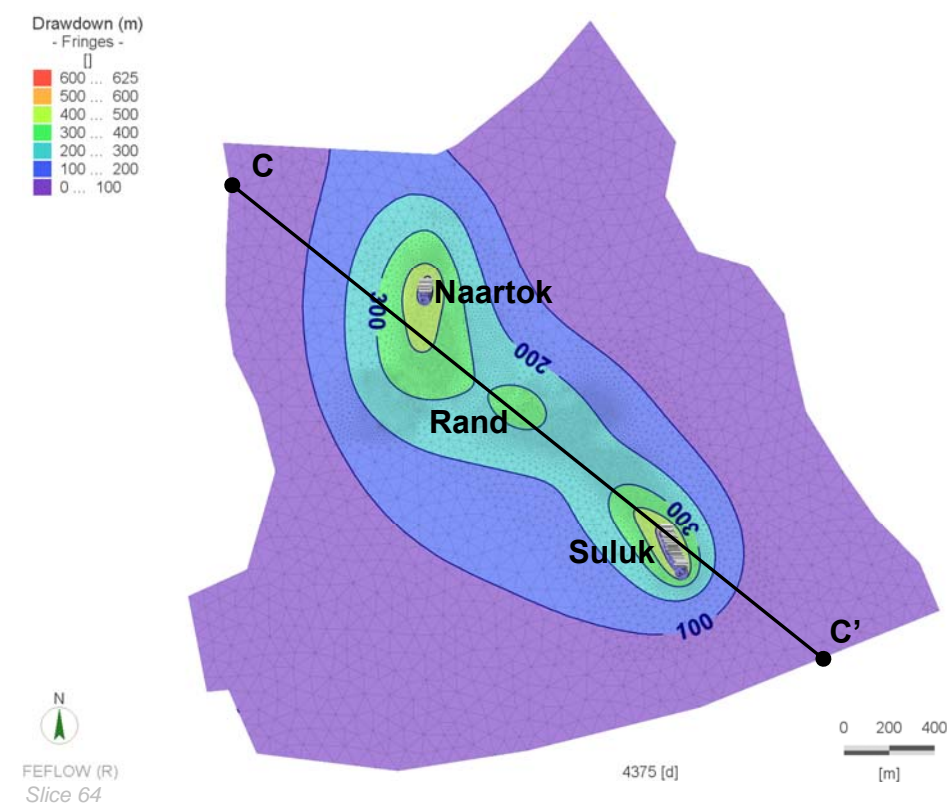
Pre-Mining Hydraulic Heads



End of Mining Hydraulic Heads



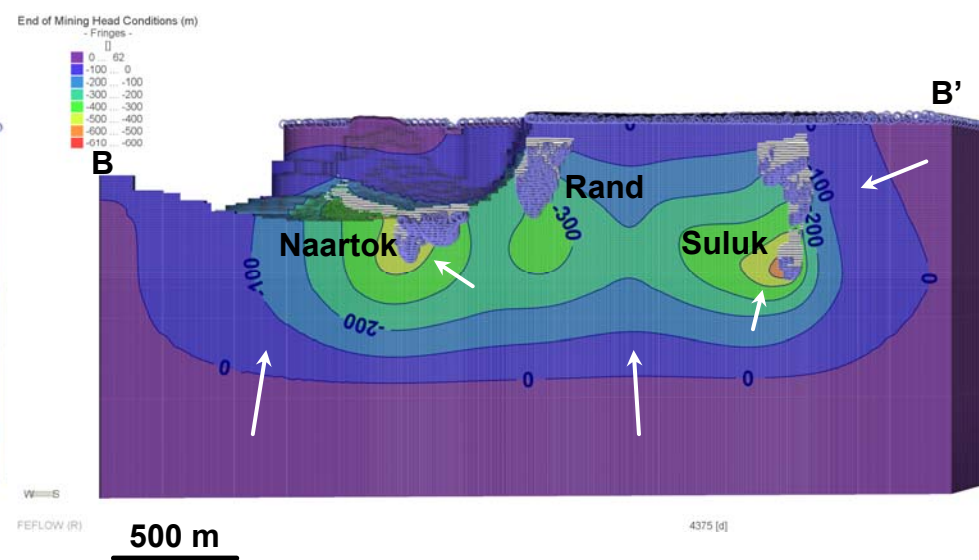
Maximum Drawdown



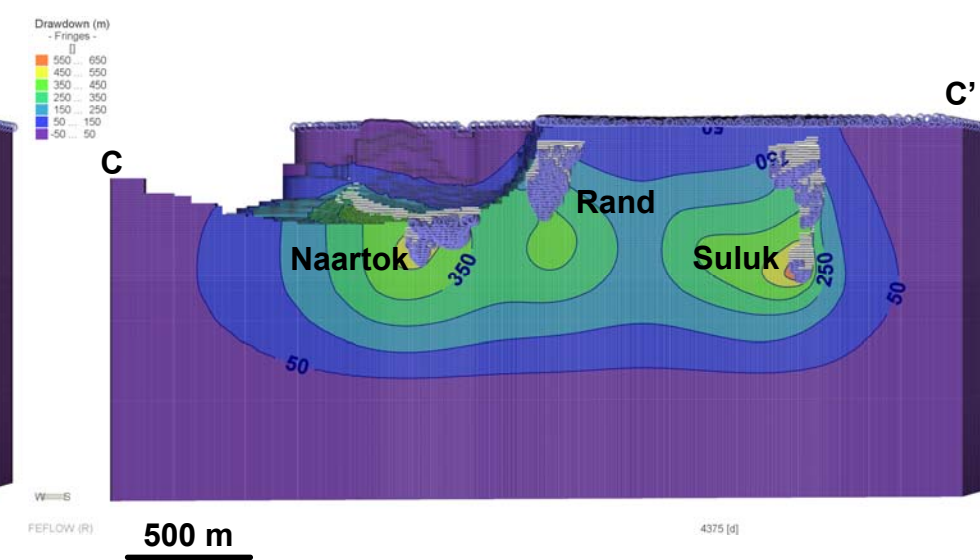
Pre-Mining Hydraulic Heads



End of Mining Hydraulic Heads



Maximum Drawdown



* white arrows = flow direction

srk consulting

Job No: 1CT022.013
Filename: 1CT022.013_FEIS_Fig_11x17_Lndscp.pptx

TMAC
RESOURCES

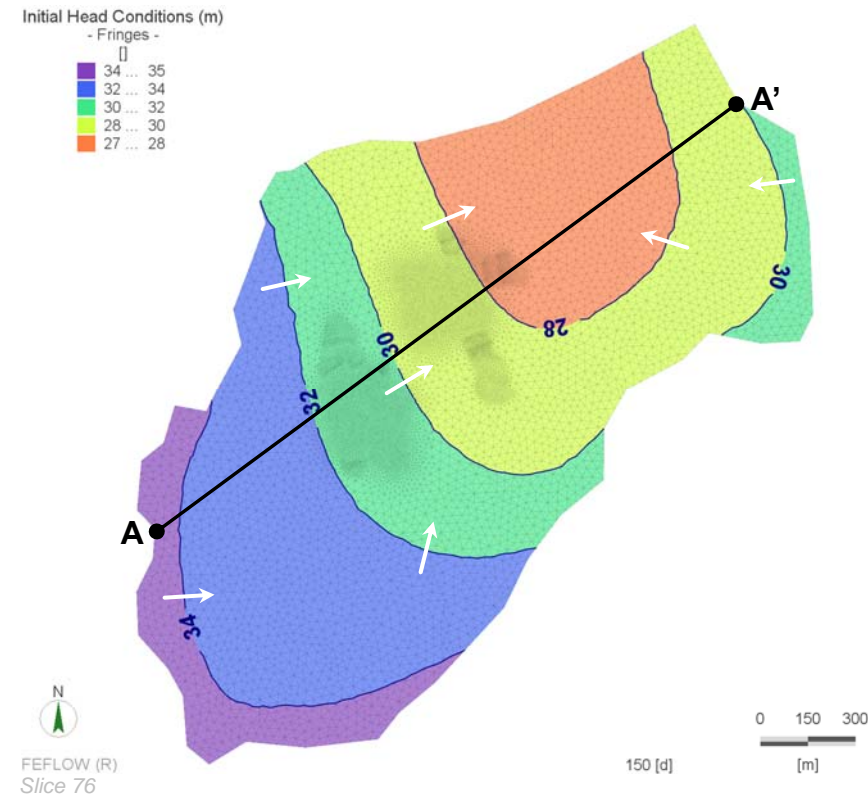
Hope Bay Project

Hydrogeology Modelling

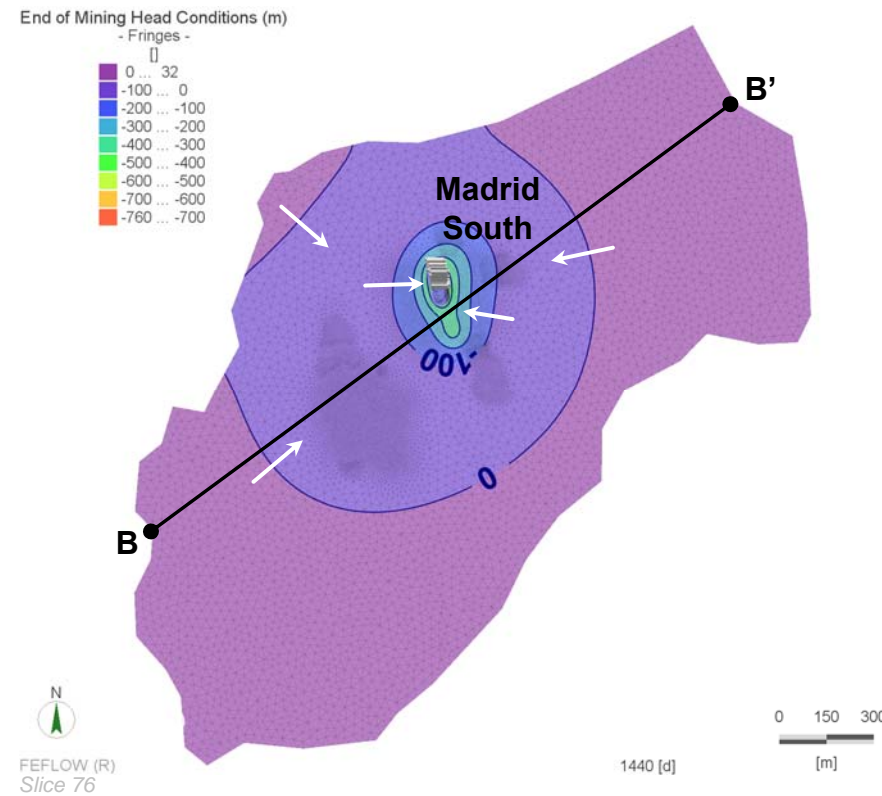
**Hydraulic Head Predictions
at Madrid North**

Date: Nov. 2017	Approved: GF	Figure: 31
--------------------	-----------------	----------------------

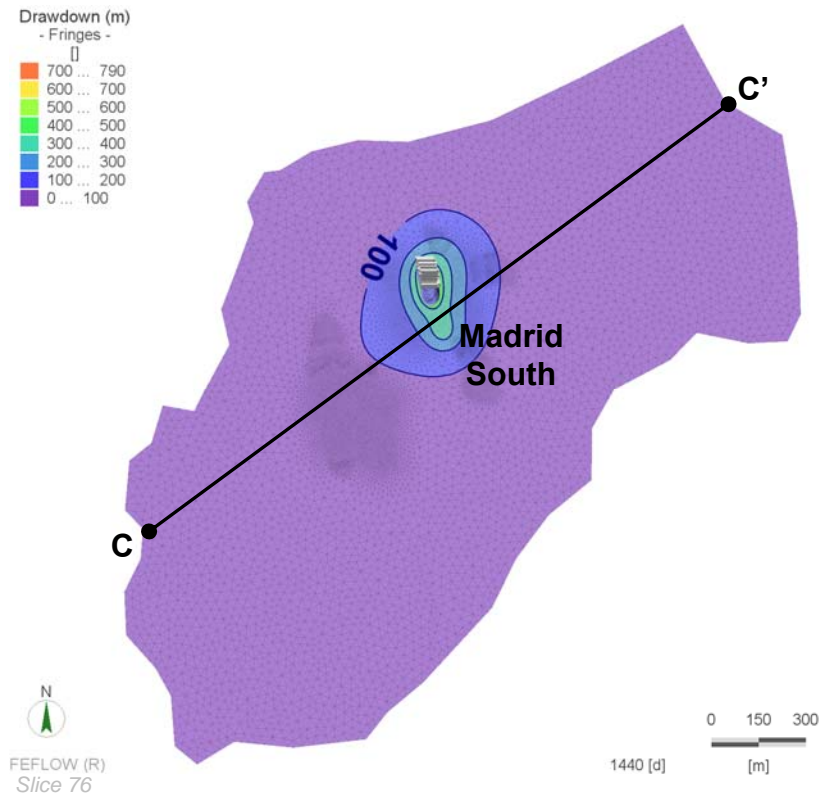
Pre-Mining Hydraulic Heads



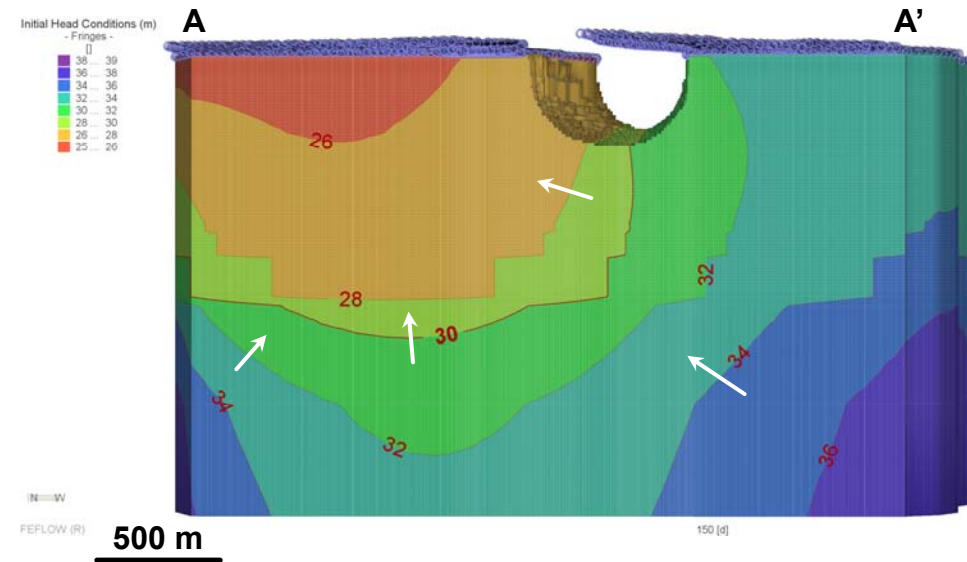
End of Mining Hydraulic Heads



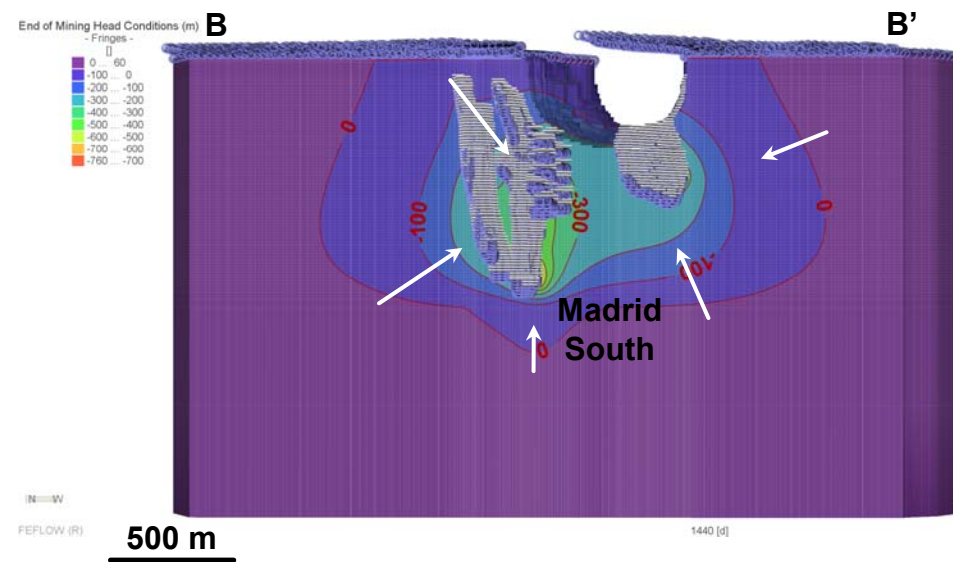
Maximum Drawdown



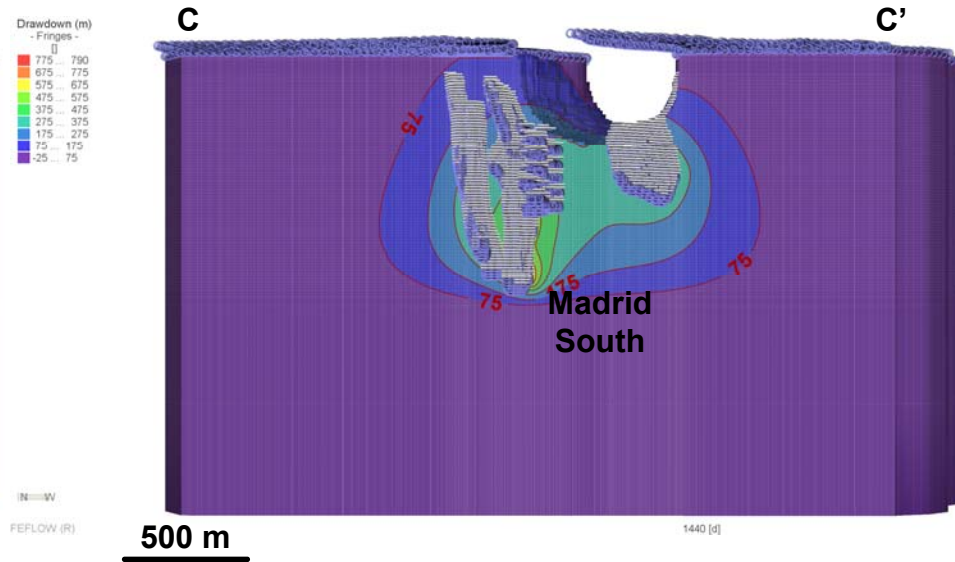
Pre-Mining Hydraulic Heads



End of Mining Hydraulic Heads



Maximum Drawdown



* white arrows = flow direction



Job No: 1CT022.013
Filename: 1CT022.013_FEIS_Fig_11x17_Lndscp.pptx

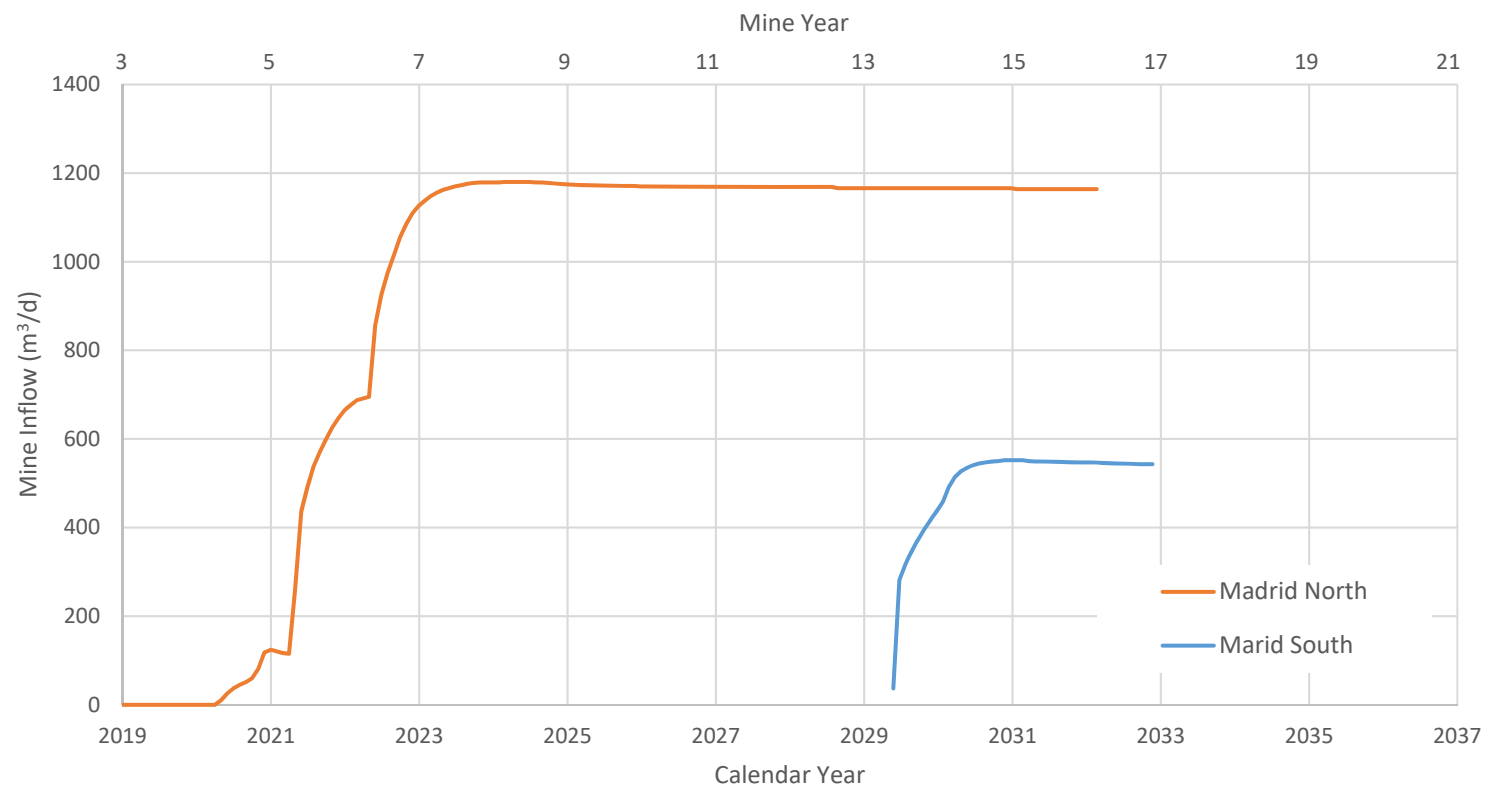


Hope Bay Project

Hydrogeology Modelling

**Hydraulic Head Predictions
at Madrid South**

Date: Nov. 2017	Approved: GF	Figure: 32
--------------------	-----------------	----------------------



Source: !MADRID_upd-oct2016_v13.0-V15.0_BASECASE_Inflow_&_Conc_Predictions_20161107_rev2.xlsx



Hydrogeological Modeling

Predicted Mine Inflows

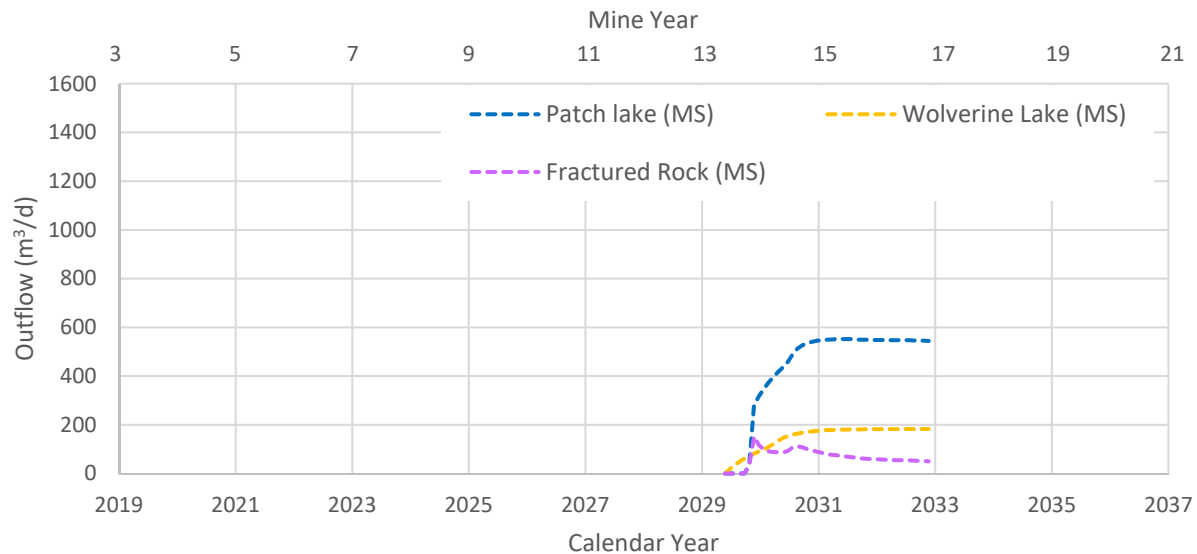
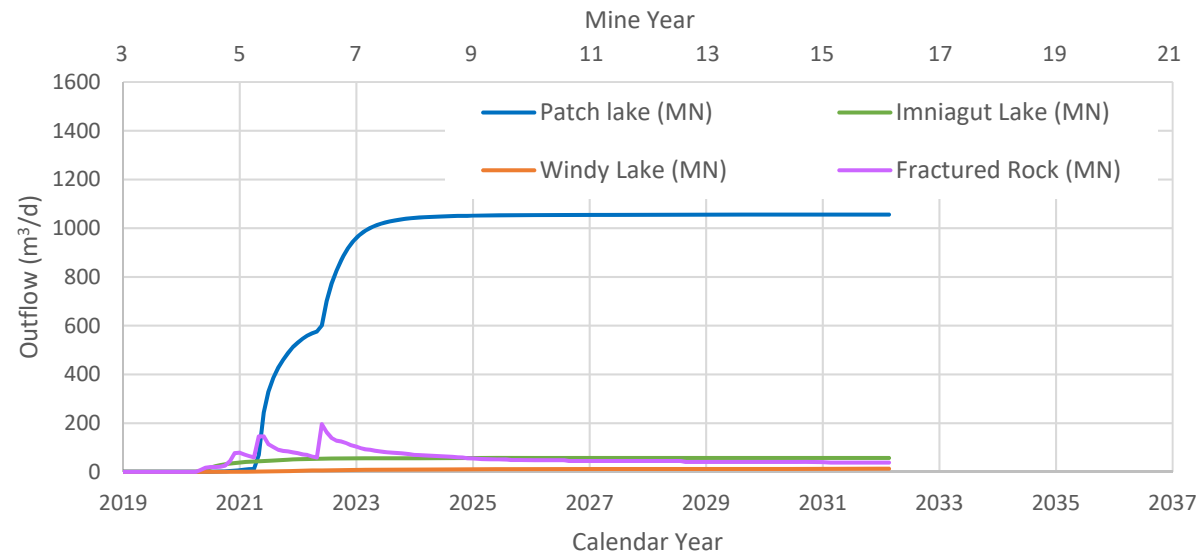
Job No: 1CT022.013
Filename: 1CT022.013_FEIS_Fig_8x11_Lndscp.pptx

Hope Bay Project

Date:
Nov. 2017

Approved:
GF

Figure: **33**



Source: !MADRID_upd-oct2016_v13.0-V15.0_BASECASE_Inflow_&_Conc_Predictions_20161107_rev2.xlsx



Hydrogeological Modeling

Predicted Infiltrations of Water
from Lakes

Job No: 1CT022.013
Filename: 1CT022.013_FEIS_Fig_8x11_Lndscp.pptx

Hope Bay Project

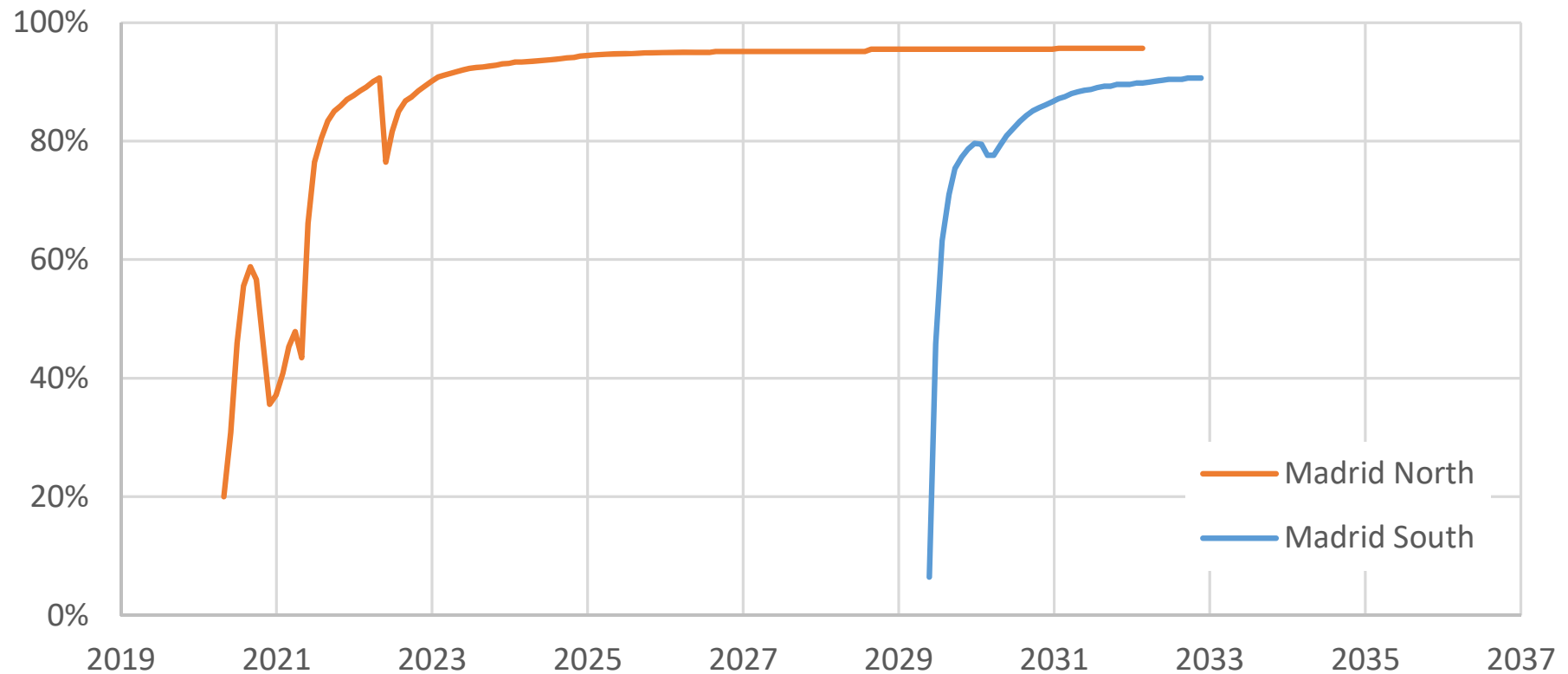
Date:
Nov. 2017

Approved:
GF

Figure: **34**

Note:
MS, Madrid South
MN, Madrid North

Contributions from Lakes to Mine Inflows (%)



Source: !MADRID_upd-oct2016_v13.0-V15.0_BASECASE_Inflow_&_Conc_Predictions_20161107_rev3.xlsx



Hydrogeological Modeling

Predicted Contributions of
Lake water to Mine Inflows

Job No: 1CT022.013

Filename: 1CT022.013_FEIS_Fig_8x11_Lndscp.pptx

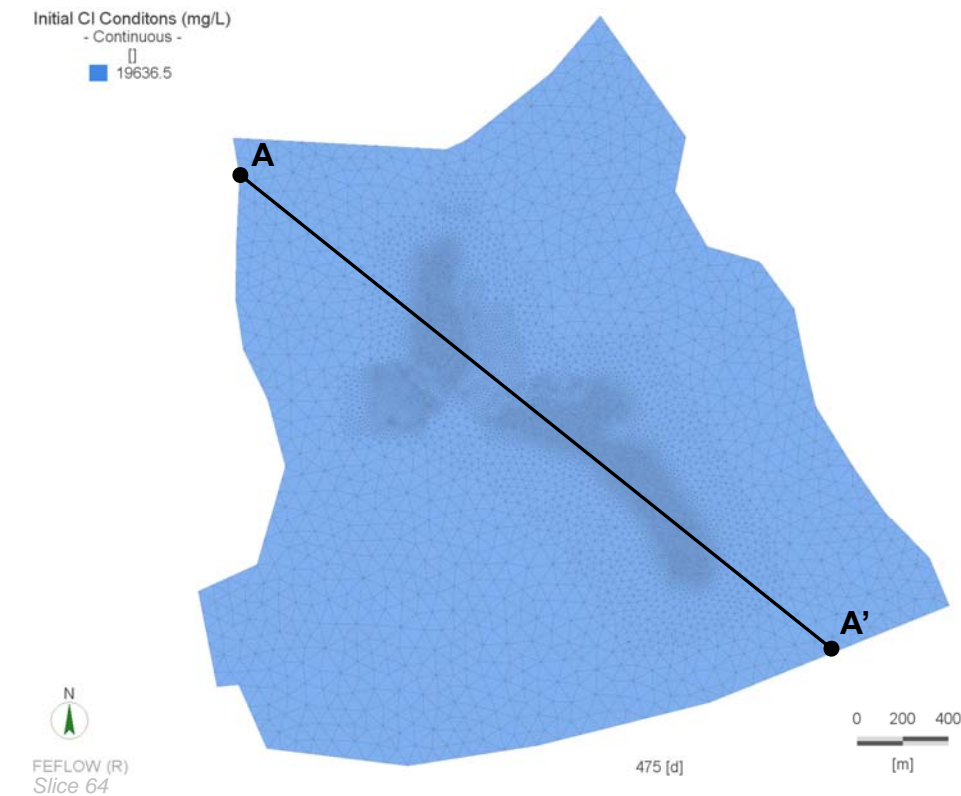
Hope Bay Project

Date:
Nov. 2017

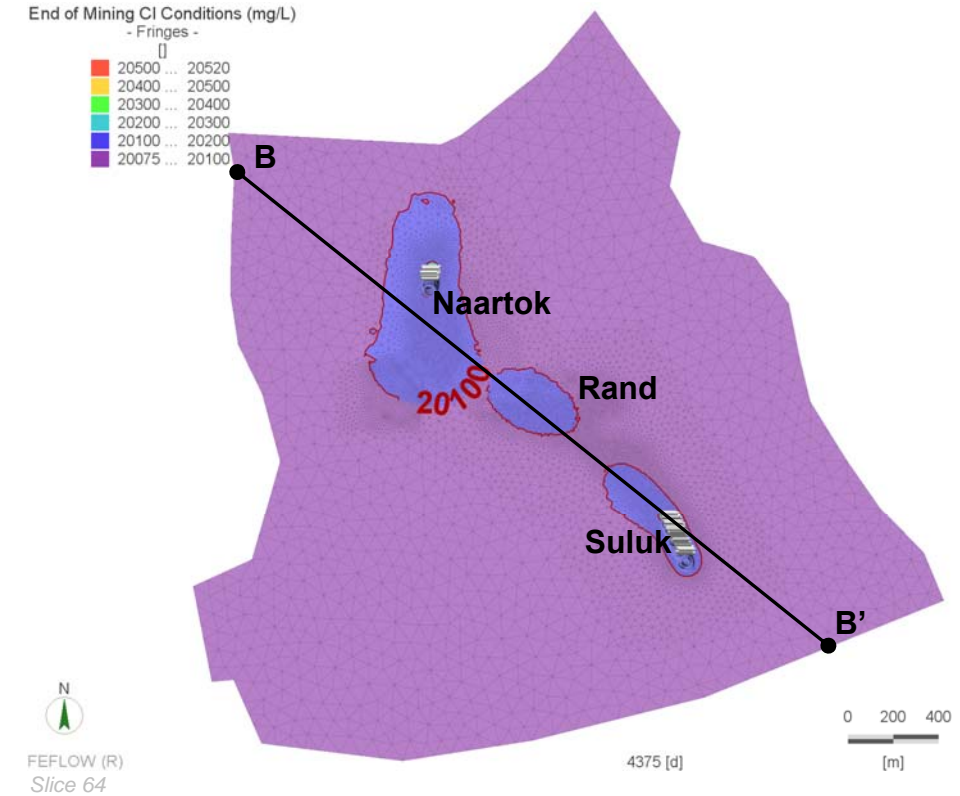
Approved:
GF

Figure: **35**

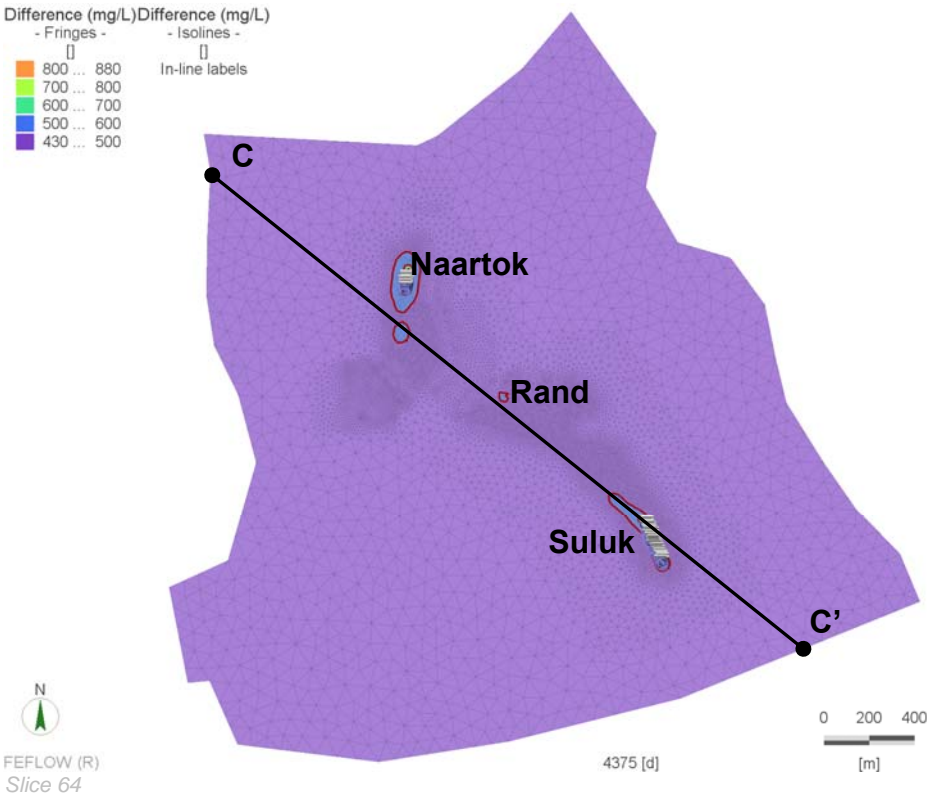
Pre-Mining Cl Concentration



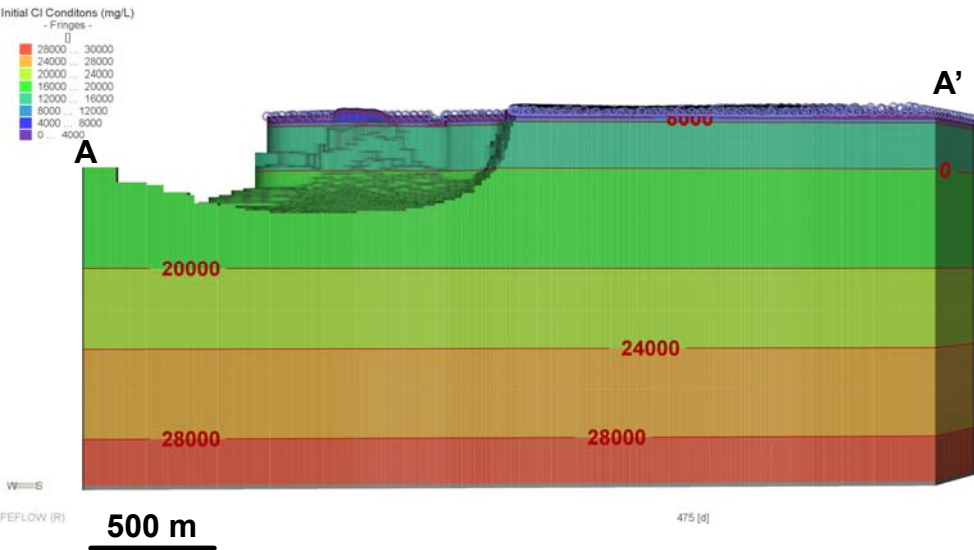
End of Mining Cl Concentration



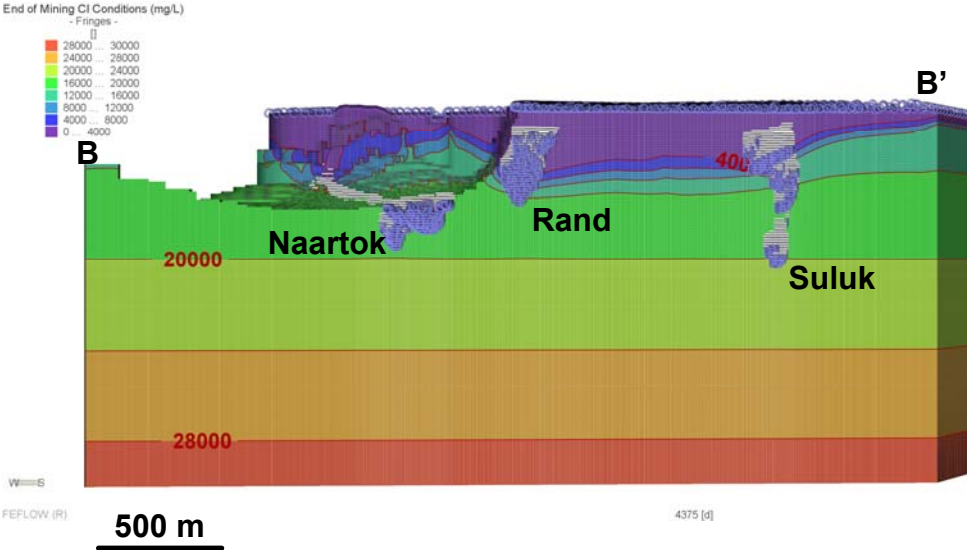
Difference
(End of Mining minus Pre-Mining)



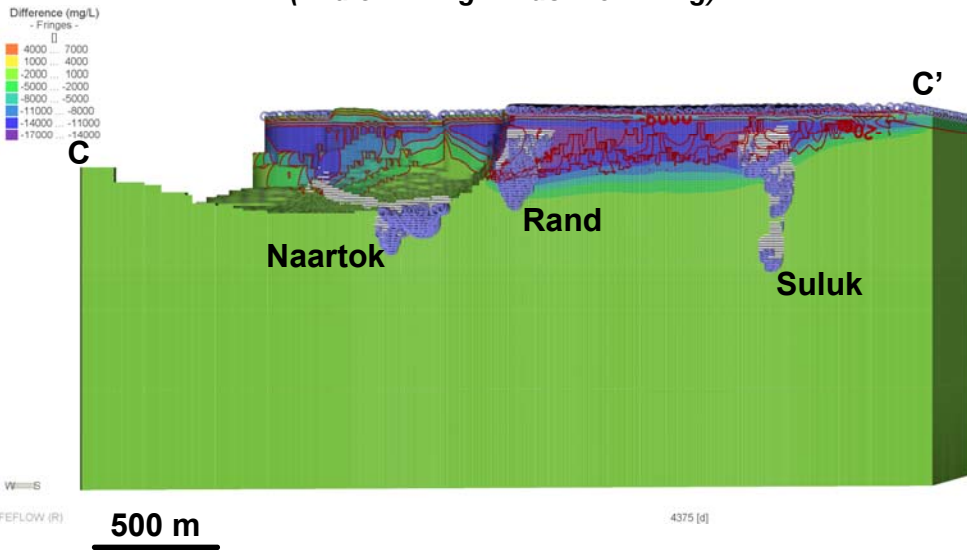
Pre-Mining Cl Concentration



End of Mining Cl Concentration



Difference
(End of Mining minus Pre-Mining)



* white arrows = flow direction

srk consulting

Job No: 1CT022.013
Filename: 1CT022.013_FEIS_Fig_11x17_Lndscp.pptx

TMAC
RESOURCES

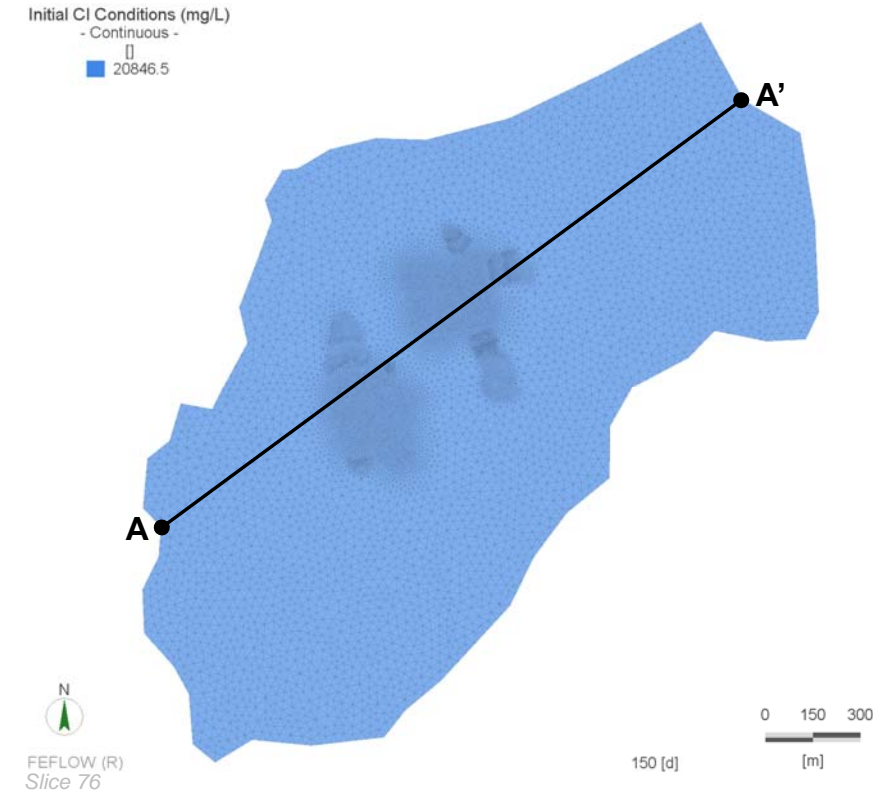
Hope Bay Project

Hydrogeology Modelling

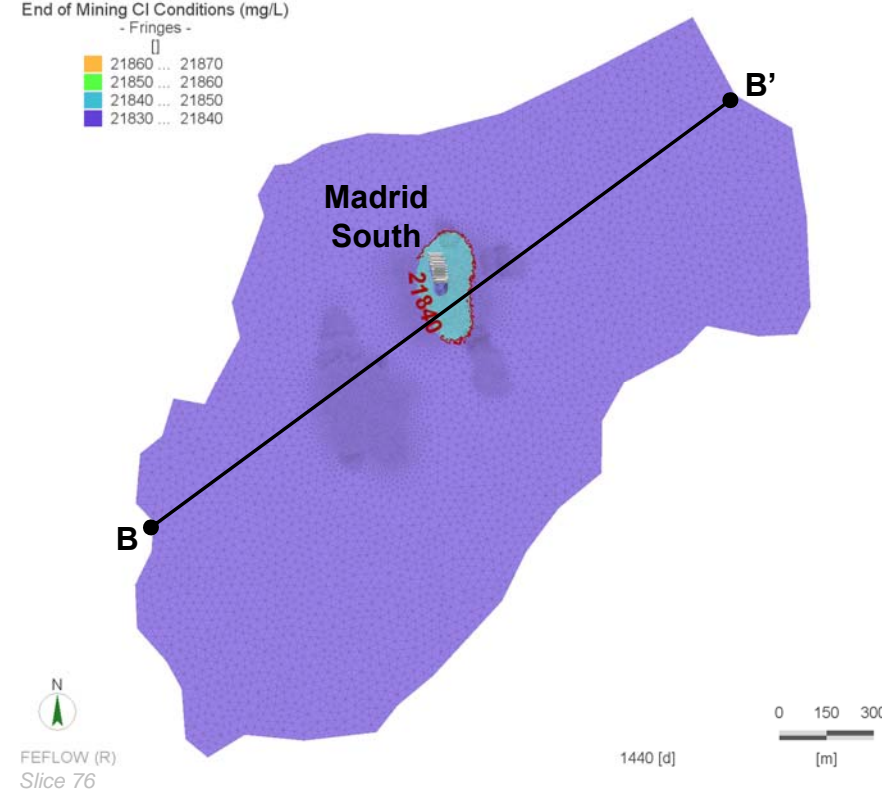
Chloride Concentration
Predictions at Madrid North

Date: Nov. 2017
Approved: GF
Figure: 36

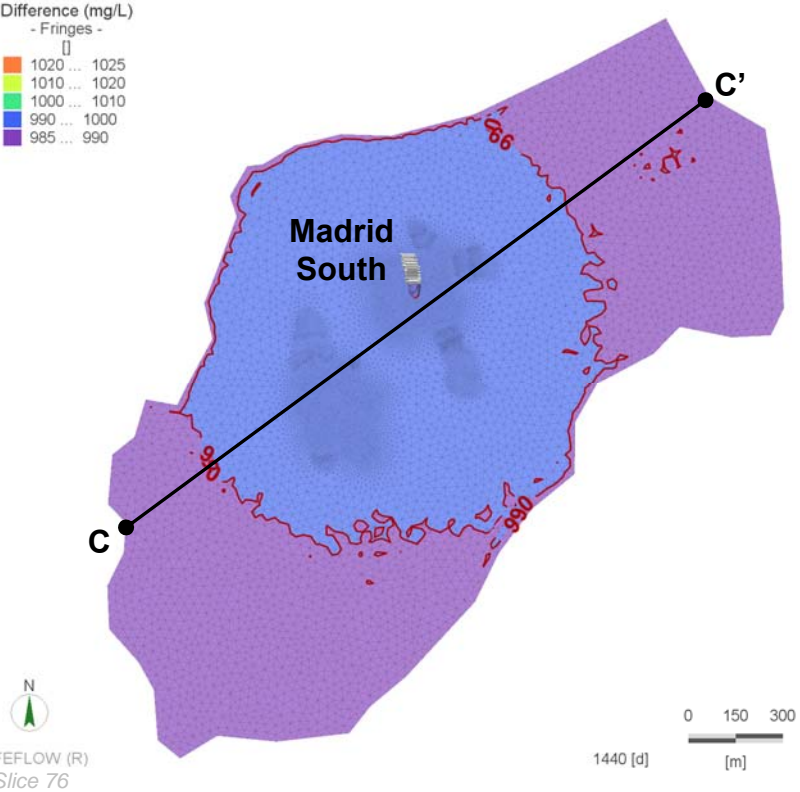
Pre-Mining Cl Concentration



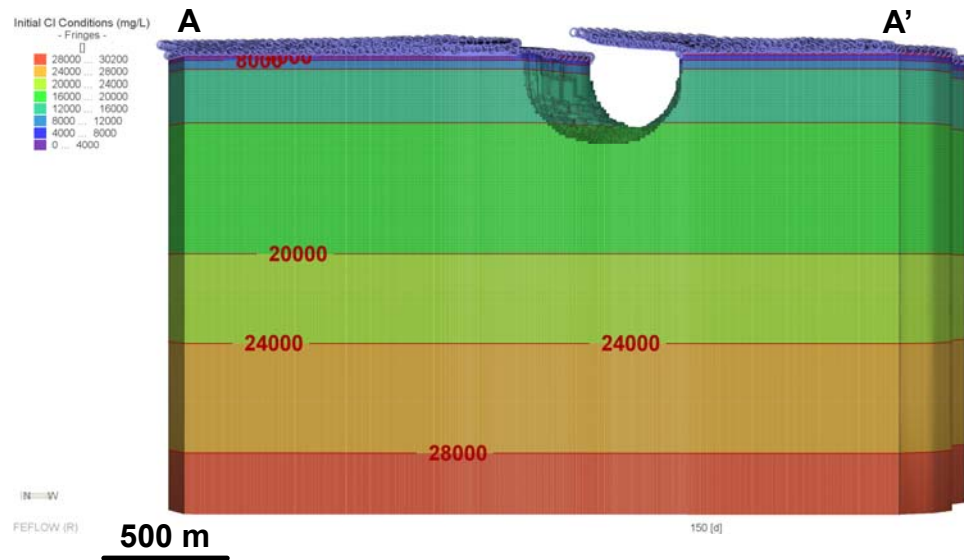
End of Mining Cl Concentration



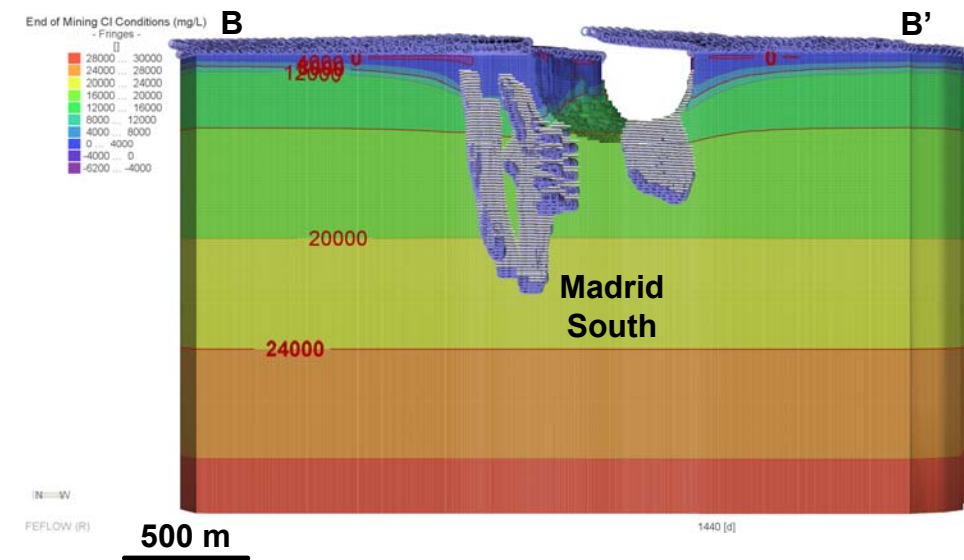
Difference
(End of Mining minus Pre-Mining)



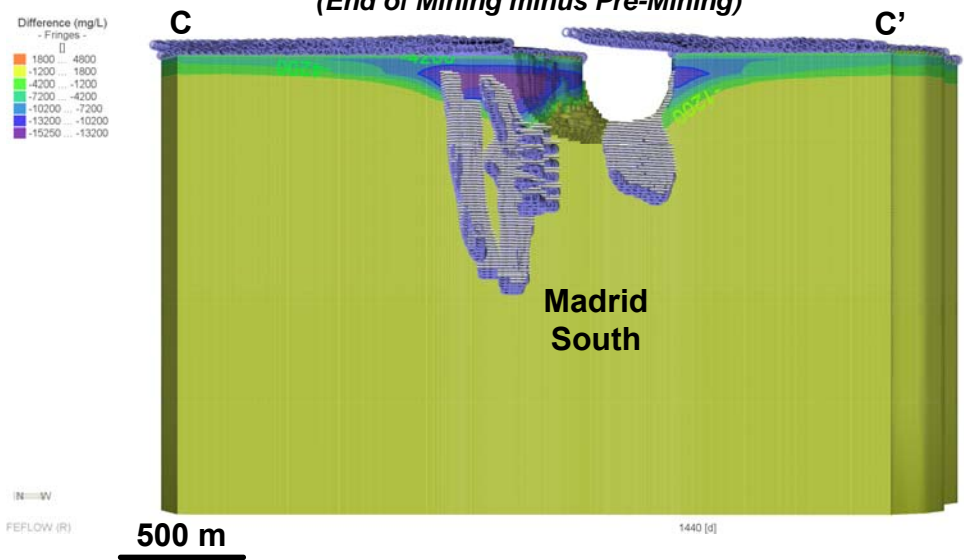
Pre-Mining Cl Concentration



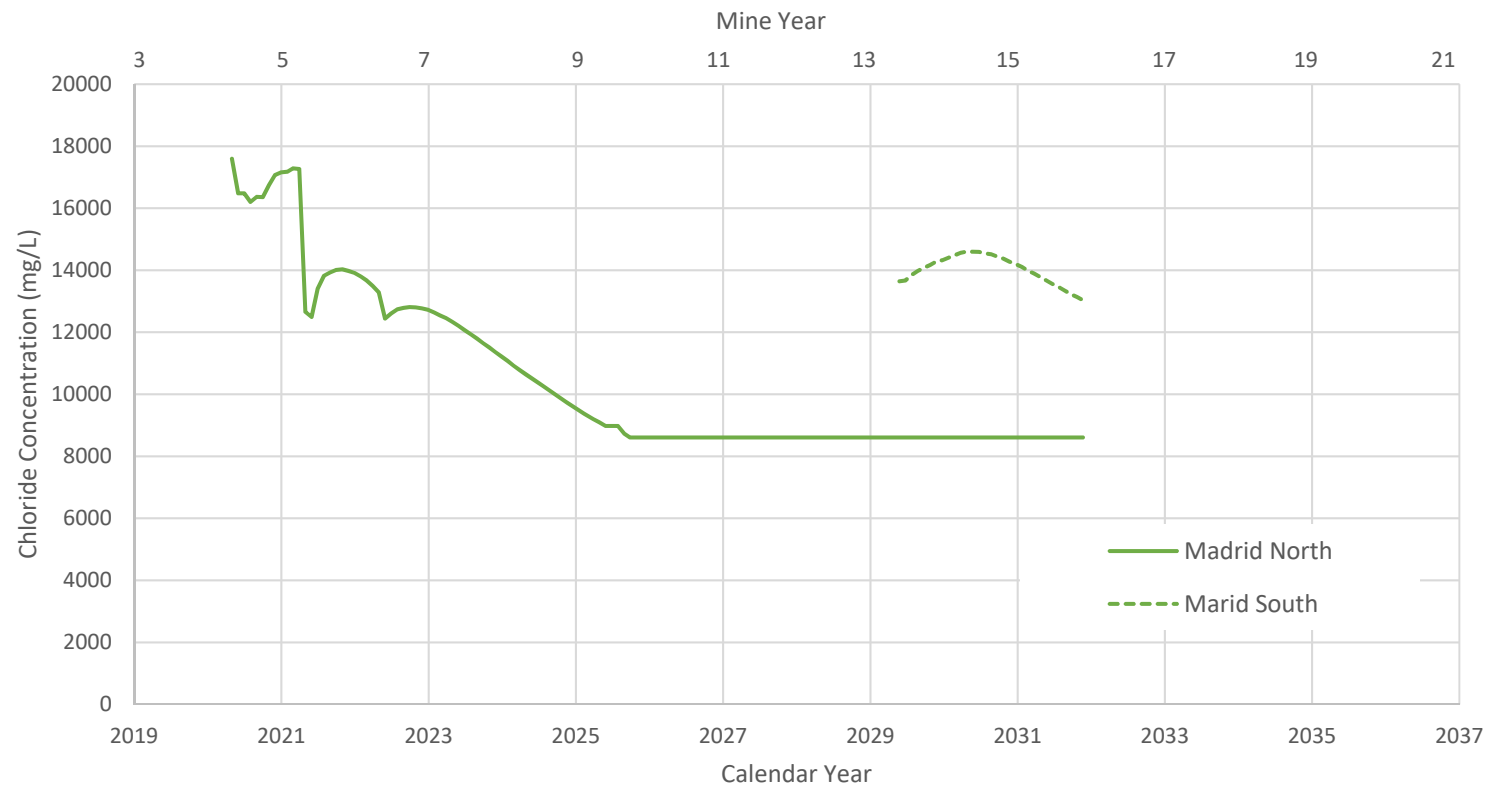
End of Mining Cl Concentration



Difference
(End of Mining minus Pre-Mining)



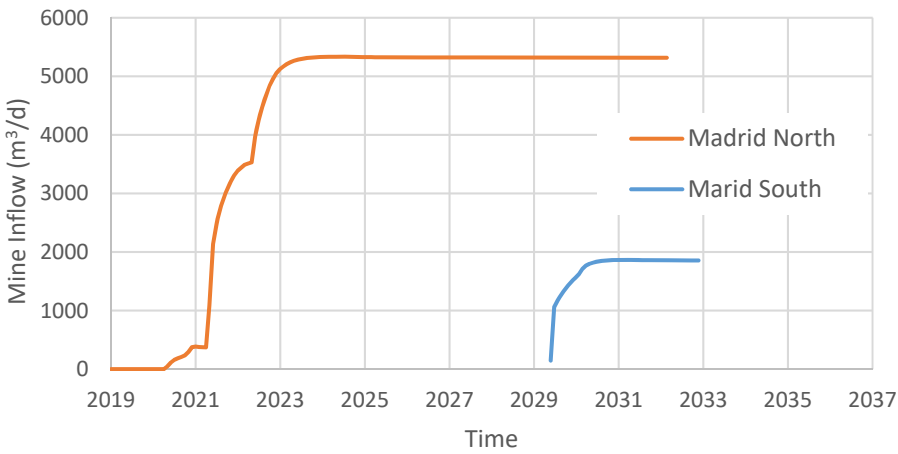
* white arrows = flow direction



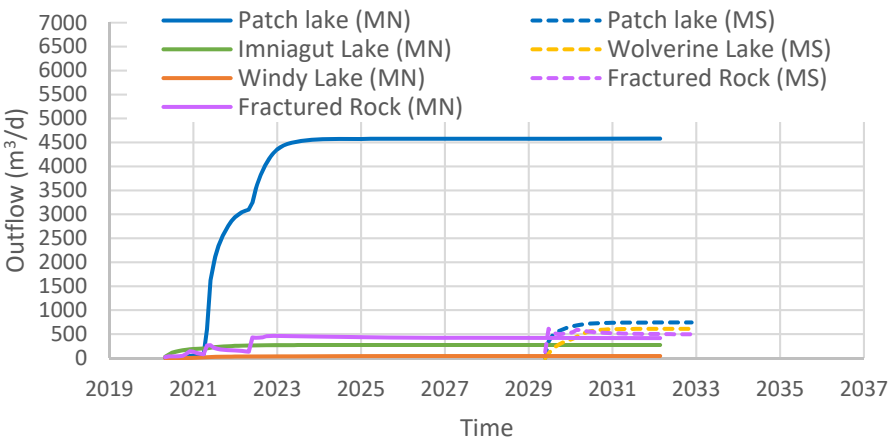
Source: MADRID_v3_BASECASE_Inflow_&_Conc_Predictions.xlsx

		Hydrogeological Modeling		
		Predicted Chloride Concentrations of Mine Inflows		
Job No: 1CT022.013 Filename: 1CT022.013_FEIS_Fig_8x11_Lndscp.pptx	Hope Bay Project	Date: Nov. 2017	Approved: GF	Figure: 38

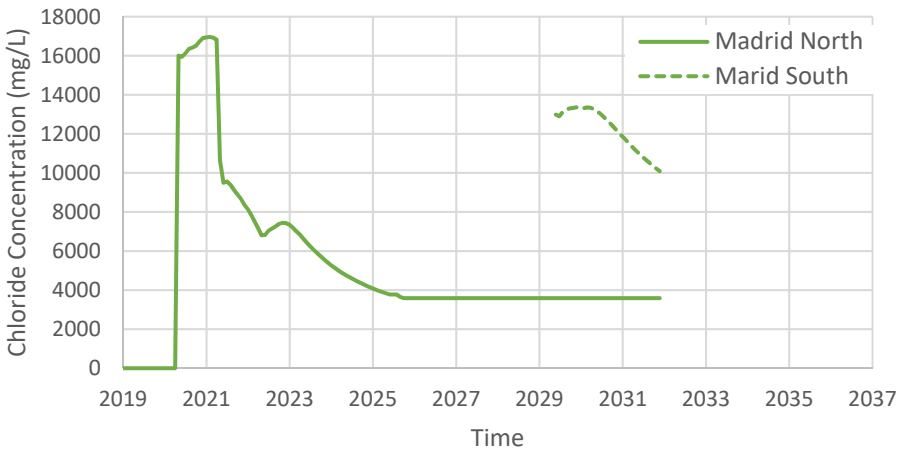
Sensitivity: Kxyz based on arithmetic mean
Predicted mine inflows



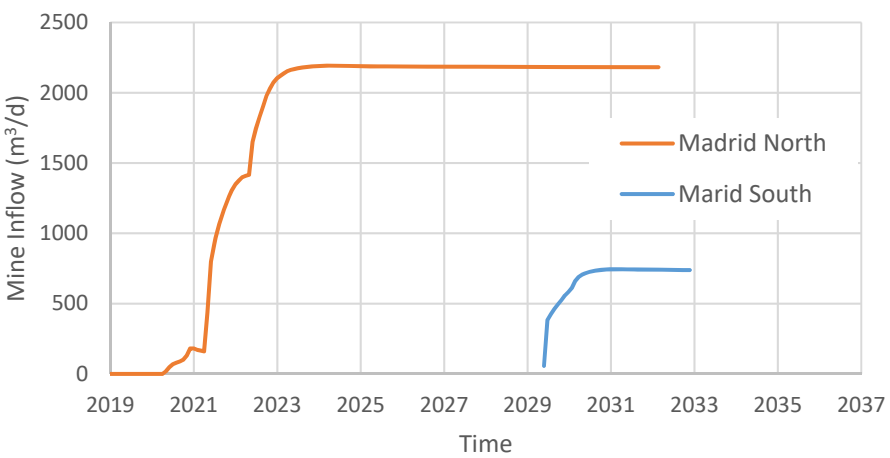
Predicted infiltrations of water from lakes



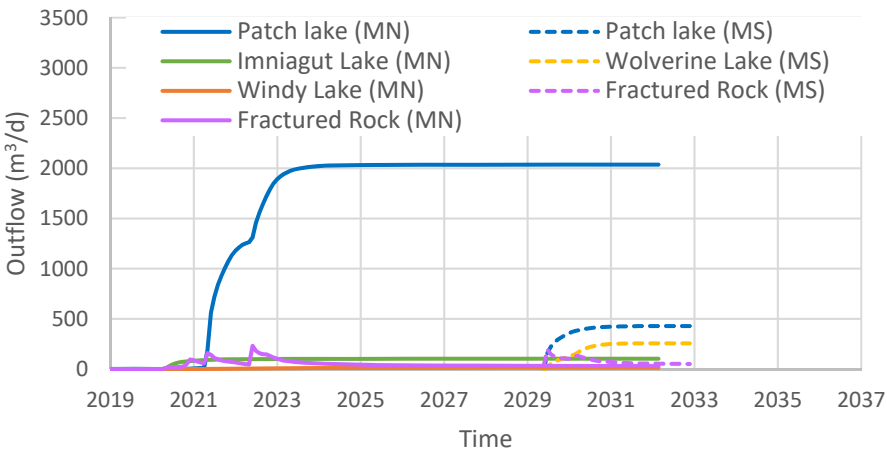
Predicted chloride concentrations of mine inflows



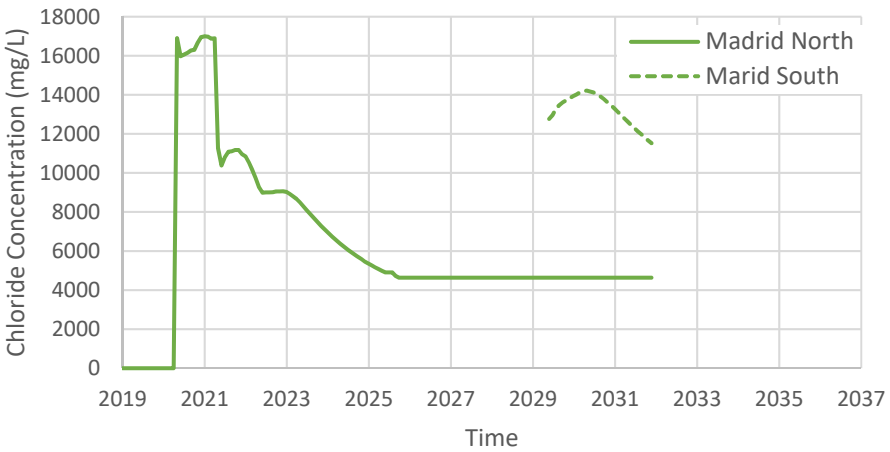
Sensitivity: Kz based on arithmetic mean
Predicted mine inflows



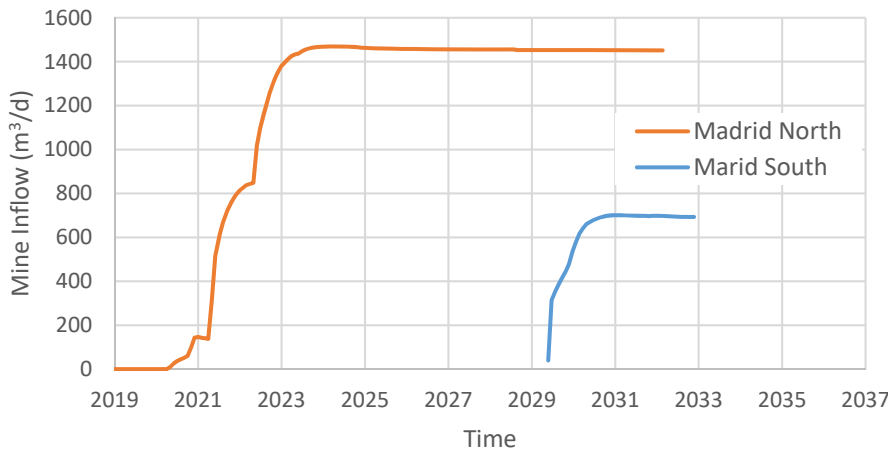
Predicted infiltrations of water from lakes



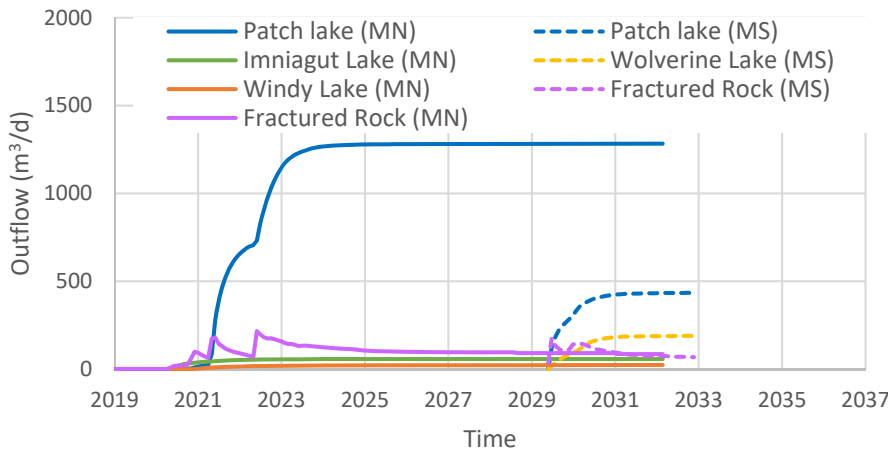
Predicted chloride concentrations of mine inflows



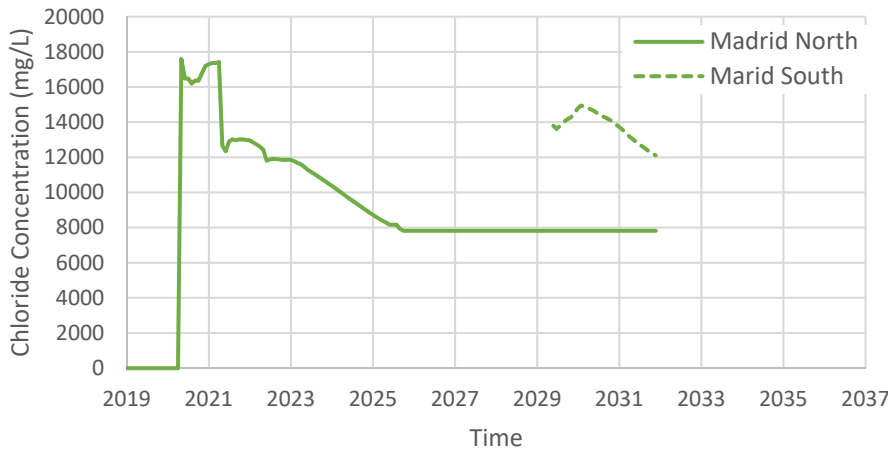
Sensitivity: High K Fault
Predicted mine inflows



Predicted infiltrations of water from lakes



Predicted chloride concentrations of mine inflows

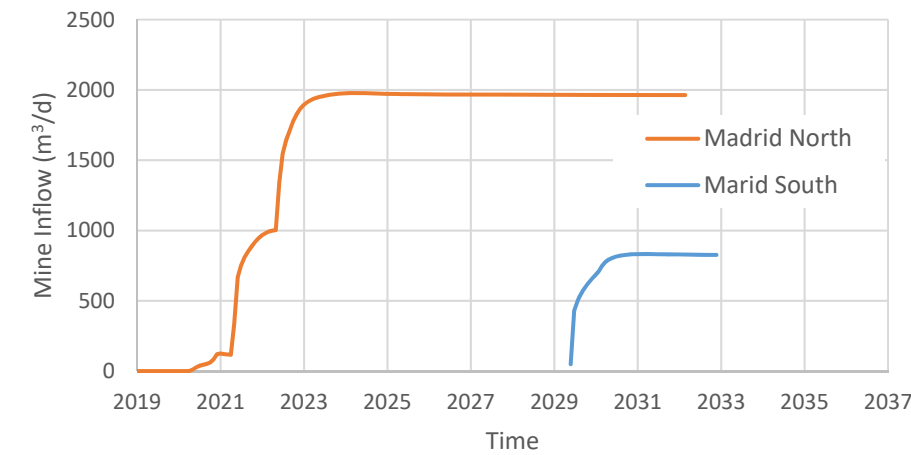


Note:
MS, Madrid South
MN, Madrid North

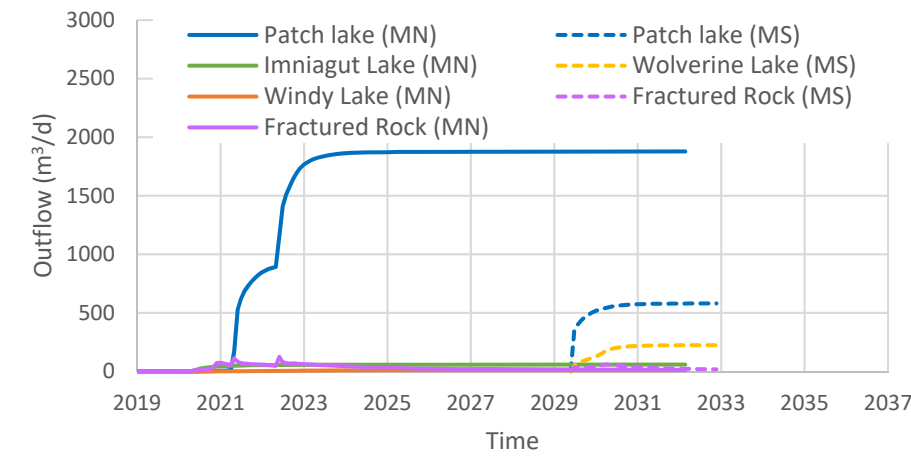
Sources:
IMADRID_upd-oct2016_v13.1-V15.1_BASECASE_Inflow_&_Conc_Predictions_20161107_rev1.xlsx
IMADRID_upd-oct2016_v13.2-V15.2_BASECASE_Inflow_&_Conc_Predictions_20161107_rev1.xlsx
IMADRID_upd-oct2016_v13.3-V15.3_BASECASE_Inflow_&_Conc_Predictions_20161107_rev1.xlsx

Sensitivity: K Lake Sediments (x10)

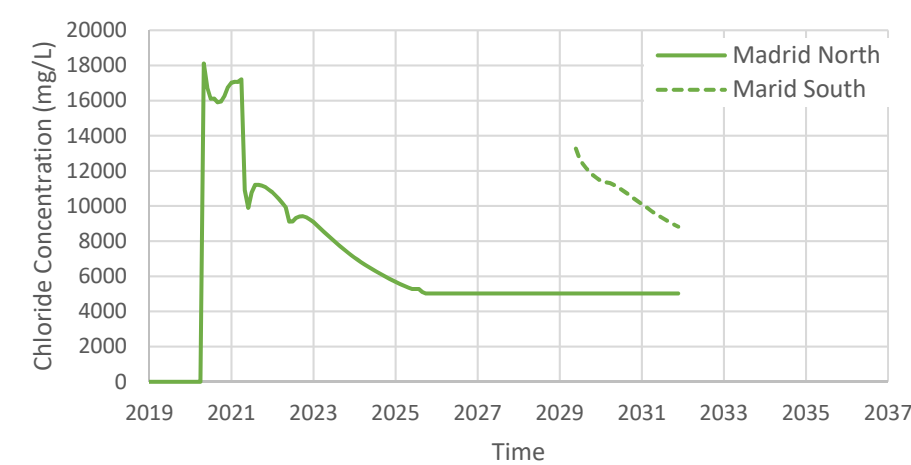
Predicted mine inflows



Predicted infiltrations of water from lakes

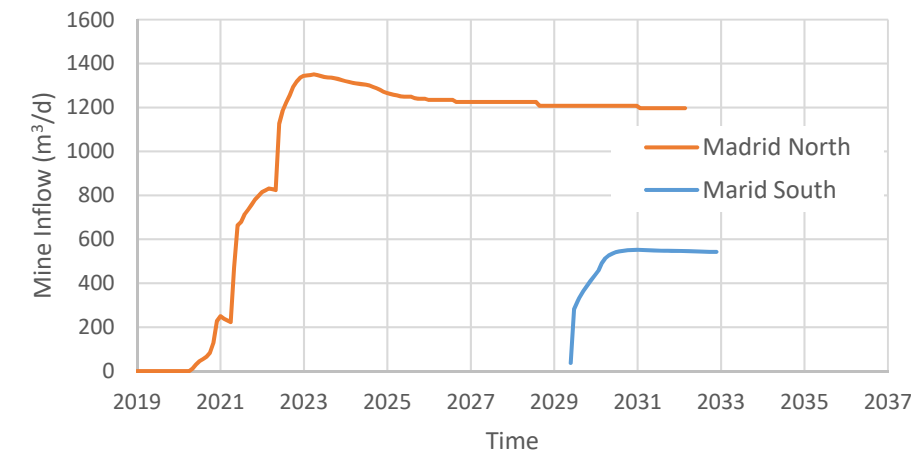


Predicted chloride concentrations of mine inflows

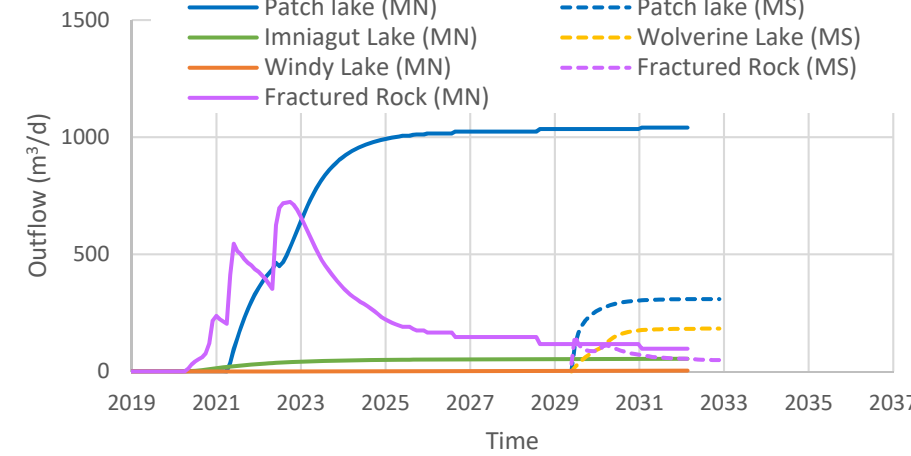


Sensitivity: Storage Coefficients (x10)

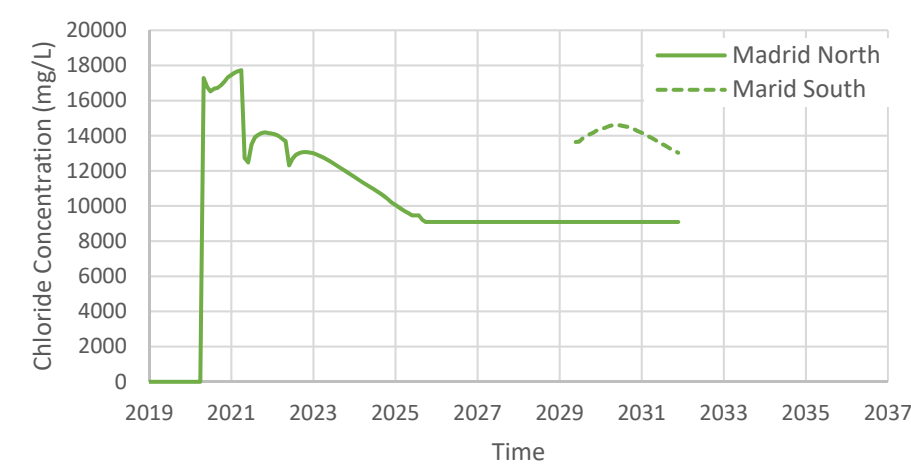
Predicted mine inflows



Predicted infiltrations of water from lakes

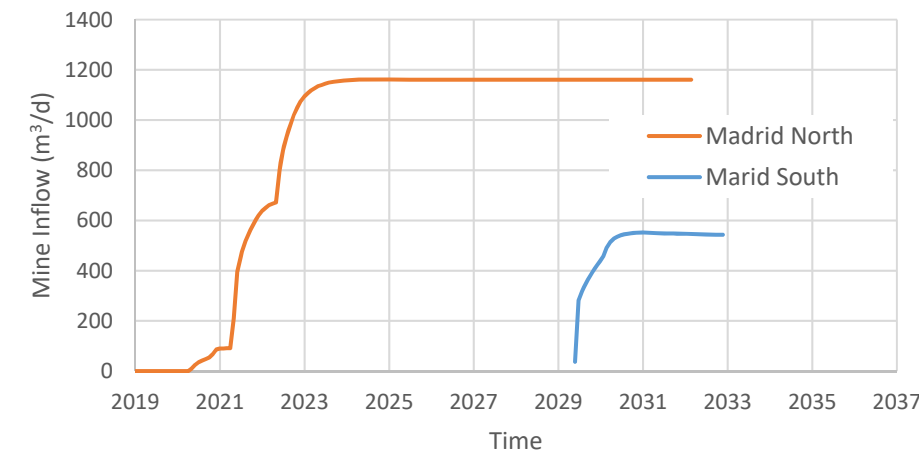


Predicted chloride concentrations of mine inflows

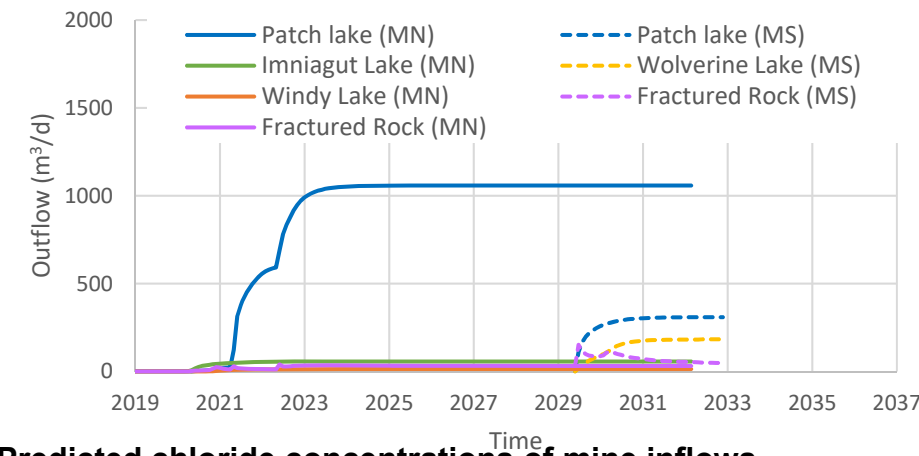


Sensitivity: Storage Coefficients (x0.1)

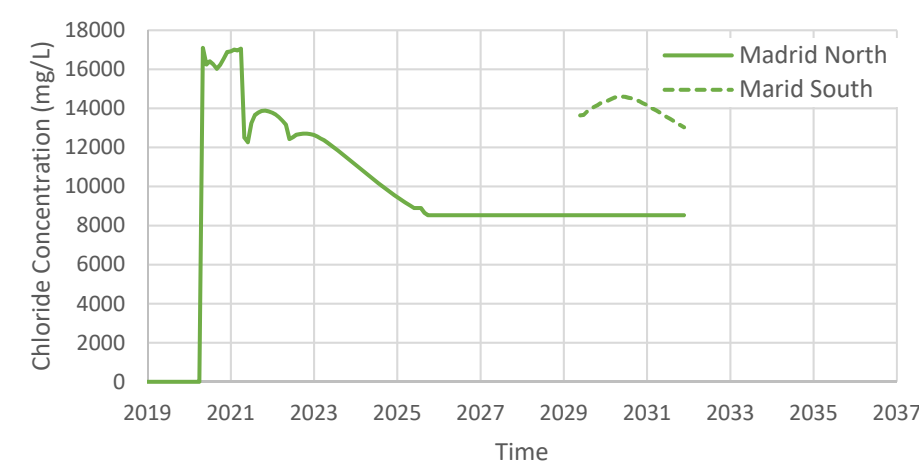
Predicted mine inflows



Predicted infiltrations of water from lakes



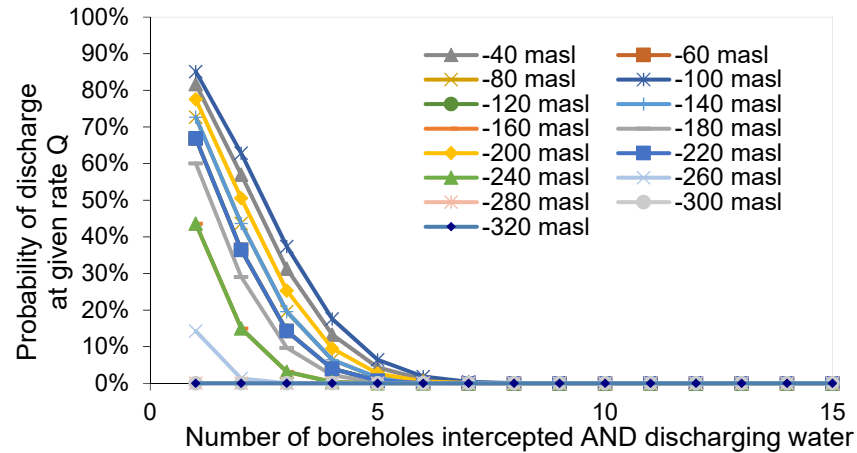
Predicted chloride concentrations of mine inflows



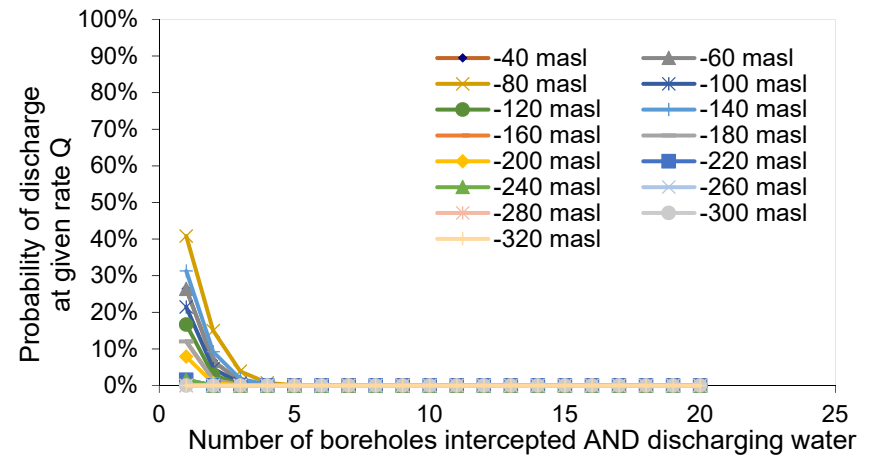
Note:
MS, Madrid South
MN, Madrid North

Sources:
IMADRID_upd-oct2016_v13.4-V15.4_BASECASE_Inflow_&_Conc_Predictions_20161107_rev1.xlsx
IMADRID_upd-oct2016_v13.6-V15.6_BASECASE_Inflow_&_Conc_Predictions_20161107_rev1.xlsx
IMADRID_upd-oct2016_v13.7-V15.7_BASECASE_Inflow_&_Conc_Predictions_20161107_rev1.xlsx

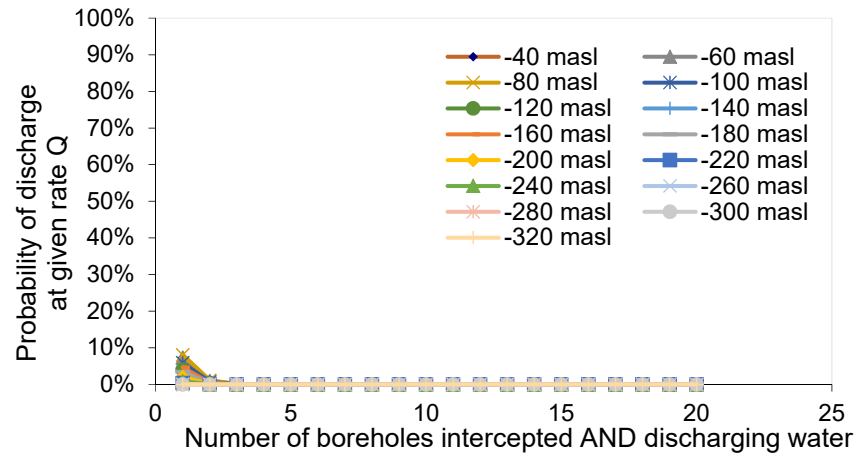
**probability of boreholes discharging water,
where distance = 0m to mine workings**



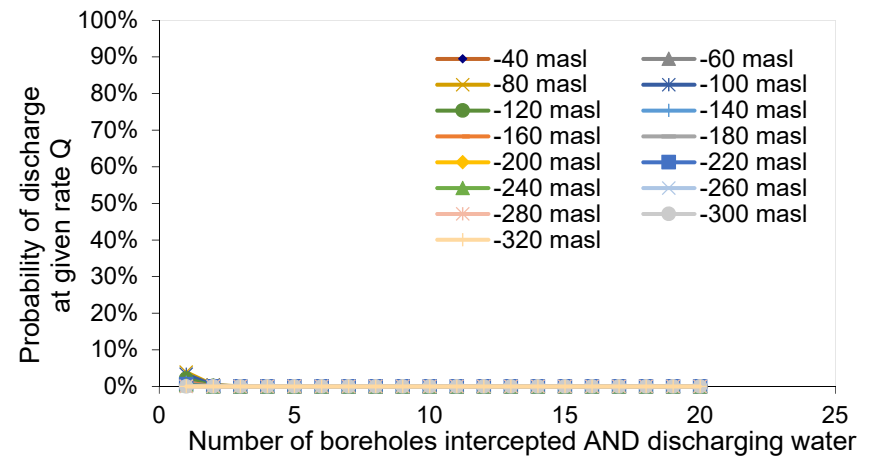
**probability of boreholes discharging water,
where distance > 0 to 3m to mine workings**



**probability of boreholes discharging water,
where distance > 3 to 10m to mine workings**



**probability of boreholes discharging water,
where distance > 10 to 30m to mine workings**



Source: DDH_Intersections_Rev4.xlsx



Job No: 1CT022.013
Filename: 1CT022.013_FEIS_Fig_8x11_Lndscp.pptx



Hope Bay Project

Hydrogeological Modeling

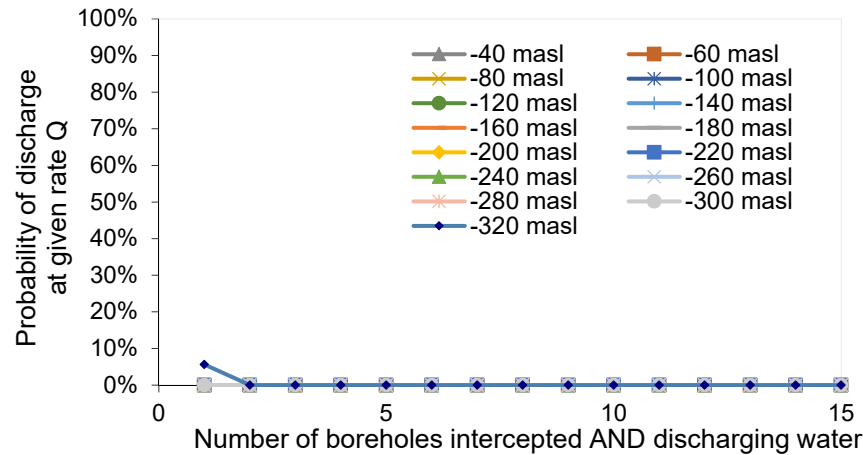
Probabilities of Intercepting Open
Hole Flowing at Maximum Rate at
Madrid North

Date:
Nov. 2017

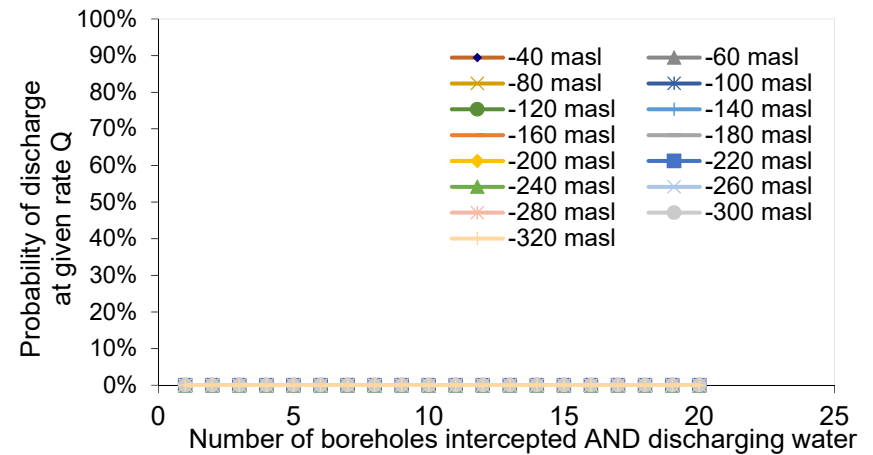
Approved:
GF

Figure: **41**

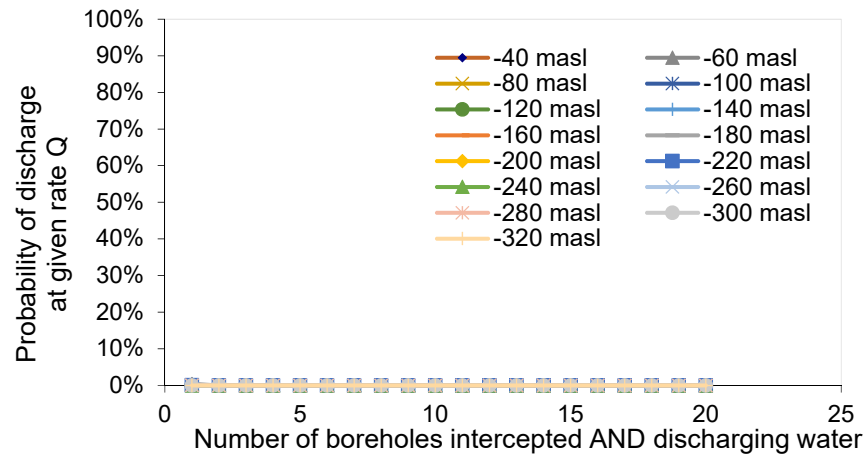
**probability of boreholes discharging water,
where distance = 0m to mine workings**



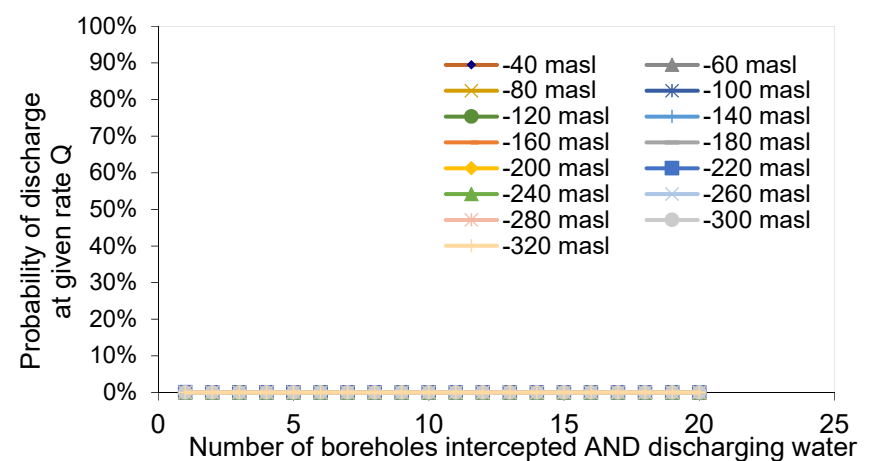
**probability of boreholes discharging water,
where distance > 0 to 3m to mine workings**



**probability of boreholes discharging water,
where distance > 3 to 10m to mine workings**



**probability of boreholes discharging water,
where distance > 10 to 30m to mine workings**



Source: DDH_Intersections_Rev4.xlsx



Job No: 1CT022.013
Filename: 1CT022.013_FEIS_Fig_8x11_Lndscp.pptx



Hope Bay Project

Hydrogeological Modeling

Probabilities of Intercepting Open
Hole Flowing at Maximum Rate at
Madrid South

Date: Nov. 2017	Approved: GF	Figure: 42
--------------------	-----------------	----------------------

Appendix A: SRK Memo, “Hope Bay Project: Lake Talik Configuration”

Memo

To:	John Roberts, PEng, Vice President Environment	Client:	TMAC Resources Inc.
From:	Christopher W. Stevens, PhD	Project No:	1CT022.013
Reviewed By:	Maritz Rykaart, PhD, PEng	Date:	November 30, 2017
Subject:	Hope Bay Project, Lake Talik Configuration		

Change Log

The following table provides an overview of material changes to this report from the previous version issued as Appendix V3-4B, Appendix A as part of the DEIS for Phase 2 of the Hope Bay Project dated December 2016.

Changes by Section

Information Request, Technical Comment, or Other Change	Section	Comments
NRCan-IR6	Section 5.2.1	Additional description of data added

1 Introduction

The Madrid-Boston Project (the Project) is a gold mining and milling undertaking of TMAC Resources Ltd (TMAC). The Project is located 705 km northeast of Yellowknife and 153 km southwest of Cambridge Bay in Nunavut Territory, and is situated east of Bathurst Inlet. The Project comprises three distinct areas of known mineralization plus extensive exploration potential and targets. The three areas that host mineral resources are Doris, Madrid, and Boston.

The Project consists of two phases; Phase 1 (Doris Project), which is currently being carried out under an existing Water Licence, and Phase 2 which is in the environmental assessment stage. Phase 1 includes mining and infrastructure at Doris only, while Phase 2 includes mining and infrastructure at Madrid and Boston located approximately 10 and 60 km due south from Doris respectively.

Although the Project is located in the continuous permafrost region of Canada, an evaluation is necessary to determine if the proposed underground mines will intercept talik zones. Where these talik zones are intercepted by the mine, groundwater inflow may be encountered, requiring appropriate management. Since the extent of these talik zones cannot be completely characterized through field verification, it is best practice to model the talik configuration. This memo provides a description of the modeling and presents the predicted talik configuration for use in subsequent mine inflow modeling.

2 Lake Taliks

2.1 Definition

A talik is defined as “a layer or body of unfrozen ground occurring in a permafrost area due to local anomalies in thermal, hydrological, hydrogeological or hydrochemical conditions” (van Everdingen 2005). In most cases, taliks are formed by lakes and other water bodies which cause a local departure in terrestrial ground temperature (Smith and Hwang 1973; Burn 2002).

In this memo, reference is made to both closed and open (or through) taliks. A closed talik is an unfrozen zone beneath a water body that is enclosed at the base and the surrounding sides by permafrost (Figure 1). An open talik is an unfrozen zone beneath a water body that penetrates the permafrost completely and may connect suprapermfrost (i.e. the layer of ground above permafrost) and subpermafrost (i.e. the unfrozen ground below the permafrost) groundwater.

2.2 Talik Configuration

Lake taliks are transient features in permafrost environments. Key factors influencing talik configuration include water bottom temperature, lake size (half width or radius), present and past ground thermal regime, and long-term changes to the landscape. Present-day water bathymetry can also effect talik configuration where shallow water allows for ice to seasonally freeze to the bottom (bottom-fast ice) and conduct heat from the ground (Burn 2002; 2005; Stevens *et al.* 2010a; 2010b).

The long-term thermal and physical evolution of the landscape is a factor in the present-day configuration of taliks that extend hundreds of metres below the surface. Lunardini (1995) showed temperature at depths up to 600 metres below ground surface (mbgs) can be influenced by surface temperatures as far back as 100,000 years.

Kerr (1994a) provides radiocarbon dating and stratigraphic interpretation of glacial and post-glacial deposits from Perry Peninsula and Queen Maud Gulf, and south of the Bathurst Inlet. His work suggests that deglaciation near the Madrid and Boston mining areas was between 9 ka and 8.7 ka (Kerr 1994a). Retreating ice may have been at or near the mining areas at around 9 ka, followed by a period of rapid ice retreat and ice-free conditions by 8.7 ka. Deglaciation was accompanied by synchronous marine incursion of the isostatically depressed terrain. Sea level curves constructed for the southern Bathurst Inlet suggest drainage of the marine water by at least 5 ka years BP (Kerr 1994b).

The sub-aerial exposure of land following drainage of marine water and cold air temperatures would have led to permafrost aggradation. Over time newly formed lakes and changes in water level of existing lakes due to changes in surface hydrology and climate would result in adjustment of lake taliks to a new equilibrium.

Open taliks are expected to be present beneath some lakes at the Property. Open taliks have been inferred from ground temperature measurements collected beneath Doris, Patch, and Aimaokatalok Lakes (SRK 2011a; Appendix A). Previous thermal modeling also supports the inference of open taliks beneath Doris and Tail Lakes, which are elongated lakes with a half-width of about 475 m and 390 m, respectively (SRK 2005a).

3 Ground Conditions

3.1 Permafrost

SRK (2017) provides detailed information on the baseline ground temperature and permafrost characteristics located in the Doris Mine, and the Madrid and Boston mining areas. The average present-day temperature of permafrost is -7.6°C at the Property, with a range from -5.6°C to -9.8°C (SRK 2017). The baseline ground temperature sites do not permit for separate assessment of permafrost temperatures at each of the three mining areas.

The base of permafrost has been estimated from ten sites to be 78 to 570 metres below ground surface (mbgs) based on the 0°C isotherm. Ground temperature sites removed from the thermal effects of nearby lakes indicate the base of permafrost extends to 570 mbgs (Site 08PMD669) at the Madrid mining area and 565 mbgs (Site 08SBD380) at the Boston mining area (Table 1). At Doris, the base of permafrost extent up to 511 mbgs at Site 10WB002. The geothermal gradient calculated from the deeper extent of permafrost averages $0.021^{\circ}\text{C m}^{-1}$, with a range of $0.014^{\circ}\text{C m}^{-1}$ to $0.029^{\circ}\text{C m}^{-1}$ (Table 1).

Table 1: Summary of Base of Permafrost and Geothermal Gradient

Thermistor Site ID	Northing	Easting	Location	Location Reference	Geothermal Gradient (°C/m)	Base of Permafrost (mbgs)
SRK-50	7,559,177	433,807	Doris Mining Area	Fig. 18	0.019	394
08TDD632	7,559,370	433,915	Doris Mining Area	Fig. 18	0.024	445
10WBW002	7,559,375	433,913	Doris Mining Area	Fig. 18	0.014	511
08PMD669	7,550,955	433,300	Madrid North Mining Area	Fig. 13+16	0.018	570
TM00141	7,546,691	435,141	Madrid South Mining Area	Fig. 13+17	0.023	346
08PSD144	7,548,990	435,178	Patch Lake Island	Fig. 13+15	-	78
08SBD380	7,504,780	441,080	Boston Mining Area	Fig. 5	0.017	565
08SBD381A	7,504,814	441,070	Boston Mining Area	Fig. 5	0.029	281
08SBD382	7,505,141	441,026	Boston Mining Area	Fig. 5	0.027	302
10WBW004	7,505,665	441,018	Boston Mining Area	Fig. 5	0.018	326
97NOD176	7,504,962	441,481	Boston Mining Area	Fig. 5	0.019	556
All Sites				Average	0.021	398
				Minimum	0.014	78
				Maximum	0.029	570
				Count	10	11

Water quality data collected from the Doris Central Westbay well (Site 10WBW001) indicates saline connate groundwater which is comparable to quality measurements observed at the Boston mining area. The lowest freezing point depression calculated from the concentration of dominate components of the groundwater was estimated to be -1.9°C (SRK 2011b). For the purpose of modeling talik extent, ground temperatures warmer than -2°C are expected to be unfrozen.

It should be recognized that the connection between surface water, mined structures, and subpermafrost groundwater is also a function of the hydraulic properties of the bedrock, the geological structures, and the hydraulic gradients that drive water movement; i.e. unfrozen ground does not necessarily constitute significant groundwater movement.

3.2 Lake Bottom Water Temperature

Table 2 shows average lake bottom water temperature (LbT) recorded during the month of April, July, August, and September for five lake locations over the period of 2010-2014 (ERM 2015; ERM 2014; Rescan 2012; Rescan 2011a). The lake bottom water temperatures are based on the deepest measurements collected at each site.

Table 2: Summary of Lake Bottom Water Temperatures

Location	Data Source (See notes)	Temperature (°C)					Ice Thickness (m)
		April	July	August	September	LbT	
Doris Lake North	1,3,4,5,6	1.5	7.8	11.0	6.2	4.7	1.8
Doris Lake South	1,3,4,5,6	1.0	9.0	10.7	5.7	4.2	1.9
Reference Lake A	1	1.6	-	4.3	-	2.5	1.8
Reference Lake B	1,3,4,5,6	2.6	9.1	11.1	3.9	5.5	1.7
Reference Lake C	2	2.0	-	8.3	-	4.1	1.9
Reference Lake D	1,3,4,5,6	0.8	11.4	12.1	2.5	4.6	1.9
Little Roberts Lake	1,3,4,5,6	0.7	10.6	10.9	3.4	4.1	1.9
Wolverine Lake	1	1.4	-	13.2	-	5.3	1.8
Patch Lake North	1	1.2	-	10.8	-	4.4	2.1
Patch Lake South	1	2.1	-	10.3	-	4.8	1.9
P.O. Lake	1	0.2	-	10.0	-	3.5	1.9
Ogama Lake	1	1.8	-	10.0	-	4.5	1.8
Doris Lake North	1	1.1	-	10.0	-	4.1	2.0
Doris Lake South	1	0.9	-	9.7	-	3.8	2.0
Naiqunnguut Lake	1	1.4	-	10.2	-	4.3	1.9
Nkhatok Lake	1	0.4	-	11.7	-	4.2	1.9
Glenn Lake	1	0.5	-	9.9	-	3.6	2.0
Imniagut Lake	1	-	-	12.2	-	-	2.0
Little Roberts Lake	1	1.3	-	10.0	-	4.2	2.1
Stickleback Lake	2	1.1	-	11.2	-	4.5	1.8
Trout Lake	2	0.8	-	12.6	-	4.7	1.8
Windy Lake	1,2	2.0	-	10.1	-	4.7	1.8
Aimaokatalok Lake: Station 2	2	-	-	11.6	-	-	-
Aimaokatalok Lake: Station 5	2	0.0	-	14.8	-	4.9	1.8
Aimaokatalok Lake: Station 6	2	2.3	-	12.1	-	5.6	1.6
Aimaokatalok Lake: Station 11	2	0.1	-	12.1	-	4.1	1.6
Aimaokatalok Lake: Station 13	2	-	-	13.9	-	-	-
All Sites					Average	4.4	1.9
					Minimum	2.5	1.6
					Maximum	5.6	2.1
					Count	24	25

Notes:

1. Average monthly temperature collected over the period of 2009- 2014 (see data source)
2. Annual lake bottom temperature (LbT) calculated using Equation 1
3. Ice thickness measured from ice auger hole drilled in April
4. Data source: 1 – Rescan (2010), 2 – Rescan (2011a), 3 – Rescan (2011b), 4 – Rescan (2012), 5 – ERM Rescan (2014), 6 – ERM (2015)

Mean annual lake bottom water temperature was calculated as a weighted mean of April and August temperatures:

$$LbT = 8LbT_{Apr} + 4LbT_{Aug} / P \quad \text{Eq. 1}$$

where:

LbT = mean annual lake bottom water temperature (°C)

LbT_{Apr} = measured lake bottom water temperature in April (°C)

LbT_{Aug} = measured lake bottom water temperature in August (°C)

P = is the period of time

Based on Equation 1, April water temperature is assumed to be representative of the period of ice cover (October to May). August water temperatures represent the warmest measurements and likely over-estimate water temperature throughout the ice-free period. Therefore, a conservative water temperature is computed using this approach, and allowed for in the thermal models.

The annual lake bottom water temperature is calculated to average of +4.4°C, with a range from +2.5°C to +5.6°C (Table 2). A value of +4.4°C is considered to be reasonable for base case conditions.

4 Regional Talik Model

4.1 Analytical Model

The critical lake dimension required for open (through) lake taliks was assessed using a one-dimensional (1D) steady state analytical model for lakes. The regional model was development to provide regional context for taliks in the area. The thermal models used for this assessment are presented by Mackay (1962), Smith (1976), and Burn (2002) for study sites in the Canadian Arctic, and have been used for talik characterization at other proposed mine projects located in the continuous permafrost region of mainland Nunavut, including the Back River Project (SRK 2015), Meliadine (Golder 2013), Kiggavik (Areva Resources Canada 2011), High Lake (Wolfden Resources Inc. 2006), Doris (SRK 2005b), and Meadowbank (Cumberland Resources Ltd. 2005) projects.

The temperature profile beneath the centre of a circular lake without terraces has been modeled by Mackay (1962) as:

$$T_z = T_g + \frac{z}{l} + (LbT - T_g) \left(1 - \frac{z}{\sqrt{z^2 + R^2}} \right) \quad \text{Eq. 2.}$$

Where:

T_z = temperature at depth z (°C)

LbT = Average annual lake bottom water temperature (°C)

T_g = average annual ground temperature (°C)

l = inverse of the geothermal gradient (m °C⁻¹)

z = depth below bottom of lake (m)

R = radius of the lake (m)

The temperature profile beneath symmetrical elongated lakes without terraces has been modeled by Smith (1976) as:

$$T_z = T_g + \frac{z}{l} + \frac{LbT - T_g}{\pi} \left(2 \tan^{-1} \frac{w}{z} \right) \quad \text{Eq. 3.}$$

Where:

T_z = Temperature at depth z (°C)

LbT = Average annual lake bottom water temperature (°C)

T_g = Average annual ground temperature (°C)

l = inverse of the geothermal gradient (m °C⁻¹)

z = depth below bottom of lake (m)

w = half-width of an elongated lake (m)

For conservatism, shallow-water terraces (lake terraces) which may be thermally influenced by bottom-fast ice were not considered in the analytical model. Table 3 shows the base case and sensitivity values using the in the 1D model. Base case values are representative of average measurements from the mining areas.

Table 3: Thermal Modeling Input Values for Analytical Talik Model

Parameter	Value (Base Case)	Value (Sensitivity Analysis)
Ground temperature (T_g)	-7.6°C	-5°C to -9°C
Mean annual lake-bottom temperature (LbT)	+4.4°C	+3°C to +6°C
Geothermal heat flux (G)	0.021°C m ⁻¹	0.014 to 0.029°C m ⁻¹

Notes:

1. Measured mean annual permafrost temperature is -7.6°C and mean annual lake bottom temperature is +4.4°C
2. Average geothermal gradient calculated from ground temperature measurements is 0.021°C m⁻¹

4.2 Model Assumptions

The modeling, as presented, is based on the following assumptions:

- Lake geometry is defined in the models as either circular or elongate, and does not account for actual lake geometries which can be quite complex.
- Modeling does not account for the thermal influence of adjacent lakes (lateral heat flow) and spatial variability in ground surface temperature. However, the sensitivity to lake-bottom temperature (LbT) and permafrost temperature are considered (Table 3).
- Water depth is assumed to be greater than the maximum thickness of seasonal ice, and the thermal influence of bottom-fast ice is not considered, making the results more conservative.
- Ground thermal properties and complex mechanisms for heat flow such as convection are not accounted for in the model.
- Geothermal heat flux is based on an average value calculated from ground temperature measurements with sensitivity around the range of values collected at the Property (Table 3).

- Steady-state models are used and therefore the transient effects, such as paleo-climate (i.e. long-term changes in ground surface and water temperature) are not considered.

Talik will naturally adjust to changes in climate and evolution of the landscape. Over the time scale of the Project, the most immediate effects would be an increase in extent of the talik beneath the shoreline, and possible subsidence and erosion of the shoreline at locations with ice-rich permafrost. A reduction in lake ice growth due to climate change would also be expected to widen and deepen existing taliks beneath shallow water bodies which rely on seasonal heat loss through the establishment of bottom-fast ice (Burn 2002; 2005; Stevens *et al.* 2010a; 2010b). The natural development of new ponds at the Property would also result in newly formed closed taliks. On the time scale of hundreds to thousands of years, open taliks may form as permafrost degrades beneath these recently formed water bodies. Natural lowering of lake water level or even complete drainage due to climate change may also result in permafrost aggradation beneath the former lake basin and long-term freezeback of taliks.

4.3 Model Results

The estimated critical dimensions for open (through) taliks beneath lakes at the Property are summarized in Table 4 and Table 5. The findings are based on a groundwater freezing point depression of -2°C and are graphically depicted in Figure 2 and Figure 3.

For the base case scenario, open taliks are estimated to occur beneath circular lakes with a diameter >224 m (i.e. lake radius of >112 m). For elongated lakes, the critical lake width is estimated to be >104 m wide (i.e. lake half-width >52 m).

Sensitivity of the critical lake dimension to change in the geothermal gradient is shown in Figure 4 and Figure 5.

Table 4: Circular Lake Critical Radius for Open (Through) Taliks Based on -2°C Isotherm

Permafrost Temperature	Annual Lake Bottom Temperature (LbT)				
	+3.0°C	+4.0°C	+4.4°C	+5.0°C	+6.0°C
-9.0°C	169 m	159 m	155 m	151 m	144 m
-8.0°C	138 m	129 m	126 m	122 m	117 m
-7.6°C	123 m	115 m	112 m	109 m	104 m
-7.0°C	108 m	101 m	98 m	95 m	91 m
-6.0°C	80 m	74 m	72 m	70 m	67 m
-5.0°C	54 m	50 m	49 m	47 m	44 m

Table 5: Elongated Lake Critical Half-width for Open (Through) Taliks Based on -2°C Isotherm

Permafrost Temperature	Annual Lake Bottom Temperature (LbT)				
	+3.0°C	+4.0°C	+4.4°C	+5.0°C	+6.0°C
-9.0°C	83 m	76 m	73 m	70 m	65 m
-8.0°C	66 m	60 m	58 m	55m	50 m
-7.6°C	60 m	54 m	52 m	49 m	45 m
-7.0°C	50 m	45 m	43 m	41 m	38 m
-6.0°C	36 m	32 m	30 m	28 m	26 m
-5.0°C	23 m	20 m	19 m	17 m	15 m

5 Site-specific Talik Model

5.1 Approach

Lake talik configuration adjacent to the Boston and Madrid mining areas was estimated using 2D thermal modeling. The model results were fitted to field observations of the -2°C isotherm, and therefore use calculated heat flow as a basis for estimating talik geometry. The modeling was carried out using a finite element code SVHeat developed by SoilVision Systems Ltd. with the FlexPDE solver.

5.1.1 Model Setup and Inputs

A long-term mean annual ground surface temperature was applied to the upper model boundary over areas of land. Long-term ground surface temperature was based on a projection of the thermal gradient from deep ground temperature measurements to the surface. The projected ground surface temperature reflects approximate paleo-surface temperature, which is typically colder than present day permafrost temperature calculated from the baseline ground temperature sites (SRK 2017). At the Madrid and Boston mining areas, the long-term ground surface temperature was estimated to be -9.6°C (Site 08PMD669) and -9.2°C (Site 08SBD380), respectively. A long-term ground surface temperature was used to more closely estimate talik configuration and the base of permafrost which result from paleo conditions. The geothermal gradient applied to the lower boundary of the model was based on Site 08PMD669 for Madrid Mining Area and Site 08SBD380 for the Boston mining area (Table 1).

A mean annual lake bottom water temperature of +4.4°C was applied to the upper boundary for lakes (Table 2). Lake width was based on current extent of water bodies at the underground mining areas. At Aimaokatalok Lake adjacent to the Boston mining area, an annual temperature of -2°C was also applied to lake areas with a water depth less than 1.3 m (i.e. water depth that is two-thirds of the mean annual ice thickness). A value of -2°C was applied to the shallow water lake terrace based on measured temperatures from similar environments (Burn 2002; 2005). The ice across these shallow water lake terraces freezes to the bottom with sufficient heat loss from the lake bottom to sustain permafrost beneath the shallow water terraces of Arctic lakes (Mackay 1992; Burn 2002). The thermal regime of shallow water was not considered at the Madrid underground mining areas due to the relatively rapid increase in water depth from shore.

Model simulations were based on a time step of one year. Table 5 summarises the thermal properties used in the transient lake talik model. The frozen and unfrozen thermal conductivity and heat capacity for bedrock (basalt) was based on previous thermal modeling at Hope Bay (SRK 2005; SRK 2011a).

Table 5: Bedrock Thermal Properties 2D Lake Talik Model

Material	Degree of Saturation (%)	Porosity	Thermal Conductivity (kJ m ⁻¹ day ⁻¹ °C ⁻¹)		Volumetric Heat Capacity (kJ m ⁻³ °C ⁻¹)	
			Unfrozen	Frozen	Unfrozen	Frozen
Basalt Bedrock	100	0.05	260	260	2,380	2,133

5.1.2 Model Assumptions

The 2D thermal modeling, as presented, is based on the following assumptions:

- Lake geometry is defined by current lake extent and does not account for historic lake configuration which can be complex.
- Lake-bottom geometry is not directly considered in the model sections. The relatively shallow lake depths would have limited impact on talik configuration deep below the ground surface.
- Surface topography is not considered in the model sections due to low relatively relief across the Property and its limited influence on talik configuration.
- Long-term paleo ground surface temperatures are based on values projected from deep ground temperature measurements, and do not capture more recent variability in surface temperature.
- Ground thermal properties and complex mechanisms for heat flow such as convection are not accounted for in the model.

5.2 Boston Mine Area

The Boston underground mine will be located on the east side of Aimaakatalok Lake (Figure 6). A total of four sections were used to model the lake talik.

5.2.1 Ground Temperature Measurements

Deep ground temperature measurements have been collected from three deep inclined wells which extend beneath Aimaakatalok Lake; well 08SBD381A, 08SBD382, and 10WBW004 (Figure 7). Well 08SBD380 and 97NOD176 are two additional deep wells that have been drilled inland near the Boston mine workings.

Table 6 summarizes the position of the 0°C and -2°C isotherms for the Boston mining area. At 08SBD380 and 97NOD176, the ground temperature has been measured to a maximum depth of 241 mbgs and 247 mbgs, respectively. The base of permafrost is not directly incepted by these wells and the lowermost thermistors nodes indicate relatively cold permafrost temperatures (-5.1°C at 08SBD380 and -5.5°C at 97NOD176). The projected base of permafrost based on the

0°C isotherm is 565 mbgs at 08SBD380 and 556 mbgs at 97NOD176 (Table 6). The -2°C isotherm is projected to be 430 mbgs at 08SBD380 and 449 mbgs at 97NOD176. At site 08SBD380, the drill hole is orientated at an inclined angle toward Stickleback Lake. Based on the depth of the 0°C and -2°C isotherm and relatively cold temperatures measured from the lowermost thermistor node, it can be inferred that permafrost continues in the direction of Stickleback Lake and beyond the extent of the underground mine.

Ground temperatures measured at three sites beneath Aimaokatalok Lake provide information on the extent of the lake talik adjacent to the shoreline (Figure 6 and Figure 7). Figure 8 shows the depth of the -2°C isotherm and its distance from shore for these sites. The water bathymetry for the three areas with ground temperatures beneath the lake are shown in Figure 9. At site 08SBD382, the -2°C isotherm is up to 115 m from the lake shoreline and located at a depth of 224 mbgs. At site 08SBD381A and 10WBW004, the -2°C isotherm is 17 and 42 metres from shore and located between 202 and 209 mbgs (Table 6).

Table 6: Boston Mining Area Depth of 0°C and -2°C Isotherm from Ground Temperature Data

Site	Location	Maximum Instrumented Depth (mbgs)	-2°C Isotherm (mbgs)	0°C Isotherm (mbgs)
08SBD380	Near Underground Mine	241	430	565
97NOD176	Near Underground Mine	247	449	556
08SBD381A	Extends Beneath Lake	291	202	281
08SBD382	Extends Beneath Lake	313	224	302
10WBW004	Extends Beneath Lake	399	209	326

Notes:

1. Digital data not available for 97NOD176, depth and temperature determined from graphical form of data
2. Thermistor node depth corrected for vertical depth using downhole well survey and surface elevation
3. Depth shown as vertical metres below ground surface (mbgs)

For sites 08SBD381A and 08SBD382, the -2°C is located beneath water depths which are not expected to seasonally freeze to the bottom and therefore do not experience thermal conduction of heat through bottom-fast ice cover. The presence of floating ice at these locations implies that there is no significant means to vertically remove heat gained from the water and the lake bottom. At site 10WBW004, the -2°C isotherm is located beneath water depths that are about two-thirds the maximum ice thickness (i.e. an ice thickness of 1.3 m). It has been suggested that water depth less than two-thirds the maximum later winter ice thickness is required to sustain permafrost beneath shallow water margins of Arctic lakes impacted by bottom-fast ice (Mackay 1992; Burn 2002). This finding was also in agreement with shallow-water permafrost located within the nearshore zone of the Beaufort Sea (Stevens *et al.* 2010b).

Therefore, under present-day lake configuration the offshore position of the -2°C isotherm cannot be explained by heat loss from seasonal bottom-fast ice. Lateral heat flow from the adjacent land also does not explain the current talik extent beneath the lake. Significantly colder ground surface temperatures and lake bottom-temperatures would be required for the talik to extend beneath the Aimaokatalok Lake. Figure 8 shows the expected configuration of the Aimaokatalok Lake talik for

steady state compared to the position of the measured position of the -2°C isotherm. For steady state talik configuration to meet the field observations, the mean annual ground surface temperatures would need to be around -20°C .

We postulate that the lateral extent of permafrost beneath Aimaokatalok Lake is a direct physical consequence of the rise in lake level through time. Over time, permafrost formed through terrestrial exposure to cold air temperatures has been submerged with lake expansion. The talik is currently responding to the thermal forcing from the current lake and the talik will adjust to new conditions and evolve with the lake. The talik would be expected to adjust to equilibrium conditions on the time scale of hundreds to thousands of years.

5.2.2 Model Results

The 2D model sections were setup to simulate possible expansion of Aimaokatalok Lake and to allow for talik adjustment to meet ground temperature measured at the site. The model was run for 5,000 years which is estimated to be the approximate duration of time since drainage of the post-glacial marine incursion. The following major periods were included in the thermal model:

- From model year 0 to 4.5 ka, the lake was assumed to occupy a smaller area defined by current water depths greater than 5 m deep. This water depth represents the approximate transition from a relatively shallow to steep gradient in the water depth profile; i.e. the change in water depth verses distance (Figure 9). It was thus assumed that lake expansion would be most rapid across areas with a water depth less than 5 m deep where the gradient is shallow.
- From model year 4.5 to 5.0 ka, the lake was allowed to expand and flood the existing permafrost. This step was included in the model to allow for the interpreted adjustment of the talik over time. The position of the -2°C isotherm modeled was then selected to closely fit to the equivalent isotherm measured at sites 08SBD381A, 08SBD382, and 10WBW004.

Figures 10 to 13 show the model results for the Boston mining area. Table 7 shows a comparison between the model fit and the ground temperatures for the -2°C isotherm which represents the transition from frozen to unfrozen conditions at the three sites. In all cases, the model fit is conservative and underestimates the measured depth of the talik.

Table 7: Measured and Model Fit for Talik Surface

Model Section	Thermistor Site ID	Model (-2°C Isotherm)	Measured (-2°C Isotherm)
T1	10WBW004	192	209
T2	08SBD382	215	224
T3	08SBD381A	196	202

Notes:

1. Model position of the -2°C isotherm based on manual fit to field data

5.3 Madrid Mining Area

The Madrid mining area consist of two distinct mines along the west side of Patch Lake. The northern mine (Madrid North) will be located between Windy Lake and Patch Lake, and the southern mine (Madrid South) will be located between Wolverine Lake and Patch Lake.

The 2D models included five sections for Madrid North and four sections for Madrid South (Figure 14). The model sections extend across the underground mining areas with an orientation that is approximately perpendicular to the long axis of the adjacent lakes. The modeled data was fit to the position of the -2°C isotherm measured at Madrid North. At Madrid South, the -2°C isotherm is located beyond the instrumented depth of the ground temperature cable. At this site, the modeled data was fit to the lowermost thermistor sensor (node).

5.3.1 Ground Temperature Measurements

Deep ground temperature measurements have been collected from three inclined wells; 08PMD669, 08PSD144, and TM00141 at the Madrid mining areas (Figure 14 and Figure 15).

Well 08PSD144 is located beneath an island centred within Patch Lake (Figure 16). Ground temperature measurements at the site indicate relatively shallow permafrost beneath the island (base of permafrost 78 mbgs) due to the surrounding heat from the lake.

Well 08PMD669 is located within the area of the Madrid North underground mine workings (Figure 17) and is instrumented to a maximum depth of 474 mbgs. The base of permafrost is 570 mbgs at this location.

Well TM00141 is located within the Madrid South underground mine between Wolverine Lake and Patch Lake (Figure 18). The well extends toward Patch Lake. Ground temperature measured from lowermost thermistors node is -2.6°C at 225 mbgs. The projected base of permafrost is 346 mbgs, intercepting the talik at the edge of the Patch Lake. The range in depth to the base of permafrost at Madrid North and Madrid South is similar to comparable measurements made at the Doris Mining Area (Table 1; Figure 19).

Table 8: Madrid Mining Area Depth of 0°C and -2°C Isotherm from Ground Temperature Data

Site ID	Location	Maximum Instrumented Depth (mbgs)	-2°C Isotherm (mbgs)	0°C Isotherm (mbgs)
08PMD669	Madrid North	474	438	570
08PSD144	Patch Lake Island	275	50	78
TM00141	Madrid South	225	303	346

Notes:

1. Thermistor node depth corrected for vertical depth using downhole well survey and surface elevation
2. Depth shown as vertical metres below ground surface (mbgs)

5.3.2 Model Results

Figures 20 to 24 show the model results for the Madrid North mining area. Lake expansion was not considered in the 2D thermal models since it is not supported by ground temperature data collected at the Madrid mining areas. Table 9 shows a comparison between site ground temperature measurements and the model fit. In all cases, the model fit is conservative and underestimates the depth of the talik

Table 9: Measured and Model Fit for Talik Surface

Model Section	Thermistor Site ID	Model (-2°C Isotherm)	Measured (-2°C Isotherm)
T2 (Madrid North)	08PMD669	412	438
T2* (Madrid South)	TM00141	258	303

Notes:

1. Asterisk indicates model fit with lowermost thermistor sensor.

At Madrid North, the model was fit to the -2°C isotherm at site 08PMD669. At this site, the lowermost sensor (node) measures -1.3°C at 474 mbgs. The equivalent isotherm estimated by the model is located at 453 mbgs or 21 m less than the measured depth.

Figures 25 to 28 show the model result for the Madrid South mining area. At Madrid South, the model was fit to the lowermost thermistor sensor (node) at site TM00141 which measures -2.6°C. The projected depth of the -2°C isotherm is 303 mbgs at the site. The equivalent isotherm estimated by the fitted model is located 258 mbgs. The model underestimates the position of the -2°C by 45 m.

Disclaimer—SRK Consulting (U.S.), Inc. has prepared this document for TMAC Resources Inc.. Any use or decisions by which a third party makes of this document are the responsibility of such third parties. In no circumstance does SRK accept any consequential liability arising from commercial decisions or actions resulting from the use of this document by a third party.

The opinions expressed in this document have been based on the information available to SRK at the time of preparation. SRK has exercised all due care in reviewing information supplied by others for use on this project. While SRK has compared key supplied data with expected values, the accuracy of the results and conclusions from the review are entirely reliant on the accuracy and completeness of the supplied data. SRK does not accept responsibility for any errors or omissions in the supplied information, except to the extent that SRK was hired to verify the data.

6 References

- Areva Resources Canada Inc. 2011. Kiggavik Project Environmental Impact Statement Technical, Appendix 5B: Geology and Hydrogeology Baseline.
- Burn CR. 2002. Tundra lakes and permafrost, Richards Island, western Arctic coast, Canada. *Canadian Journal of Earth Sciences* 39: 1281–1298.
- Burn CR. 2005. Lake-bottom thermal regimes, western arctic coast, Canada. *Permafrost and Periglacial Processes* 16: 355–367.
- Cumberland Resources Ltd. 2005. Meadow bank Gold Project: Final Environmental Impact Statement.
- ERM Rescan. 2014. Doris North Project: 2013 Aquatic Effects Monitoring Program Report. Prepared for TMAC Resources Inc. by ERM Rescan: Yellowknife, Northwest Territories.
- ERM. 2015. Doris North Project: 2014 Aquatic Effects Monitoring Program. Prepared for TMAC Resources Inc. by ERM Consultants Canada Ltd.: Yellowknife, Northwest Territories.
- Golder Associates 2013. Meliadine. Draft Environmental Impact Statement - Volume 7 Freshwater Environment - Appendix 7.2-A Groundwater Quality Baseline Report.
- Kerr, D.E. 1994a. Late Quaternary Stratigraphy and Depositional History of the Parry Peninsula-Perry River Area, District of Mackenzie, Northwest Territories. *Geological Survey of Canada Bulletin* 465. 34 p.
- Kerr, D.E. 1994b. Late Quaternary History of the Parry Peninsula to Perry River Region, Northwest Territories. PhD. Dissertation. University of Alberta.
- Lunardini V.J. 1995. Permafrost Formation Time. CRREL Report 95-8, US Army Corps of Engineers, Cold Regions Research & Engineering Laboratory, April 1995.
- Mackay J.R. 1962. Pingos of the Pleistocene Mackenzie delta area. *Geographical Bulletin*, 18: 21-63.
- Mackay, J.R. 1992. Lake stability in an ice-rich permafrost environment: examples from the western Arctic coast. In *Aquatic ecosystems in semi-arid regions: implications for resource management*. Edited by R.D. Robarts and M.L. Bothwell. National Hydrology Research Institute, Environment Canada, Saskatoon, Sask., Symposium Series 7, 1–26.
- Rescan. 2010. 2009 Freshwater Baseline Report, Hope Bay Belt Project. Prepared for Hope Bay Mining Limited by Rescan Environmental Services Ltd.
- Rescan. 2011a. Hope Bay Belt Project: 2010 Freshwater Baseline Report. Prepared for Hope Bay Mining Limited by Rescan Environmental Services Ltd.

- Rescan. 2011b. Doris North Gold Mine Project: 2010 Aquatic Effects Monitoring Program Report. Prepared for Hope Bay Mining Limited by Rescan Environmental Services Ltd.: Vancouver, British Columbia.
- Rescan. 2012. Doris North Gold Mine Project: 2011 Aquatic Effects Monitoring Program Report. Prepared for Hope Bay Mining Limited by Rescan Environmental Services Ltd.
- Smith MW. and Hwang CT. 1973. Thermal disturbance due to channel shifting, Mackenzie Delta, N.W.T., Canada. Second International Conference on Permafrost. U.S.S.R., National Academy of Science, Washington, D.C., 51-60.
- Smith M.W. 1976. Permafrost in the Mackenzie delta, Northwest Territories. Geological Survey of Canada. Paper 75-28.
- SRK 2015a. Hope Bay Doris North Project Thermal Modelling – Permafrost between Doris and Tail Lakes.
- SRK. 2005b. Groundwater Assessment, Doris North Project, Hope Bay, Nunavut.
- SRK 2009. Hope Bay Gold Project: Stage 2 Overburden Characterization Report. Report submitted to Hope Bay Mining Ltd.
- SRK 2011a. Hope Bay Project – Geotechnical Design Parameters. Report prepared for Hope Bay Mining Limited.
- SRK 2011b. Stage 2 Geotechnical and Hydrogeological Assessment for Doris Central and Connector Underground Mines. Prepared for Hope Bay Mining Limited.
- SRK 2015. Back River Project: Goose Property Talik Thermal Modeling. Prepared for Sabina Gold & Silver Corp.
- SRK 2017. Hope Bay Project: Thermal Modelling to Support Run-of-Quarry Pad Design. Prepared for TMAC Resources Inc.
- Stevens CW. 2010a. Interannual Changes in Seasonal Ground Freezing and Near-surface Heat Flow beneath Bottom-fast Ice in the Near-shore Zone, Mackenzie Delta, NWT, Canada. Permafrost and Periglacial Processes 21: 256-270.
- Stevens CW. 2010b. Modeling Ground Thermal Conditions and the Limit of Permafrost within the Nearshore Zone of the Mackenzie Delta, Canada. Journal of Geophysical Research. 115: F04027.
- van Everdingen, R. (ed.). 2005. Multi-language glossary of permafrost and related ground-ice terms. Boulder, CO: National Snow and Ice Data Center.
- Wolfden Resources Inc. 2006. High Lake Project Environmental Impact Statement.

Figures
